The compound eyes of mantis shrimps (Crustacea, Hoplocarida, Stomatopoda). I. Compound eye structure: the detection of polarized light

N. J. MARSHALL[1], M. F. LAND[1], C. A. KING[2] AND T. W. CRONIN[2]

[1] *School of Biological Sciences, University of Sussex, Falmer, Brighton BN1 9QG, U.K.*
[2] *Department of Biological Sciences, University of Maryland, Baltimore County, Catonsville, Maryland 21228, U.S.A.*

CONTENTS

SUMMARY

Stomatopod crustaceans possess compound eyes divided into three distinct regions: two peripheral retinae – the dorsal and ventral hemispheres – and the mid-band. Throughout the eye, in particular in the mid-band, there are many structural adaptations that potentially enable different portions of the eye to perform different visual tasks. A high degree of optical overlap between these eye regions allows the parallel sampling of various parameters of light from one direction in space. In consecutive papers, we present structural evidence that stomatopods have the receptors necessary for colour and polarization vision.

The first paper describes the retinal structures that suggest the existence of polarization sensitivity in stomatopods. mid-band rows five and six, together with the hemispheres, are probably involved in this visual process. By using two strategies, rhabdomal modification and varying the orientation of similar ommatidial units in the three eye regions, stomatopods have the capacity to analyse polarized light in a very detailed manner. All the species included in this study live in shallow, tropical waters where polarized light signals are abundant. It therefore seems likely that their eyes have evolved to take advantage of such environmental cues.

Structural evidence also suggests that all retinular cells in rows one to four of the mid-band, and the distal most retinular cells (R8) over most of the retina, are not sensitive to polarized light. These mid-band rows are instead adapted for colour detection. This function of the stomatopod retina and structural features concerned with colour sensitivity are described in paper II (*Phil. Trans. R. Soc. Lond.* B **334**, 57–84 (1991)).

1. INTRODUCTION

Stomatopods, or mantis shrimps, are highly aggressive, predatory marine crustaceans. They live in cavities or burrows, which they may excavate themselves, and from which they stalk and kill other crustaceans, annelids, molluscs and fish (Caldwell & Dingle 1976). They possess two large raptorial limbs which, with a rapid strike, can smash or spear prey. Mantis shrimps are commonly classified by using this functional distinction as 'smashers or spearers'. Four modern superfamilies of stomatopod exist; the Bathysquilloidea,

Phil. Trans. R. Soc. Lond. B (1991) **334**, 33–56
Printed in Great Britain

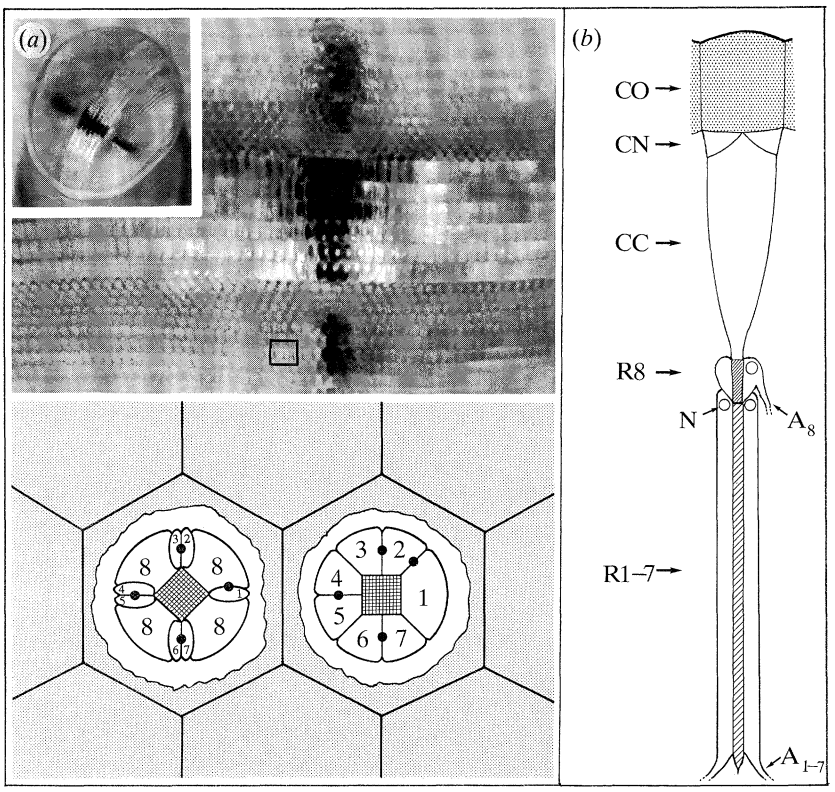

Figure 1. (*a*) Left eye of *Gonodactylus chiragra*. The photograph is of the mid-band with some peripheral ommatidia and the inset is a frontal view of the whole eye. Stomatopod eyes can rotate about the eye stalk axis by up to 70° and the mid-band is often not held horizontally. However, to simplify the description of the eye's anatomy (in particular the direction of microvilli relative to the outside world) the text and all subsequent figures presume the mid-band is horizontal, unless otherwise stated.

Beneath the photograph is an expanded, diagrammatic view of the portion of the ventral hemisphere within the box above. Two of the hexagonal facets found in the peripheral retinae are 'cut away' to reveal the arrangement of retinular cells in these ommatidia. The R8 cell level is shown on the left and the R1–7 level on the right (figure 16). As explained further in the text (§3*d*(iv)), the dorsal and ventral halves of the eye are mirror images of each other; as are the right- and left-hand eye. The cell arrangement shown here is for the bottom half of the left-hand eye, viewed looking into the eye from in front of the shrimp. The black dots mark the position of the four cone cell projections and cell numbering is based on the position of these relative to the R1–7 cells; it conforms with that of Hallberg (1977) and is not the same as that of Marshall (1988). Cell 1 is always the largest cell and cell 2 is flanked on both sides by cone cell projections. Note the two directions of microvilli in the rhabdoms represented by the cross-hatch.

(*b*) A generalized ommatidium in longitudinal (or sagittal) section: CO, cornea; CN, corneagenous cells; CC, crystalline cones; N, nucleus; A8, axon of retinular cell 8; A1–7, axons of R1–7 cells.

Squilloidea, Lysiosquilloidea and Gonodactyloidea (Manning *et al.* 1984).

A notable feature of stomatopods is their large and often highly mobile eyes which have been called '... the most amazing compound eye(s)' (Horridge 1977). They are obviously important in locating and tracking prey (Cronin *et al.* 1988; Land *et al.* 1990) and are arranged optically in such a way that each eye views the same area in visual space, simultaneously with three parts of the eye (Horridge 1978; Marshall 1988). With such a system, monocular range-finding is theoretically possible (Exner 1891). The 'trinocular' nature of these eyes is clearly visible anatomically, as each eye consists of two peripheral ommatidial groups, or hemispheres, divided by a mid-band region (Manning *et al.* 1984).

Mid-bands are composed of two rows of ommatidia in the squilloids and six rows in the lysiosquilloids and gonodactyloids. Bathysquilloids, which are deep-sea animals, tend to have reduced or simplified eyes with no mid-band present. Externally, facets in six-row mid-bands often appear different from those in the hemispheres. Those in the gonodactyloidae for instance are considerably larger and dorsoventrally elongate (table 2 and figure 1), suggesting that these six rows are functionally specialized (Schiff & Abbott 1989). Two-row mid-band ommatidia are similar to those in the hemispheres, and probably perform a similar function as the rest of the eye (Schiff *et al.* 1986*a*). This account is mainly concerned with six-row mid-bands and how their structure and function differs from the rest of the eye.

The ommatidia in the hemispheres are structurally like those of other malacostracans described (Eguchi & Waterman 1966). The rhabdom is fused with interdigitating orthogonal microvilli throughout and there is a single, relatively short, distally placed retinular cell, R8, overlying seven cells R1–7, which supply most of the rhabdom (figures 1 and 16). The rhabdoms of the mid-band, however, although clearly derived from

this basic form, possess many novel features. These include brightly coloured intrarhabdomal filters, a tiering system unique in the crustaceans, and R8 cells with unidirectional microvilli (Marshall 1988). In fact, each of the six mid-band rows has its own characteristic modifications and these specializations suggest that this group of ommatidia operates as a colour and polarized light analyser.

In the first of the two papers presented here, we describe the structure and ultrastructure of the mid-band and hemispheres of several stomatopods: *Gonodactylus chiragra*, *Gonodactylus oerstedii*, *Odontodactylus scyllarus* and *Pseudosquilla ciliata* (Gonodactyloidae); *Coronis scolopendra*, *Lysiosquilla sulcata*, *Lysiosquilla scabricauda* and *Lysiosquilla tredecimdentata* (Lysiosquilloidae). We use this number of species both to emphasize similarities in design of the stomatopod retina and also to illustrate the slight modifications to this basic design found in each of the species. Some figures also contain information concerning the retina of *Oratosquilla solicitans* (Squilloidae), a stomatopod with a two row mid-band, which is included here for comparative purposes. The eyes of this superfamily are more thoroughly described in Schiff (1963), Schiff *et al.* (1986*a*) and Schönenberger (1977).

The second of the two papers (Marshall *et al.* 1991; hereafter referred to as paper II) describes the most unusual features of stomatopod eyes, the brightly coloured intrarhabdomal filters (Marshall 1988), and also discusses other photostable and photosensitive pigments present (Cronin & Marshall 1989*a*, *b*). It now seems likely that all stomatopods with six row mid-bands possess up to eleven distinct visual pigments, individually positioned in the various retinal areas described here. This unique combination of structural organization, photostable filters and multiple photopigments, may provide these shrimps with a sharply tuned colour sampling system.

Within all the retinae described here there is the potential for a complex and possibly unique polarized light analysis system. Many crustaceans are theoretically capable of this visual sense using the orthogonal, interdigitating microvilli often found in their retinae (Snyder 1973; Waterman 1981). Here each cell is maximally sensitive to light whose *E*-vector is parallel to the microvilli it carries. There are therefore, two populations of cells in the retina, one possessing microvilli perpendicular to the other. Such eyes are, in the nomenclature of Bernard & Wehner (1977), said to be capable of 'two dimensional' polarization sensitivity. In other words, it is likely that two information channels are present, the orthogonal receptor sets potentially providing two opponent signals. Stomatopods also possess microvilli arrayed in two directions in nearly all eye regions. However, by compartmentalizing the eye into three areas and arranging the receptors in each area differently, more potential information channels have been created, enabling a very detailed analysis of polarized light in the environment.

If stomatopods are processing polarized light, this task is made more complicated by their impressive repertoire of eye movements (Cronin *et al.* 1988; Land *et al.* 1990). Particularly important in this respect is a rotational degree of freedom of the eyes about the eyestalk axis. Each eye can be rotated by up to 70° and this will change the orientation of the microvilli within it relative to any plane of polarized light the animal is looking at. In theory this ability could be used in combination with a single direction microvillar array to analyse polarized light patterns in a serial manner (Kirschfeld 1973). This unusual eye movement means that in describing the structure of the eye, in particular the microvillar orientation, we have had to choose a fixed eye orientation. For a variety of reasons, explained in the caption to figure 1, the orientation chosen is with the mid-band horizontal.

2. MATERIALS AND METHODS

Stomatopods were obtained from tropical marine suppliers, hand caught in the Fort Pierce area of Florida, or supplied by Dr R. Caldwell of the University of California, Berkeley. All animals were kept in aquaria on a 12 h:12 h light:dark cycle. They were fed live or frozen shrimp. Animals used for microscopy were allowed to acclimatise to this régime for several days and were killed during the light phase so as to obtain fully light-adapted eyes.

Of a variety of fixatives used, best fixation was obtained with a mixture of 4% glutaraldehyde and 0.5% paraformaldehyde in 0.1 M PIPES buffer with 2% sucrose and 1 mM EGTA (percentages by mass). Tissue was fixed at 4 °C overnight and post-fixation done in 1% osmium tetroxide in PIPES buffer plus 2% sucrose, for 3 h. After dehydration in a series of ethanols, the material was passed through two changes of propylene oxide. It was rotated overnight in a mixture of 50% Spurs resin and 50% propylene oxide from which it was transferred into pure Spurs resin and again rotated overnight before embedding. Shrinkage of around 20% was presumed for tissue treated in this way.

For light microscopy (LM), material was sectioned at 1 or 2 μm and stained with toluidine blue. For transmission electron microscopy (TEM), thin sections were cut by using glass or diamond knives, stained with uranyl acetate and lead citrate and examined on a Jeol 100C or a Zeiss EN 10CA. All drawings or photographs of transverse sections are arranged as if the observer is looking into the eye from the outside. It is important to bear this in mind when considering the symmetries in the retinal morphology (see §3*d*(iv)).

3. RESULTS

The eye is divided into three parts, two hemispheres positioned dorsally and ventrally (figure 1) and a mid-band consisting of six morphologically distinct rows of ommatidia. The dorsal hemisphere typically contains around 15% more ommatidial rows than the ventral hemisphere, making the eye slightly asymmetrical dorso-ventrally.

Stomatopod ommatidia are similar to those of many other apposition-eyed crustaceans (Waterman 1981): they consist of cornea, crystalline cone, pigment cells

Table 1.

(Eye stalk length is measured from the front of the cornea to the back of the eye stalk where its flexible joint attaches to the head. Cornea length is measured, viewing the eye's dorsal surface, from the front of the cornea to the point at which it joins the calcified eye stalk. Cornea height is measured, viewing the eye from in front, along a sagittal line perpendicular to the mid-band.)

	G.c.	O.s.	P.c.	C.s.	L.t.	O.o.
animal size/mm	80	140	90	70	110	140
no. facets per eye	8800	12000	9500	3000	6500	3500
no. facets in AZ	95	270	140	170	300	—
eye stalk length/mm	7.0	5.0	6.0	3.8	7.5	5.5
cornea length/mm	2.5	2.8	2.6	1.9	4.0	2.5
cornea height/mm	2.3	4.8	3.0	2.4	9.0	6.5

and eight retinular cells. The fused rhabdom contains interdigitating orthogonal microvilli, throughout most of the retina, and is surrounded by a clear, palisade layer along its entire length. A basement membrane at which the rhabdom terminates divides the retina from underlying nerve plexi.

(*a*) *Cornea*

The dioptric units, cornea and crystalline cones, are described for several stomatopod species, by Schiff *et al.* (1986*b*) and are therefore only mentioned briefly here.

Facets in dorsal and ventral hemispheres of all species are hexagonal, arranged in rows parallel to the mid-band, and in many gonodactyloid stomatopods are considerably smaller in size than the dorso-ventrally alongate facets of the mid-band (figures 1–15). Facets of the mid-band in the lysiosquilloids are less distinct, being hexagonal and similar in size, or in the case of rows two and four, smaller than those in the hemispheres (table 2). Within both superfamilies there is a common asymmetry to be seen in the mid-band; the facets of rwo three are large compared to those of two and four, and rows five, six and one are of a similar, intermediate size (figures 2–15 and table 2). This external morphology indicates two things. Firstly, the mid-band rows probably perform the same functions in different species, and secondly, the various mid-band rows have different functions.

Throughout the eyes of all species corneal facets are bi-convex and are secreted by two corneagenous cells which they overlie (figure 16). Those in the mid-band are more curved on both surfaces, and all lenses focus a sharp image onto the rhabdom tips.

(*b*) *Crystalline cones*

There are four homogeneous crystalline cone cells per ommatidium. Their nuclei are positioned distally in a pyramidal, fused projection which makes contact with the underside of the corneal facet and is surrounded by the corneagenous cells (figure 16). The cones are round or ovoid, in transverse section. From their widest point, just below the corneagenous cells, they taper proximally until a few microns above the retina. Here a thin cone tail is formed which makes direct contact with the distal tip of the rhabdom. Just distal to this point, the boundary between cone cells becomes scalloped and irregular. After contacting the retina, each cone cell sends a thin process proximally, between the retinular cells, to the basement membrane (figures 1 and 28–31).

Along a sagittal section of the eye, cones vary considerably in length (figures 4, 7, 11 and 15), becoming shorter towards the dorsal and ventral edges of the eye and also medially and laterally. Those of the mid-band ommatidia are often slightly shorter than their immediate neighbours in the hemispheres. If an acute zone is present, cones here are around 20% longer than in neighbouring areas.

(*c*) *Pigment cells*

These cells are described in some detail in paper II and are therefore only listed here. The pigment cells of crustacean eyes can be put in six general classes (Hallberg & Elofsson 1989), and five of these exist in stomatopod eyes (Schönenberger 1977). They are: retinular cell pigment (of which there are several types unique to mantis shrimps), distal pigment, proximal pigment, inter-ommatidial pigment and basal pigment.

(*d*) *Retinular cells and rhabdom*

The structure of rhabdoms in both the mid-band and the hemispheres is based on a two-tiered design, typical of many crustacea. There is a relatively small R8 cell as the top tier, and this overlies a longer tier constructed by the R1–7 cells. In the hemispheres and rows five and six of the mid-band, R1–7 cells contribute to the entire length of the lower tier. However in rows one to four of the mid-band the R1–7 tier is subdivided into two: a distal region (DR1–7) and a proximal region (PR1–7). These mid-band rows are therefore three tiered and this is most easily seen in rows two and three. These two rows each contain two coloured intrarhabdomal filters which are positioned between the three rhabdom sections (figure 16).

Figure 16 is a diagrammatic representation of the retina in longitudinal section. Within this five levels are drawn, A, B, C, D and E, each representing a transverse section through the receptors of the retina. Figures 17, 20 and 21 form a montage of these levels and enable a comparison of the retinal cells in each tier and in each ommatidial row or region. Level A, for instance, is a section through the distal R8 cell tier.

This overall view of the retina is needed to compare the various microvillar directions found in each subsection of the eye.

A remarkable feature of mid-band ommatidia, particularly in the gonodactyloids, is the amount of space these six rows occupy within the eye. In *G. chiragra*, for instance, 30% of the total retinal volume is taken up by the mid-band rhamdoms whereas the 35 rows of the dorsal hemisphere and 30 rows of the ventral hemisphere occupy the remainder (figures 4 and 7). The disproportionate volume is partly due to an increase in rhabdom size. For the four gonodactyloid species examined, mid-band rhabdoms were found to be, on average twice as wide as those of the hemispheres. In the lysiosquilloids this was also true of some mid-band rows, but only over a limited portion of their length. All ommatidial dimensions are summarized in table 2.

(i) *R8 cells (level A)*

In both the mid-band and the hemispheres, each rhabdom has a single, distally placed R8 cell (named by convention with past literature, e.g. Waterman 1977) which forms a layered, orthogonal set of microvilli in all retinal areas except rows five and six (figures 23 and 24).

Stomatopod R8 cells are four-lobed and cross-shaped in transverse section, resembling a four-leafed clover (figures 17 and 18). Except for rows five and six, which are described shortly, each 'leaf' or lobe builds microvilli in one direction to meet the microvilli of the opposite 'leaf' at the rhabdom's mid-line. The R8 cell nucleus is consistently positioned within a particular lobe which also forms a thin axon that projects proximally, close to cells 1 and 7, through the basement membrane (figures 17, 46 and 48). Between the lobes of R8 are thin upward-projecting processes of R1–7 but at this level, these cells make no contribution to the rhamdom (figure 18). Stomatopod R8 cells are like those found in other malacostracans (Waterman 1981) although the final orientation of microvilli relative to those of R1–7 is different. This is clarified below when the R1–7 part of the retina is described.

Schönenberger (1977) identified a basal R8 cell in *Squilla mantis*. In the squilloid examined here, *Oratosquilla solicitans*, a distal R8 cell is present although it seems degenerate (figure 26). The cell produces few, disorganized microvilli which are smaller than those in the R1–7 cells. This is the first clear demonstration of a distal R8 cell in a squilloid stomatopod. Schiff & Abbott (1989) mention the presence of small distally-placed microvilli, and Waterman (1981) notes that R8 cells are present in many stomatopods.

The position of R8 nucleated lobes in all species indicates a dorso-ventral mirror symmetry that exists in the retina and for which the plane of reflection divides row 2 and row 3 of the mid-band (figures 17 and 49). Symmetry will be considered in more detail in §3*d*(iv).

In mid-band rows one to four, R8 cell rhabdoms are square in transverse section and possess microvilli that are laid down in two directions (⤫). That is, they are orthogonally layered within a single cell making it probably that these cells are not concerned with the analysis of polarized light (figures 23 and 49). The R8 rhabdoms of the hemispheres also contain bi-directional microvilli. However, the direction of microvilli in these retinal regions is often different in each hemisphere. In *C. scolopendra*, for instance, R8 microvilli are (⇢⇡) in the dorsal hemisphere and (⤫) in the ventral hemisphere (that is with the 'fixed eye' orientation of figure 1).

R8 rhabdoms in rows five and six contribute over 20% of the entire rhabdom length (row one R8 is also unusually long; table 2). In transverse section they are elliptical or spindle-shaped except distally where they join the cones, and proximally on fusing to the R1–7 rhabdom. Here they match the shape of cone or rhabdom (figures 16 and 24). The spindle length varies among the species examined but is consistent in all species in its orientation in these two rows (figure 27). There is a difference of 90° between the two rows in the orientation of the long axis of the spindle. It is parallel to the mid-band in row six and perpendicular to it in row five (figure 49).

The microvilli of R8 cells in rows five and six are unidirectional, perpendicular to the long axis of the ellipse and are unlayered. As figure 49 illustrates, R8 microvilli of these two rows are therefore orthogonal to each other and arranged medio-laterally (⇢) in row five and dorso-ventrally (⇡) in row six).

A large proportion of the microvilli in each row five or six R8 rhabdom are laid down by the two lobes of this retinular cell situated on the long sides of the spindle. The remaining 'spindle end' microvilli are constructed by the two smaller lobes of this unusual R8 cell and, perhaps surprisingly, run in the same direction as the majority of microvilli in these rhabdoms (figure 24).

(ii) *R1–7 cells (levels C – DR1–7 and E – PR1–7)*

Rhabdoms of the hemispheres are like those of decapods and other malacostracans (Waterman 1981; see figures 1 and 16). The R1–7 rhabdom is contributed to by all seven retinular cells along its entire length and this is also the case in rows five and six of the mid-band. Mid-band rows one to four, however, are highly unusual in the way their R1–7 rhabdom is constructed as this portion of rhabdom is divided into two tiers (figures 16–22). The rhabdom in these four rows therefore consists of three tiers; one R8 and two R1–7 tiers. The rest of the retina is two tiered; one R8 and one R1–7.

Dorsal and ventral hemispheres. In gonodactyloid stomatopods, the rhabdoms in the hemispheric retinal regions are notably smaller in diameter than those of the mid-band (table 2). Rhabdoms of the lysiosquilloid mid-band are of a similar diameter, Although clearly different from those of the hemispheres. In all species, rhabdoms in the hemispheres are longest next to the mid-band and diminish in length towards the dorsal and ventral 'edges' of the eye (figures 4, 7, 11 and 15). All rhabdoms become shorter medially and laterally. The seven retinular cell nuclei are positioned distally

Table 2.

	D/μm						*f*/μm						*a*/μm						*l*/μm					
	G.c.	O.s.	P.c.	C.s.	L.t.	O.o.	G.c.	O.s.	P.c.	C.s.	L.t.	O.o.	G.c.	O.s.	P.c.	C.s.	L.t.	O.o.	G.c.	O.s.	P.c.	C.s.	L.t.	O.o.
edge	50	40	30	50	100	100	95	54	90	50	250	120	5	7	8	7	8	5	125	20	110	100	250	200
R8	—	—	—	—	—	—	—	—	—	—	—	—	—	—	—	—	—	—	12	3	10	10	25	5
R1–7	—	—	—	—	—	—	—	—	—	—	—	—	—	—	—	—	—	—	105	17	100	90	225	195
d.hem.	60/40	90/60	50/40	75/65	120/110	133/115	570	513	540	500	1000	410	5	7	8	7	8	5	540	530	430	480	750	520
R8	—	—	—	—	—	—	—	—	—	—	—	—	—	—	—	—	—	—	40	50	40	50	75	5
R1–7	—	—	—	—	—	—	—	—	—	—	—	—	—	—	—	—	—	—	500	480	390	430	675	515
v.hem.	60/40	86/60	50/40	75/65	120/110	133/115	530	485	540	360	1000	390	5	7	8	7	8	5	540	480	420	450	750	500
R8	—	—	—	—	—	—	—	—	—	—	—	—	—	—	—	—	—	—	40	50	40	50	75	5
R1–7	—	—	—	—	—	—	—	—	—	—	—	—	—	—	—	—	—	—	500	430	380	400	675	515
MB row 1	90/50	120/60	90/60	90/65	100/110	150/95	510	500	430	340	750	350	7	10	10	10	8	5	600	670	510	600	600	400
R8	—	—	—	—	—	—	—	—	—	—	—	—	—	—	—	—	—	—	115	140	100	180	90	5
DR1–7	—	—	—	—	—	—	—	—	—	—	—	—	—	—	—	—	—	—	265	350	220	240	300	485
PR1–7	—	—	—	—	—	—	—	—	—	—	—	—	—	—	—	—	—	—	220	180	190	180	210	—
MB row 2	80/50	110/60	80/60	65/65	70/110	150/95	440	480	385	330	700	350	7	10	10	10	8	5	640	670	550	625	650	490
R8	—	—	—	—	—	—	—	—	—	—	—	—	—	—	—	—	—	—	85	100	70	90	50	5
F1	—	—	—	—	—	—	—	—	—	—	—	—	—	—	—	—	—	—	35	29	14	10	20	485
DR1–7	—	—	—	—	—	—	—	—	—	—	—	—	—	—	—	—	—	—	280	303	240	280	215	—
F2	—	—	—	—	—	—	—	—	—	—	—	—	—	—	—	—	—	—	15	48	18	20	—	—
PR1–7	—	—	—	—	—	—	—	—	—	—	—	—	—	—	—	—	—	—	225	190	208	225	365	—
MB row 3	100/50	140/60	100/60	75/65	110/110	—	420	460	325	315	650	—	12	10	10	10	8	—	650	670	640	640	700	—
R8	—	—	—	—	—	—	—	—	—	—	—	—	—	—	—	—	—	—	55	48	50	60	50	—
F1	—	—	—	—	—	—	—	—	—	—	—	—	—	—	—	—	—	—	30	30	18	15	20	—
DR1–7	—	—	—	—	—	—	—	—	—	—	—	—	—	—	—	—	—	—	335	240	320	285	260	—
F2	—	—	—	—	—	—	—	—	—	—	—	—	—	—	—	—	—	—	20	70	22	—	—	—
PR1–7	—	—	—	—	—	—	—	—	—	—	—	—	—	—	—	—	—	—	210	282	230	280	370	—
MB row 4	80/50	110/60	80/60	65/65	60/100	—	440	490	385	340	700	—	7	10	10	10	8	—	640	670	550	550	650	—
R8	—	—	—	—	—	—	—	—	—	—	—	—	—	—	—	—	—	—	87	100	70	80	75	—
DR1–7	—	—	—	—	—	—	—	—	—	—	—	—	—	—	—	—	—	—	280	390	250	260	250	—
PR1–7	—	—	—	—	—	—	—	—	—	—	—	—	—	—	—	—	—	—	273	180	230	210	325	—
MB row 5/6	90/50	120/60	100/60	90/65	125/110	—	475	510	430	400	750	—	7	10	10	10	8	—	600	670	500	530	600	—
R8	—	—	—	—	—	—	—	—	—	—	—	—	—	—	—	—	—	—	145	150	125	100	75	—
DR1–7	—	—	—	—	—	—	—	—	—	—	—	—	—	—	—	—	—	—	455	520	375	430	525	—

Table 2. (*cont.*)

	d/μm						Mv size						no. of Mv per layer						$\Delta\rho$/degrees					
	G.c.	O.s.	P.c.	C.s.	L.t.	O.o.	G.c.	O.s.	P.c.	C.s.	L.t.	O.o.	G.c.	O.s.	P.c.	C.s.	L.t.	O.o.	G.c.	O.s.	P.c.	C.s.	L.t.	O.o.
edge	—	—	—	—	—	—	—	—	—	—	—	—	—	—	—	—	—	—	3.0	7.5	5.0	8.0	1.3	2.3
R6	7	7	5	8	8	5	0.05	0.05	0.05	0.05	0.05	0.04	6	5	—	9–12	—	—	—	—	—	—	—	—
R1–7	9	15	8	10	10	24	0.05	0.07	0.05	0.05	0.05	0.06	8	5	—	9–12	8	13–15	—	—	—	—	—	—
d.hem.	—	—	—	—	—	—	—	—	—	—	—	—	—	—	—	—	—	—	0.5	0.8	0.8	0.8	0.5	0.7
R8	7	7	5	8	8	6	0.05	0.05	0.05	0.05	0.05	0.04	4–6	5	4–25	—	—	—	—	—	—	—	—	
R1–7	9	12	8	10	10	25	0.05	0.07	0.05	0.05	0.05	0.06	8	5	—	8–12	8	13–15	—	—	—	—	—	—
v.hem.	—	—	—	—	—	—	—	—	—	—	—	—	—	—	—	—	—	—	0.5	0.8	0.8	1.1	0.5	0.7
R8	7	7	5	8	8	6	0.05	0.05	0.05	0.05	0.05	0.04	4–6	5	—	4–25	—	—	—	—	—	—	—	—
R1–7	9	12	8	10	10	25	0.05	0.07	0.05	0.05	0.05	0.06	8	5	—	8–12	8	13–15	—	—	—	—	—	—
MB row 1	—	—	—	—	—	—	—	—	—	—	—	—	—	—	—	—	—	—	0.8	1.1	1.3	1.7	0.6	0.8
R8	10	10	10	10	10	6	0.05	0.05	0.05	0.05	0.05	0.04	4–6	3–5	—	—	—	—	—	—	—	—	—	—
DR1–7	10	17	12	12	12	25	0.05	0.07	0.05	0.05	0.05	0.06	2–18	4–13	—	2–21	8	13–15	—	—	—	—	—	—
PR1–7	11	17	11	12	12	—	0.05	0.07	0.05	0.05	0.05		—	2–20	4–13	—	1–19	—	—	—	—	—	—	—
MB row 2	—	—	—	—	—	—	—	—	—	—	—	—	—	—	—	—	—	—	0.9	1.2	1.5	1.7	0.6	0.8
R8	10	10	10	8	8	6	0.05	0.05	0.05	0.05	0.05	0.04	4–6	3–5	—	—	—	—	—	—	—	—	—	—
F1	8	10	8	9	10	25	—	—	—	—	—	—	—	—	—	—	—	13–15	—	—	—	—	—	—
DR1–7	12	16	12	10	12	—	0.05	0.07	0.05	0.05	0.06	0.06	2–20	3–13	—	1–19	1–12	—	—	—	—	—	—	—
F2	9	16	10	10	10	—	—	—	—	—	—	—	—	—	—	—	—	—	—	—	—	—	—	—
PR1–7	10	18	11	10	12	—	0.05	0.08	0.05	0.05	0.07	—	3–18	3–10	—	1–18	1–12	—	—	—	—	—	—	—
MB row 3	—	—	—	—	—	—	—	—	—	—	—	—	—	—	—	—	—	—	1.6	1.3	1.8	1.8	0.7	—
R8	10	10	10	8	8	—	0.05	0.05	0.05	0.05	0.05	—	4–6	3–5	—	—	—	—	—	—	—	—	—	—
F1	8	10	8	8	10	—	—	—	—	—	—	—	—	—	—	—	—	—	—	—	—	—	—	—
DR1–7	9	20	11	10	12	—	0.07	0.10	0.05	0.05	0.06	—	9–11	3–13	—	2–20	4–15	—	—	—	—	—	—	—
F2	8	13	10	—	—	—	—	—	—	—	—	—	—	—	—	—	—	—	—	—	—	—	—	—
PR1–7	11	15	10	8	12	—	0.08	0.12	0.05	0.05	0.08	—	11–14	3–15	—	2–17	4–15	—	—	—	—	—	—	—
MB row 4	—	—	—	—	—	—	—	—	—	—	—	—	—	—	—	—	—	—	0.9	1.2	1.5	1.7	0.6	—
R8	10	10	10	8	8	—	0.05	0.05	0.05	0.05	0.05	—	4–6	3–5	—	—	—	—	—	—	—	—	—	—
DR1–7	12	17	12	10	10	—	0.05	0.07	0.05	0.05	0.05		—	4–20	2–12	—	2–18	—	—	—	—	—	—	—
PR1–7	12	17	11	10	12	—	0.05	0.07	0.05	0.05	0.05	—	3–18	2–10	—	1–17	—	—	—	—	—	—	—	—
MB row 5/6	—	—	—	—	—	—	—	—	—	—	—	—	—	—	—	—	—	—	0.8	1.1	1.1	1.4	0.6	—
R8	15/8	30/10	20/7	14/8	20/7	—	0.04	0.04	0.05	0.05	0.05	—	—	—	—	—	—	—	—	—	—	—	—	—
DR1–7	9	20	16	14	10	—	0.05	0.07	0.05	0.05	0.05	—	5	5	—	8–13	6	—	—	—	—	—	—	—

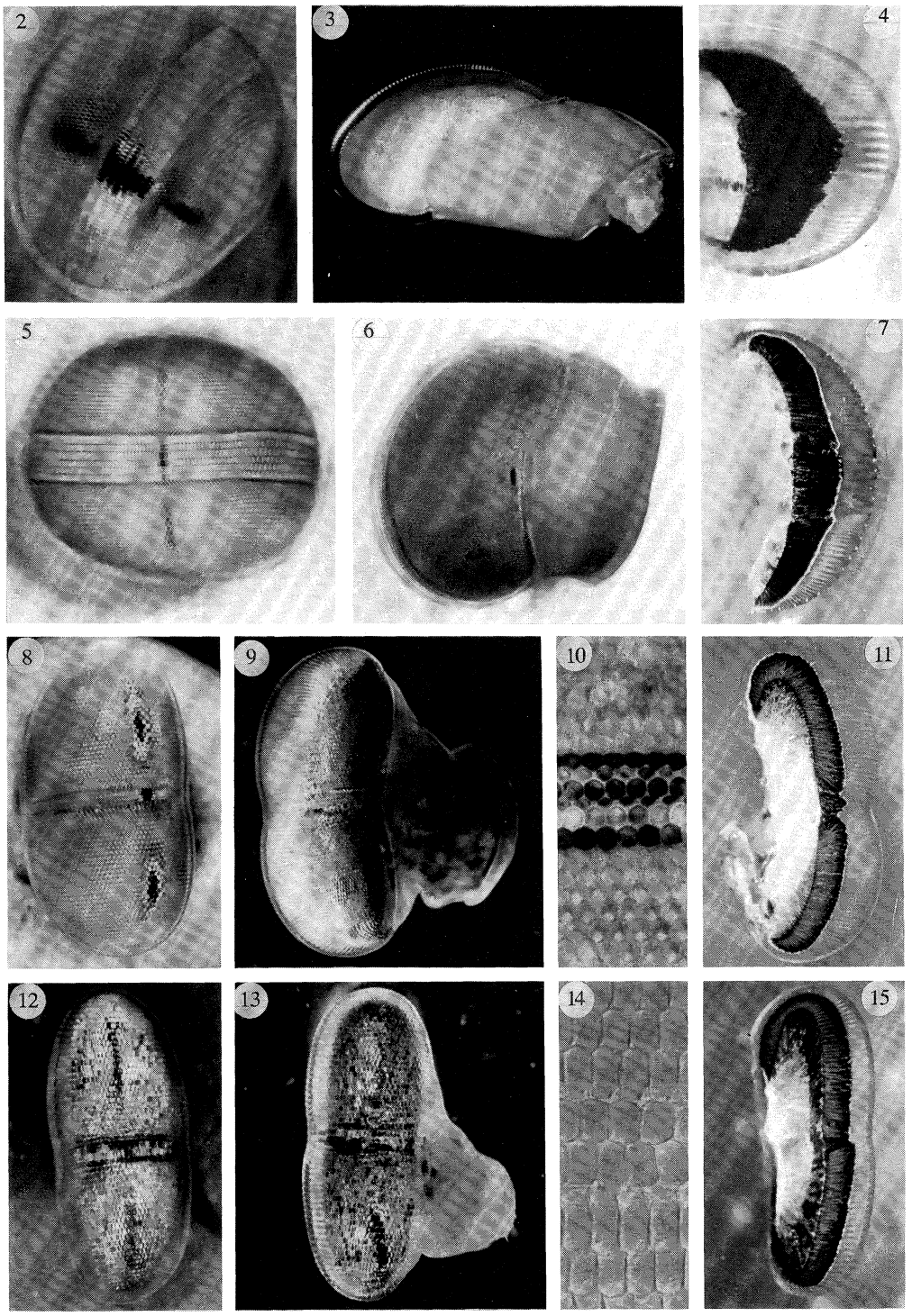

Figures 2–15. Stomatopod eyes.
Figure 2. Acute-zone in *Gonodactylus chiragra*, 15° off sagittal axis of eye.
Figure 3. Dorsal aspect of the eye of *Gonodactylus chiragra*.
Figure 4. Sagittal section through the eye of *Gonodactylus chiragra*.
Figure 5. Right eye of *Odontodactylus scyllarus* viewed from in front, directly on the sagittal axis.
Figure 6. Dorsal aspect of the eye of *Odontodactylus scyllarus*.
Figure 7. Sagittal section through the eye of *Odontodactylus scyllarus*.
Figure 8. Left eye of *Lysiosquilla tredecimdentata* viewed from in front, directly on the sagittal axis.
Figure 9. Lateral aspect of the left eye of *Lysiosquilla tredecimdentata*.
Figure 10. Close-up of the mid-band and surrounding ommatidia in *Lysiosquilla tredecimdentata*.
Figure 11. Sagittal section through the eye of *Lysiosquilla tredecimdentata*.
Figure 12. Left eye of *Oratosquilla solicitans* viewed from in front, directly on the sagittal axis. Note the position of the pseudopupil (dark facets) in this eye compared with figure 8. There is no acute-zone in this eye and only two rows of ommatidia in the mid-band.
Figure 13. Lateral aspect of the left eye of *Oratosquilla solicitans*.

(figure 16), and each cell forms an axon just prior to projecting through the basement membrane.

R1–7 rhabdoms of all stomatopod species examined are approximately square in transverse section. This is particularly apparent for *C. scolopendra* in which very near squares can be seen 'flat side down' in the ventral hemisphere and 'point down' in the dorsal hemisphere (figures 19 and 22, again, recall this is with the eyes in the 'fixed' orientation of figure 1). Microvilli in these rhabdoms are always aligned parallel to the sides of the square and are therefore arranged differently in each hemisphere. As is apparent on examination of the R8 cell level, the rhabdoms of the dorsal hemispheres are apparently rotated 45° relative to those found in the ventral hemisphere (figure 49).

Hemispheric R1–7 microvilli are constructed by all seven retinular cells and form alternating, interdigitating layers of microvilli (figure 42). The cell numbering system, explained in the caption to figure 1, recognizes the largest retinular cell as 'cell 1' and numbers subsequent cells according to their positioning in relation to the cone cell extensions. Cell 1, as it does in other crustaceans, completely occupies one of the four sides of the rhabdom and lays down more microvilli than the other six retinular cells found at this level (Hallberg 1977; Eguchi & Waterman 1968).

For the right eye of *C. scolopendra*, *G. oerstedii* and *G. chiragra*, microvilli are arranged approximately horizontally (↔) (cells 1, 4 and 5) and vertically (↕) (cells 2, 3, 6 and 7) in the ventral hemisphere, and bottom-left to top-right (↗) (cells 1, 4 and 5) and bottom-right to top-left (↖) (cells 2, 3, 6 and 7) in the dorsal hemisphere (figure 49). In *P. ciliata*, *L. sulcata*, *L. tredecimdentata* and *L. scabricauda* the dorsal and ventral hemisphere retinular cell orientation is inverted. As a result microvilli are (↔) (cells 1, 4 and 5) and (↕) (cells 2, 3, 6 and 7) in the dorsal hemisphere and (↗) (cells 1, 4 and 5) and (↖) (cells 2, 3, 6 and 7) in the ventral hemisphere (figures 45–49).

The microvilli in R1–7 here and, as will shortly be seen, in rows five and six are not arrayed in the same direction as those of the R8 cells, but at 45° to them (figure 49). This is different from most malacostracans examined to date (Waterman 1981).

Mid-band rows five and six. Rows five and six of the mid-band, below the level of R8, are very much like those found in the hemispheres. In all species examined they are wider than rhabdoms of the peripheral retinae (figures 40 and 41 and table 2) and receive contributions from by all seven retinular cells along their entire length. In this way, they resemble other malacostracan ommatidia in their cell arrangement and layering (Waterman 1981). In both rows, the R1–7 microvillar layers are the thinnest found anywhere in the retina being around six microvilli deep (table 2). This may aid polarization sensitivity (Stowe 1983).

Mid-band row five. The rhabdom of row five is a strikingly regular square shape in transverse section, positioned 'point-down' when the mid-band is held horizontal. The largest R1–7 cell, number 1, is positioned dorso-laterally and for this row, cells 1, 4 and 5 have microvilli that run from bottom right to top left (↖) (for the right eye) whereas those of cells 2, 3, 6 and 7 are positioned bottom left to top right (↗) (figure 49).

Mid-band row six. Superficially the R1–7 rhabdom of this mid-band row appears identical to that of row five: it is also a 'point-down' square in transverse section and is laid down by seven retinular cells (figure 40). However, on close examination, it is clear that the rhabdom and retinular cells are actually rotated 90° anticlockwise (for the right eye) in relation to row five (figure 49). This means the microvilli of cells 1, 4 and 5 run from bottom left to top right (↗) and those of cells 2, 3, 6 and 7 from bottom right to top left (↖). This rotational relationship between rows five and six is most obvious on examination of the R8 rhabdom of this row whose microvilli run vertically (↕) whereas those of R8 in row five run horizontally (↔). This, together with all retinal symmetries, is examined in more detail in §3*d*(iv).

Mid-band rows one to four. The layout of retinular cells in rows one to four is initially rather confusing and it is instructive to remember that they are derived from the basic malacostracan design. The hemispheres also contain 'basic malacostracan' rhabdoms with a small R8 cell overlying seven R1–7 cells (figure 16). Row one to four R8 cells are similar to those in the hemispheres, it is the R1–7 cells that have become reorganized here.

Retinular cells 1–7 in rows one to four of the mid-band construct their rhabdom as two separate blocks or tiers of microvilli, each tier being made of three or four cells (cell numbers 1, 4 and 5 or 2, 3, 6 and 7 respectively, figures 28–33). Rows one, three and four stacks cells 1, 4 and 5 over 2, 3, 6 and 7, whereas in row two this plan is inverted, with cells 2, 3, 6 and 7 over 1, 4 and 5. Owing to this different arrangement between mid-band rows, the two tiers of R1–7 in these four rows are called DR1–7 and PR1–7 for distal and proximal R1–7 cells rather than using the cell numbers.

In all cells, nuclei are placed at the distal end of the tier to which they belong. Therefore there are three levels at which retinular cell nuclei are found in this retinal portion: distally in R8 cells, more proximally at the R8/DR1–7 rhabdom junction and more proximally still, mid-way down the R1–7 rhabdom, at the DR1–7/PR1–7 junction (figure 16). Although both DR1–7 and PR1–7 cells possess thin processes, extending distally into the R8 level, they play no part in rhabdom construction (figures 30–31).

Two points are notable with respect to the microvillar and cellular arrangement here and apply to all DR1–7 and PR1–7 tiers of rows one through four.

First, microvilli in these rows are positioned orthog-

Figure 14. Close-up of the mid-band and surrounding ommatidia in *Oratosquilla solicitans*; cornea dissected away and cleaned. The mid-band is flanked by two rows with small facets.

Figure 15. Sagittal section through the eye of *Oratosquilla solicitans*. Note the unusual upward skewing of the ommatidia in the ventral hemisphere.

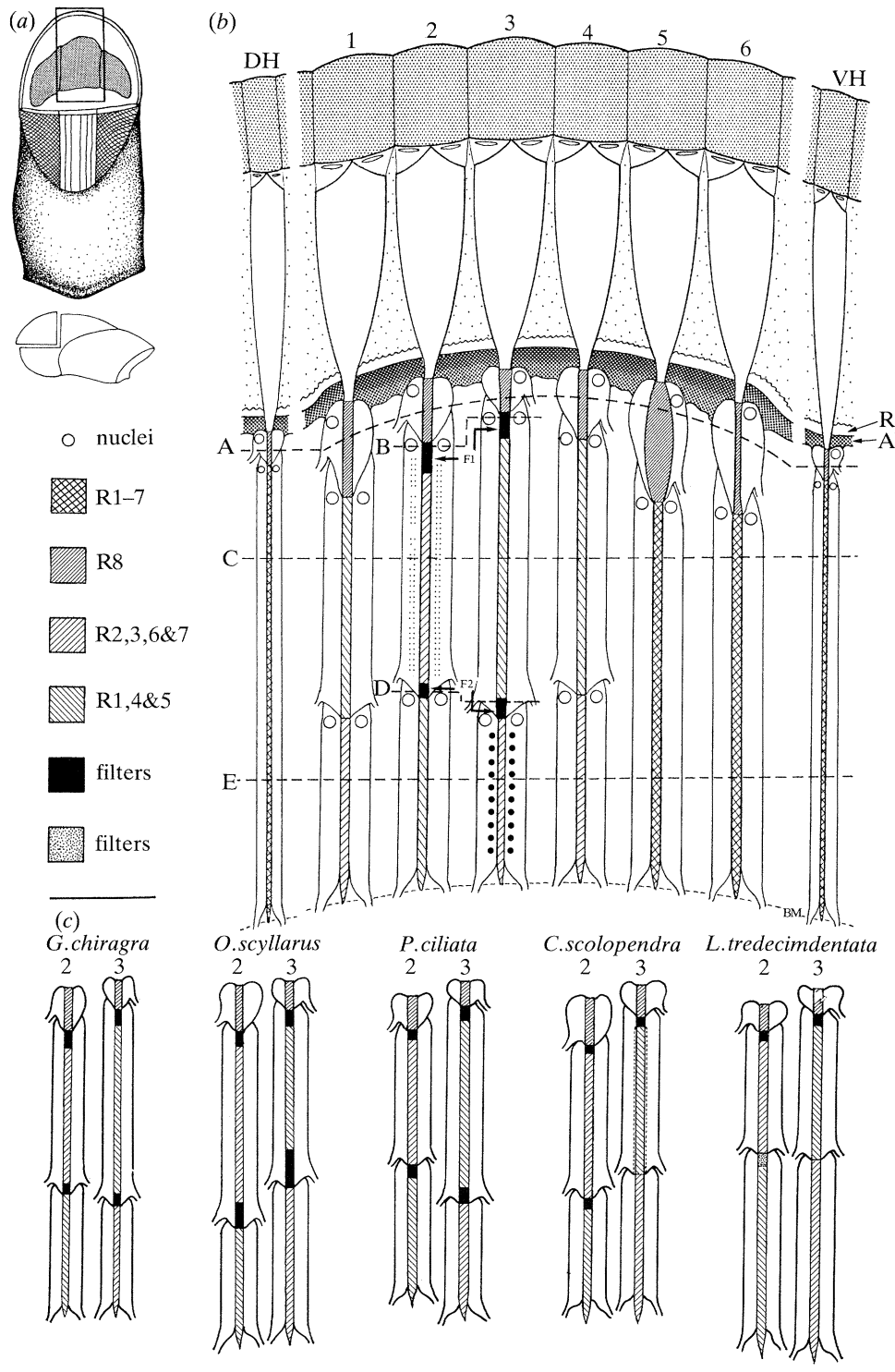

Figure 16. (*a*) The eye of *Gonodactylus chiragra* with a segment removed to show the mid-band. The inset is the eye rotated through 90° about the eye stalk axis to show the segment removed. The box contains the eye region illustrated in (*b*).

(*b*) Diagrammatic representation of the mid-band of *Gonodactylus chiragra*. All gonodactyloid and lysiosquilloid retinae are built on the same basic plan. The different levels shown here (A, B, C, D and E) are the points at which transverse sections of the retina were taken to provide a representative view of the various cell configurations in each tier. These are referred to in the text. Mid-band rows are labelled one to six from dorsal to ventral and two peripheral ommatidia are included, one from each hemisphere, for comparison. At around the point at which tiers join, the axons formed by retinular cells are shown as side-branches, not drawn all the way to the basement-membrane. Row two cells 2, 3, 6 and 7 and rows one, three and four cells 1, 4 and 5 form DR1–7 (level C). Row two cells 1, 4 and 5 and rows one, three and four cells 2, 3, 6 and 7 form PR1–7 (level E).

The filled circles in the proximal tier in row three (PR1–7) represent the heavy concentration of 'oil drops' found here (paper II). The small dots in the distal tier of row two (DR1–7) represent the red coloured 'vessicles' present in this retinal region (paper II). F1, distally placed filters; F2, proximally placed filters; RP, reflecting pigment (paper II); AP, absorbing pigment (paper II); DH, dorsal hemisphere; VH, ventral hemisphere. Scale 130 μm.

onally, (↗) and (↖), in each microvillar layer, and unlike rows five and six and the hemispheres, are therefore parallel to the more distally placed R8 cell microvilli (figure 49). The cells involved contribute to the rhabdom in an unusual manner. All row one to four retinular cells in both DR1–7 and PR1–7 produce microvilli in both orthogonal directions and contribute to all microvillar layers in their respective tiers (figures 28–33). The extent of each cell's contribution to the layers varies, with cell one (as is the case for other retinal areas) producing more microvilli than any other.

Second, in stomatopods the three-cell and four-cell groups (1, 4 and 5 and 2, 3, 6 and 7) form separate tiers, DR1–7 and PR1–7, in rows one to four. There is good evidence in many malacostracans that polarization sensitivity (PS) may be achieved through opponency between orthogonal sets of microvilli; that is between cells 1, 4 and 5 and 2, 3, 6 and 7 (Nässel 1976; Stowe 1977; Sabra & Glantz 1985; Waterman 1981). The two rhabdomal tiers in stomatopods are apparently made by the cells which in other malacostracans contribute the two information channels for analysis of polarized light. Despite this, both DR1–7 and PR1–7, here and in other mid-band rows, possess microvilli arranged, not in a single direction, but in an orthogonal manner (figures 30 and 31). The microvillar layers are less regular than those from the hemispheres or rows five and six and they tend to contain more microvilli per layer (figure 43 and table 2). These features – orthogonality within a single cell, disorganized and relatively thick layering – will reduce the overall PS of each tier (Stowe 1983). Microvillar orthogonality here, as in the R8 cell rhabdoms, appears to be an attempt to render these receptors insensitive to polarized light.

(iii) *Intrarhabdomal filters (levels B and D)*

Here one of the unique features of the gonodactyloid and lysiosquilloid retina is described, the distal and proximal intrarhabdomal filters (F1 and F2) found in rows two and three and positioned between rhabdom blocks R8 & DR1–7 and DR1–7 & PRI–7 (figure 16 and Marshall 1988). Paper II deals with their structure, colours, and their possible functions in relation to colour vision. In this paper they are described in brief as a part of the retina, and in order to allow comparisons of tier construction between species.

F1 filters are found immediately below the rhabdom of the R8 cells in rows two and three. In life and in cryosection (see Materials and Methods, paper II) they consist of strongly coloured, dense plugs of material, and are usually slightly narrower in diameter than the rhabdom. TEM shows them to be made up of small (0.1 μm) vesicles (figures 34–39). In transverse section it is apparent that these filters are divided into three or four, approximately equal-sized segments, the number of segments being the same as the number of retinular cells in DR1–7 (figures 34–39). All F1 filters are in fact constructed by the DR1–7 tier. Their length varies between rows, and quite markedly between species (table 2).

The more proximal filters in the stomatopod retina, F2s, are situated between the rhabomal portion of DR1–7 and PR1–7 of rows two and three and are in general more densely pigmented than those in the more distal F1 position (e.g. dark red or orange in row two and maroon or blue in row three). Like F1 filters, they are slightly narrower in diameter than the rhabdom (table 2), and of various lengths between rows and among species.

In some species; *G. chiragra*, *G. oerstedii* and *O. scyllarus*, row two filters differ from those found in other species; *C. scolopendra*, *L. sulcata*, *L. scabricauda* and *P. ciliata*. In the former three species row two F2 filters are constructed from four segments (figure 36), like the F1s of this row, whereas in the other four species F2s are made up of three segments (figure 35). The explanation is that F2s in the latter four species are produced by the PR1–7 cells and are therefore part of this more proximal retinal tier. The DR1–7 cells make the F1 filter in all species and in *G. chiragra*, *G. oerstedii* and *O. scyllarus*, they are also responsible for producing F2 filters. Thus row two for each of the DR1–7 cells in these three species make F1, F2 and microvilli between, implying an unusually complex intracellular organization. No row two F2s have yet been characterized in *L. sulcata* or *L. tredecimdentata*. This may be the result of the relatively small number of eyes examined in these two species (figure 16).

A second difference between the species studied exists at the F2 level of row three. These filters in the gonodactyloids consist of three segments (figures 38 and 39), which suggests they are made by the same three DR1–7 cells (1, 4 and 5) that make F1 in this row. In all lysiosquilloids, however, there is no F2 in row three. Instead the DR1–7 and PR1–7 rhabdom blocks directly abut each other. In *C. scolopendra* there is a pink sheath present around the entire length of DR1–7 which may act as a lateral filter (paper II).

(iv) *Symmetries found in the stomatopod retina*

The relative position of retinular cells within each ommatidium allows three kinds of symmetry within the retina to be discerned: (i) an overall mirror symmetry dividing rows two and three of the mid-band and involving the entire retina; (ii) a rotational symmetry between dorsal and ventral hemispheres only and (iii)

(*c*) Variations on the basic gonodactyloid/lysiosquilloid mid-band design shown in (*a*). The most obvious differences are in rows two and three of the mid-band. *Gonodactylus chiragra* rows two and three are drawn again for comparison. *Odontodactylus scyllarus* is similar to this plan but with larger filters. Row two F2 in *Pseudosquilla ciliata*, *Lysiosquilla* sp. and *Coronis scolopendra* is formed by the PR1–7 tier rather than the DR1–7. Row two F2 has been found in only one *Lysiosquilla* sp. These filters are probably present in all species, but relatively few *Lysiosquilla* sp. have been examined, hence the differently shaded filter. The lateral pigment abutting the DR1–7 rhabdom in row three of *Coronis scolopendra* is represented here by dots. Scale 200 μm.

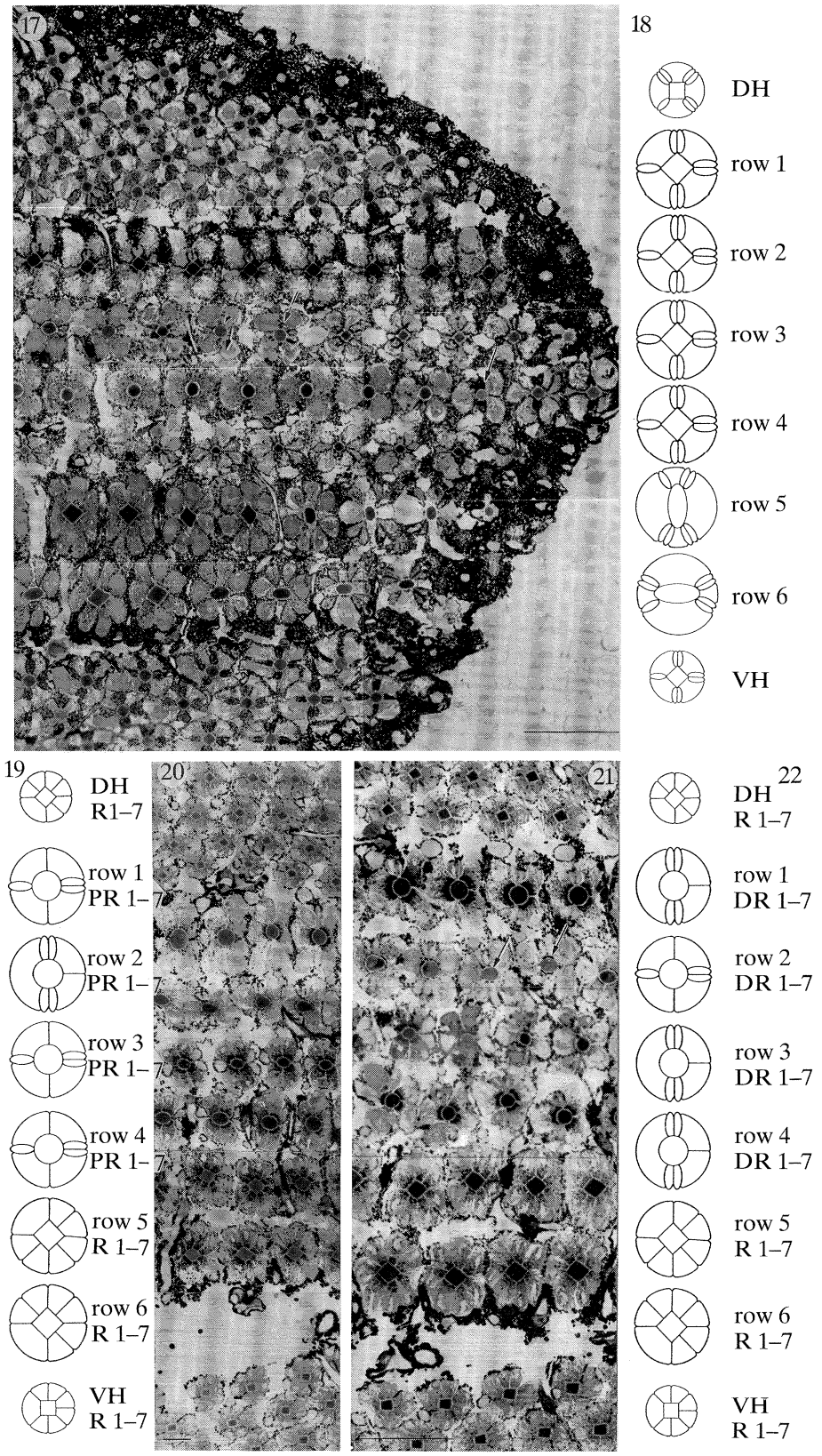

Figures 17–22. The retinular cells (levels A–R8, C–DR1–7 and E–PR1–7). Figures 17, 20 and 21 are arranged such that rhabdoms on the right of each figure are more distal than those on the left.

Figure 17. Transverse LM section of mid-band and periphery of the right eye of *Coronis scolopendra* at a distal level. Owing to the curvature of the retina, several different retinal levels, A, B and C (figure 16), can be seen in one section. In mid-band row one and four and in both hemispheres, only the R8 rhabdom (level A) is sectioned. In the remainder of the retina, R1–7, DR1–7 (level C), in rows two and three, and F1 filters (level B: arrowed in the figure) are sectioned (see figures 34–39). Scale 100 μm.

Figure 18. Diagrammatic representation of the R8 cells in figure 17 level A in the retina. R1–7 cells are also present

a rotational symmetry involving only rows five and six of the mid-band.

Overall retinal mirror symmetry. As with many arthropods (Nässel 1976; Hallberg 1977; Tomlinson 1988), a plane of symmetry exists running horizontally through the eye. Ommatidia, and therefore retinular cells, in one half are mirror images of those in the other half. For gonodactyloid and lysiosquilloid stomatopods, the line of symmetry is positioned between rows two and three of the mid-band. In the squilloids where there are only two mid-band rows it lies between these two rows. On sectioning down through the retina in the transverse plane, this relationship is first visible in the R8 cells (figure 49).

The location of cone cell processes is a more reliable indicator of all the symmetries found throughout the retina and determines the numbering of retinular cells R1–7 (figure 1). In the dorsal half of the (left) eye, cells are arranged in numerical sequence clockwise from the large cell number 1 through to 7 while for the ventral half the eye, the sequence is anticlockwise. Cell 2 is the only cell flanked on both sides by cone cell extensions, and this asymmetry is a clear indication of the cellular arrangement in the various retinal regions.

Species-specific rotational symmetry between hemispheres. With the exception of *O. solicitans*, in all species examined, one hemisphere's ommatidia are not simply mirror images of the other. This also is first apparent at the R8 cell level (figures 17, 18 and 49) but is clearest on examination of transverse sections of R1–7 cells. Each species examined is described below.

1. *O. solicitans.* Peripheral rhabdoms and retinular cells in this species are simple mirror images of each other. The plane of reflection is between the two mid-band rows. Rhabdoms in both dorsal and ventral peripheral eye regions, and the mid-band, are square with the 'flat side down' in transverse section. Unlike the other species described here, mid-band rhabdoms in *O. solicitans* are much like those of the hemispheres in all respects (figure 47). Cell 1 is positioned laterally in both hemispheres and, for the left eye, cell numbering (1 through 7) is clockwise in the dorsal hemisphere and anticlockwise in the ventral hemisphere.

2. *Gonodactylus chiragra* and *Coronis scolopendra.* In both these species, for the right eye, the ventral retinular cells and rhabdoms are rotated 45° clockwise relative to those in the dorsal hemisphere. R1–7 rhabdoms, for instance, are all square in transverse section and for the dorsal hemisphere are oriented 'point down' (figures 21, 48 and 49). Conversely in the ventral hemisphere they are positioned 'flat side down'. The handedness of the rotation is given by the position of the large cell 1, and the cone cell projections (figure 1).

3. *P. ciliata, L. scabricauda, L. tredecimdentata* and *L. sulcata.* Rotation of retinular cells in the ventral hemisphere of these four species is anticlockwise relative to the dorsal hemisphere. Also the rhabdoms are positioned differently to those of *G. chiragra* and *C. scolopendra.* This is apparent, again, in transverse section where R1–7 rhabdoms are still square but are 'flat side down' in the dorsal hemisphere and point down in the ventral hemisphere (figures 45 and 49).

4. *O. scyllarus.* Although not as apparent as in other species, the 45° rotational relationship between hemispheres is present in such that the ventral hemisphere is rotated 45° anticlockwise relative to the dorsal hemisphere (figures 46 and 49).

Row five and six rotational symmetry. This retinal transformation is common to all gonodactyloid and lysiosquilloid species examined and is most clearly indicated at the R8 cell level. The plane of rotational symmetry lies between the two rows. On examination of R8 cell nuclei and, in particular, the spindle shape these rhabdoms form in transverse section, it can be seen that for the left eye, row six retinular cells are rotated 90° clockwise with respect to row five (figure 27).

The possible significance of these three retinal symmetries is that, relative to the outside world, the microvillar directions in one portion of the retina are often different to those in another portion. Even where they are the same, as they are for instance between rows two and three of the mid-band, the mirror symmetry of the retina means that different retinular cells in each eye half produce microvilli in the same direction. (All microvillar directions for the different retinal regions of the stomatopods described here are summarized in figure 49.) As is explained further in the discussion, this means that different eye regions are sensitive to different planes of polarized light and makes possible the construction of a highly complex PS system.

(v) *Retinular cells and rhabdom; summary of major findings*

1. Rhabdoms of the peripheral retina are much like those of other malacostracans, with a relatively short, distally placed R8 cell rhabdom overlying a longer section made up of interdigitating microvilli from seven retinular cells, R1–7. Microvilli are arranged orthogonally throughout with the orientations of those in the R8 cells being 45° offset from those in the R1–7 cells underneath.

at this level as thin upward projections between these four lobes of R8. Note the 'side-down' square shape of the R8 rhabdom in the dorsal hemisphere and the 'point-down' square shaped R8 rhabdom in the ventral hemisphere.

Figure 19. Diagrammatic representation of the retinular cells and rhabdoms in figure 20 (level E, figure 16). In mid-band rows one to four, the small cells are the axonal projections of the DR1–7 cells.

Figure 20. LM transverse section of the mid-band and hemispheres in *Coronis scolopendra* PR1–7. In row one the transition between DR1–7 and PR1–7 tiers is visible, all other rows are sectioned through the PR1–7 tier only. Scale 30 μm.

Figure 21. Transverse LM section of the mid-band and hemispheres in *Coronis scolopendra* DR1–7 (level C). F2 in row two (level B, arrowed) is also visible in this section, as are the PR1–7 cells (level E) in rows two and three. All other rhabdoms are sectioned through DR1–7 rhabdom. Scale 100 μm.

Figure 22. Diagrammatic representation of the DR1–7 cells in figure 21 or 24 (level C, figure 16).

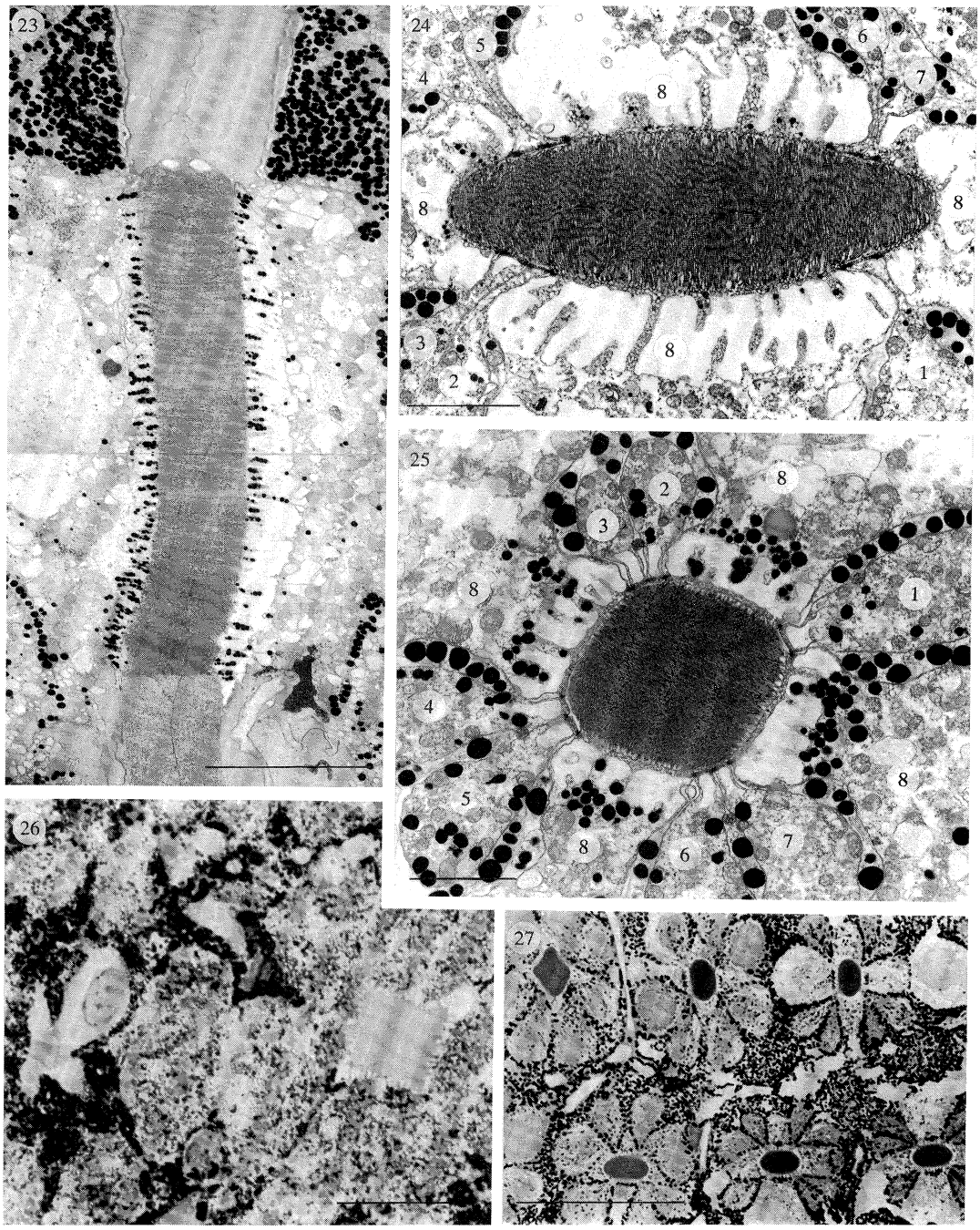

Figures 23–27. The R8 cells.

Figure 23. TEM longitudinal section of the R8 cell rhabdom of row three in *Gonodactylus chiragra*. At the top the crystalline cones, surrounded by screening pigment, join the rhabdom and at the bottom the rhabdom joins the F1 filter of this row. Scale 10 μm.

Figure 24. TEM transverse section of row six R8 rhabdom in *Pseudosquilla ciliata*. The small distal protrusions of cells 1–7 are labelled. Scale 5 μm.

Figure 25. TEM transverse section of the R8 cell of row four in *Coronis scolopendra*. The four lobes of the R8 cell and the small upward projections of R1–7 are labelled. Note the orthogonal arrangement of microvilli. Scale 5 μm.

Figure 26. Transverse LM section of R8 (left) and R1–7 (right) cells and rhabdom in the dorsal hemisphere of the left eye of *Oratosquilla solicitans*. Note the R8 cell nucleus in the upper right limb of the 'X' and the four cone cell projections visible at the R8 cell level. Scale 20 μm.

Figure 27. LM transverse section of rows five and six R8 cells in *Coronis scolopendra*. Scale 50 μm.

2. The six mid-band rows of ommatidia are morphologically different from those of the peripheral retina. In gonodactyloid species there is also an increase in size of all ommatidial components, while in the lysiosquilloids this is less obvious. The structure of the two-row mid-band ommatidia of the squilloids is the same as that of the peripheral retina in all respects.

3. Based on retinular cell placement, there are three forms of symmetry found in the retina: (i) a line of mirror symmetry between mid-band rows two and

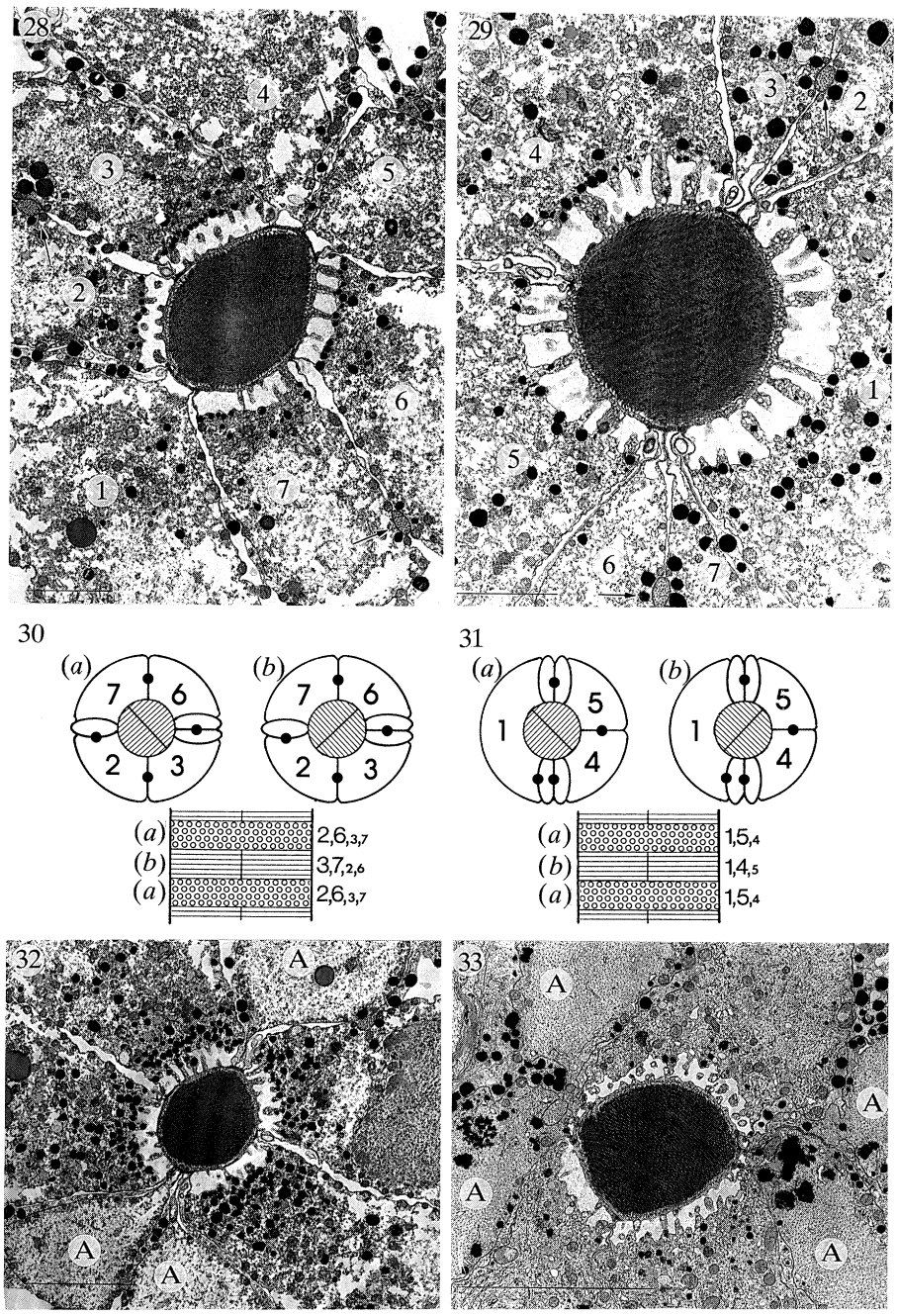

Figures 28–33. Cellular microvillar arrangement in rows one to four of the mid-band.

Figure 28. TEM transverse section of row two DR1–7 in *Coronis scolopendra*. Cells are numbered and three cone cell projections visible between cells 2 and 3, 4 and 5 and 6 and 7 are arrowed. Scale 5 μm.

Figure 29. TEM transverse section of row three DR1–7 in *Coronis scolopendra*. Cells are numbered and two of the cone cell projections visible between cells 2 and 3 and 6 and 7 are arrowed. Scale 5 μm.

Figure 30. Diagrammatic representation of a four-cell rhabdom found in the row two DR1–7 tier and rows one, three and four PR1–7 tiers (figure 16). The illustration is specifically of row one or two in a right eye (from the cone tail position, figure 1). The upper two diagrams (*a*) and (*b*) are transverse sections of layers (*a*) and (*b*) shown in the lower diagram which is a longitudinal section. The large and small numbers next to each layer are the cells responsible for the manufacture of microvilli; the large numbers are those cells which make most microvilli. Therefore in layer (*a*), for instance, cells 2 and 6 make most of the microvilli arrayed (↗) and cells 7 and 3 make a few microvilli arrayed (↗). In the next layer, (*b*), the roles are reversed to produce (↘) microvilli and cells 3 and 7 make most microvilli and cells 2 and 6 only a few.

Figure 31. Diagrammatic representation of a three-cell rhabdom found in the row two PR1–7 tier and rows one, three and four DR1–7 tiers (figure 31). Here cells 4 and 5 alternate in producing large or small amounts of microvilli for each of layers (*a*) and (*b*), and cell 1 contributes an equal amount to each layer.

Figure 32. TEM transverse section of a row three PR1–7 rhabdom in *Coronis scolopendra*. The three axons from the DR1–7 cells of this ommatidium, are labelled A. Scale 10 μm.

Figure 33. TEM transverse section of a row two PR1–7 rhabdom in *Lysiosquilla scabricauda*. The four axons of the DR1–7 cells are labelled A. Scale 10 μm.

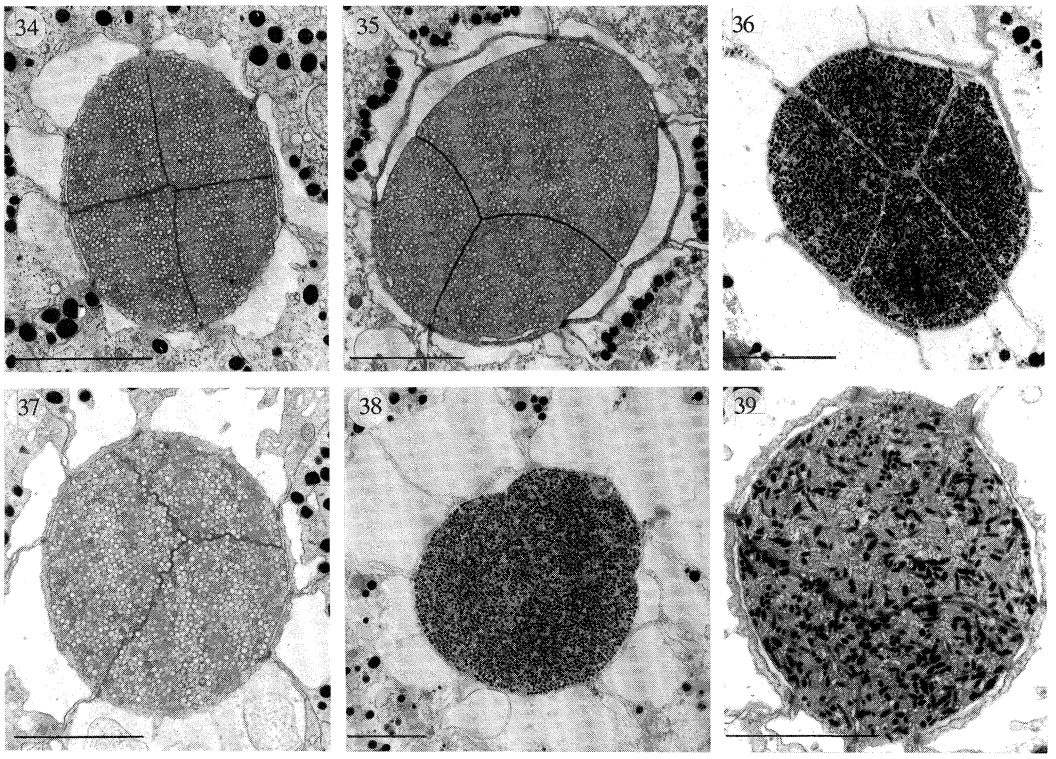

Figures 34–39. Distal and proximal filters (levels B–F1 and D–F2). Notable in these figures is the three or four part segmentation of filters depending on whether they are made by the four cell (DR1–7) tier in row two or the three cell (DR1–7) tier of row three. Differential staining of 'similar coloured' filters is also shown here. Filters in figures 36, 37 and 38 are all 'red'.

Figure 34. Row two F1 in *Gonodactylus oerstedii* (yellow, DR1–7). Scale 4 μm.

Figure 35. Row two F2 in *Coronis scolopendra* (yellow, DR1–7). Scale 4 μm.

Figure 36. Row two F2 in *Gonodactylus chiragra* (red, DR1–7). Scale 4 μm.

Figure 37. Row three F1 in *Coronis scolopendra* (red, DR1–7). Scale 4 μm.

Figure 38. Row three F2 in *Odontodactylus scyllarus* (red, DR1–7). Scale 4 μm.

Figure 39. Row three F2 in *Gonodactylus oerstedii* (purple, DR1–7). Scale 4 μm.

three involving the entire retina; (ii) rhabdoms of the dorsal and ventral hemispheres only are rotated 45° relative to one another, the exact nature of this being species specific and (iii) in all species, there is a similar 90° rotational relationship between rows five and six. All three transformations may be significant for polarization sensitivity and in this respect there are three main features to note.

Firstly, R8 cells of mid-band rows five and six possess unidirectional microvilli along unusual (spindle shaped in transverse section) lengths of rhabdom. The microvillar orientation in row five (↔), is orthogonal to that in row six (↕), suggesting some form of polarization sensitivity. Secondly, there are four microvillar directions between hemispheres. Here R1–7 microvilli are always (with the exception of *O. scyllarus*) arrayed (↔) & (↕) to (↘) & (↗) (dorsal hemisphere to ventral hemisphere) or (↘) & (↗) to (↔) & (↕) (dorsal hemisphere to ventral hemisphere). Thirdly, within a single row five or six ommatidium, three directions of microvilli exist, for row five for instance, R8 is (↔) and R1–7 are (↗) & (↘). Such arrays make the peripheral retina and rows five and six capable of complex polarization sense.

4. R1–7 cells in rows one to four of the mid-band have split into two tiers made up of three or four retinular cells DR1–7 and PR1–7. These two cell groups are equivalent to those that form the orthogonal sets of microvilli in the peripheral retina, rows five and six, and the rhabdoms of more orthodox malacostracans. Within these rows each cell supplies microvilli in two orthogonal directions. These directions, unlike the case in the periphery and rows five and six, are the same as those in the R8 cells. This may be an attempt to reduce polarization sensitivity.

5. In mid-band rows two and three, there exist photostable coloured filters, F1 and F2, positioned between R8 and DR1–7 and DR1–7 and PR1–7 respectively. These are made by the retinular cells and vary in colour depending on retinal position and species. In the Lysiosquilloidea F2s (in row three and row two) may not be present and in *C. scolopendra* row three are possibly replaced by a lateral filter.

6. Like the R1–7 cells in rows one to four, R8 cells in the remainder of the retina have orthogonal microvilli within a single cell. This structural adaptation may be an attempt to decrease sensitivity to polarized light.

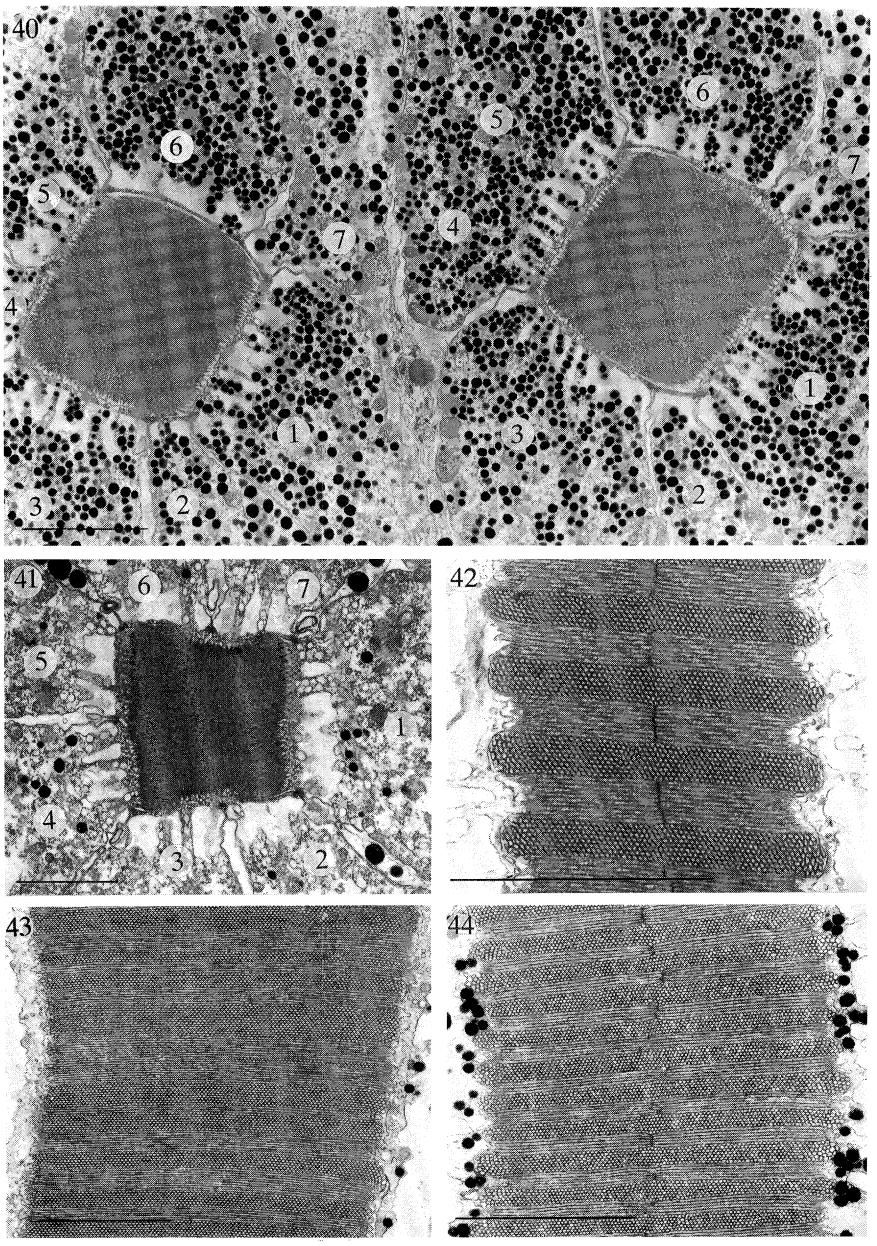

Figures 40–44. Cellular and microvillar arrangement in mid-band and periphery.
Figure 40. TEM transverse section of mid-band row six in *Pseudosquilla ciliata*, cells 1–7 are numbered. Scale 10 μm.
Figure 41. TEM transverse section of a rhabdom of the ventral hemisphere in *Coronis scolopendra*. Cells 1–7 are numbered. Scale 3 μm.
Figure 42. TEM of a dorsal hemisphere rhabdom in *Coronis scolopendra* cut in longitudinal section. Scale 3 μm.
Figure 43. TEM of row one PR1–7 *Gonodactylus chiragra* cut in longitudinal section. Scale 3 μm.
Figure 44. TEM of row six in *Gonodactylus chiragra* cut in longitudinal section. Scale 3 μm.

4. DISCUSSION

The stomatopod eye contains many unique visual adaptations, the majority of which are situated in the highly specialized mid-band ommatidia. In gonodactyloid stomatopods, the large size of mid-band facets, compared with those of the peripheral retina, is the first indication of the remarkable structures within this subsection of the eye. Most adaptations, however, concern modifications to the internal, rhabdomeric part of the ommatidium.

Dividing compound eyes up into functionally distinct regions is a relatively common strategy among the arthropods. Different regions may be obvious from external examination as they are in stomatopods (e.g. Euphausids, Land *et al.* 1979; Odonata, Sherk 1978; Amphipods, Land 1989*b*) or they may involve specializations under an apparently homogeneous array of facets (e.g. Diptera, Hardie 1986; Cladocera, Odselius & Nilsson 1983; Consi *et al.* 1989; Hymenoptera, Nilsson *et al.* 1987; and for a general review see Land (1989*a*)). The functions suggested for parts of eyes containing regional structural differences can be divided into four groups: heightened acuity, either by

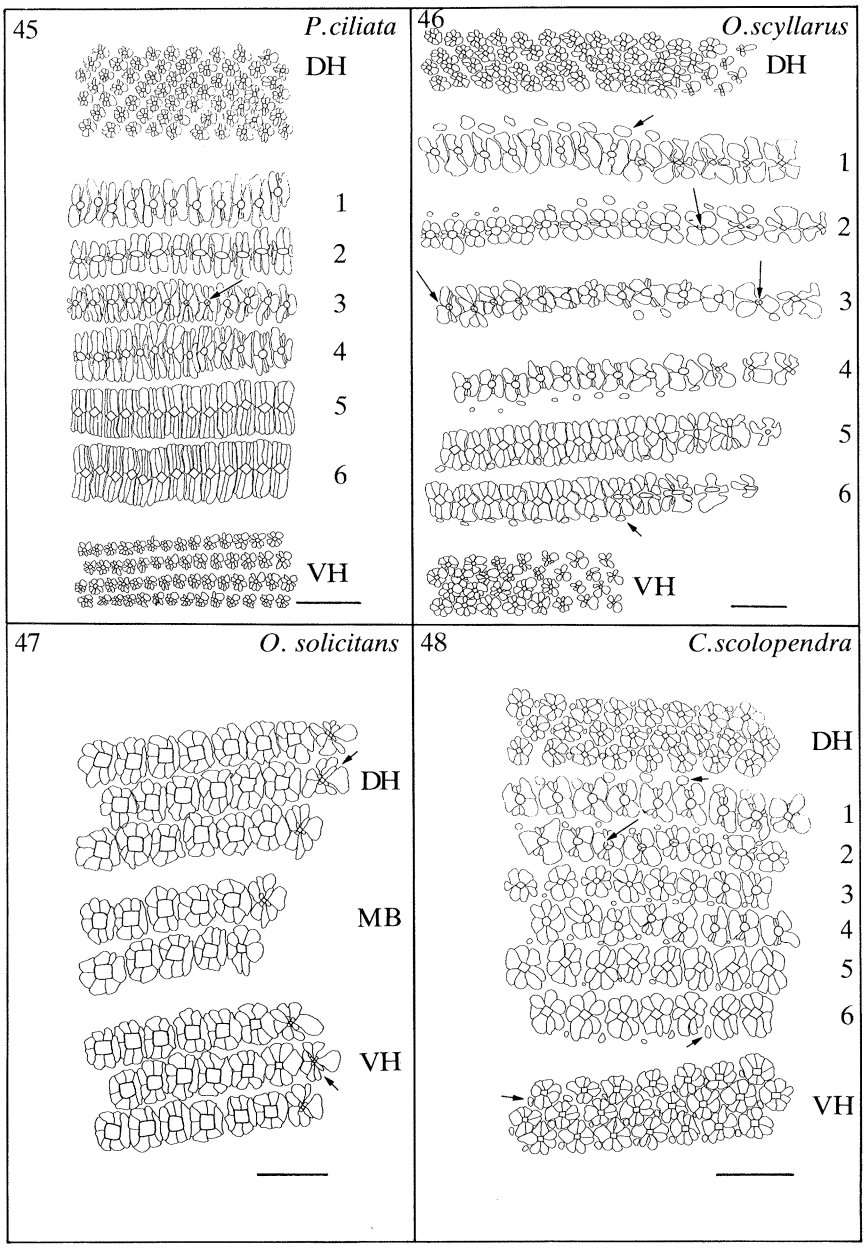

Figures 45–48. Tracings of transverse sections of the mid-band and peripheral retinae in four stomatopod species. DH, dorsal hemisphere; VH, ventral hemisphere; MB, mid-band.

Figure 45. Tracing of a transverse section of *Pseudosquilla ciliata* retina. The section is at the DR1–7–PR1–7 tier junction. A row three F2 is arrowed. Scale 100 μm.

Figure 46. Tracing of a transverse section of *Odontodactylus scyllarus* retina. The section is at the R8–DR1–7 tier junction but is so oblique that an F2 in row three is visible. This and other filters are indicated with large arrows. Small arrows indicate the position of R8 axons. Scale 100 μm.

Figure 47. Tracing of a transverse section of *Oratosquilla solcitans* retina. The section is at the R8–R1–7 tier junction and nucleated R8 lobes are arrowed. Scale 100 μm.

Figure 48. Tracing of a transverse section of *Coronis scolopendra* retina. The section is at the R8–DR1–7 tier junction. The large arrow indicates an F1 in row two and the small arrows R8 axons. Scale 100 μm.

an increase in sensitivity (van Hateren *et al.* 1989) or resolution (Zeil 1983); colour analysis (Hardie 1986; Meinertzhagen *et al.* 1983; Menzel 1981) and the analysis of polarized light (Waterman 1981; Rossel 1989).

From an examination of structure alone, it is possible to predict which areas of the tripartate stomatopod eye are involved in certain sensory modalities. Rows one to four of the mid-band, with their tiered arrangement and coloured filters arranged between tiers, potentially represent a very comprehensive analyser of coloured light in the environment (Marshall 1988; Hardie 1988; paper II). In support of this hypothesis is the finding that this eye region also contains over eight visual pigments (Cronin & Marshall 1989*a*, *b*). Mid-band rows five and six, also based purely on structural evidence, seem specifically designed for the analysis of polarized light (Marshall 1988). This is also true of the

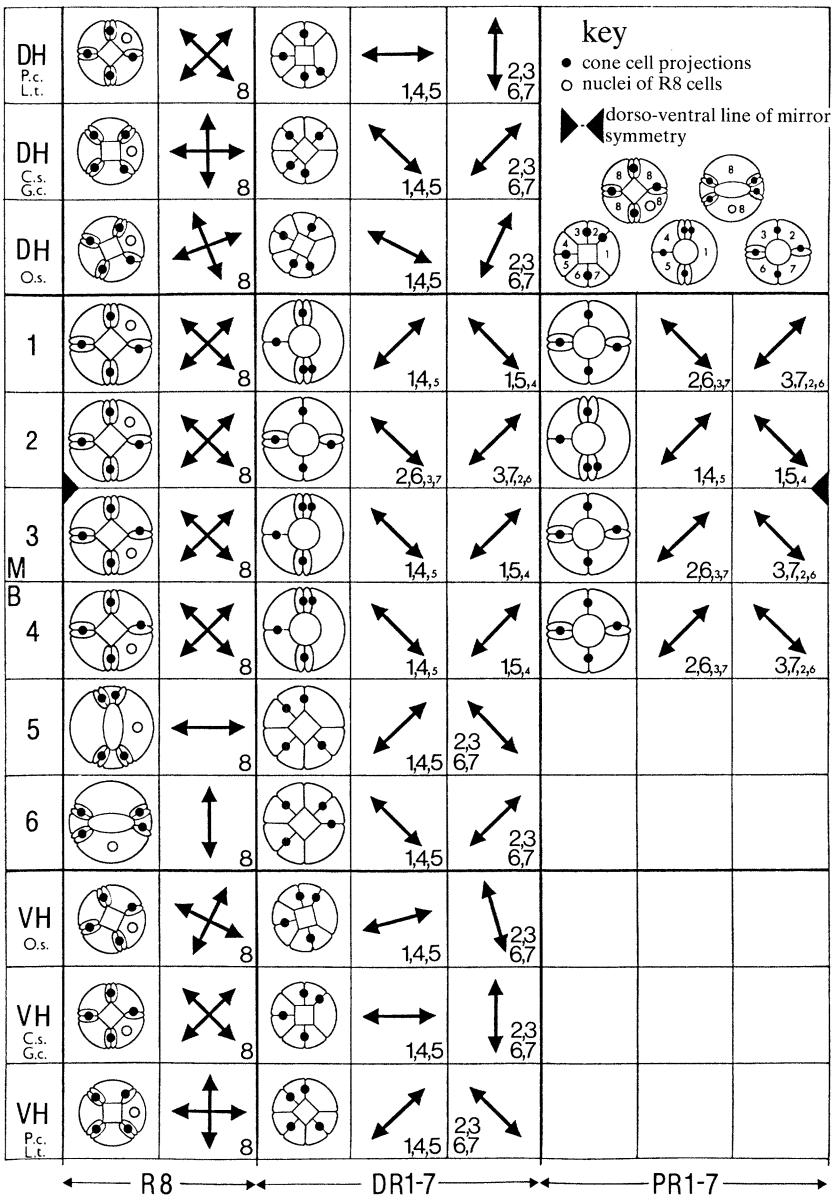

Figure 49. Summary of retinal symmetries and microvillar directions in the left eye of five stomatopod species for the fixed eye orientation explained in figure 1. The cell numbering system is explained in the key: cell 1 is always the large one and cell 2 is flanked by two cone cell projections. The three retinal tiers R8, DR1–7 and PR1–7, are delineated at the bottom of the figure. The arrows on the right of each diagrammatic representation of the retinular cells indicate the microvillar directions found within that retinal region and the cells involved. Small numbers indicate that only a few microvilli are supplied by that cell (figures 30 and 31). Crossed arrows indicate those regions where orthogonal microvilli are supplied by the R8 cell (with probable polarization blindness the result).

P.c., *Pseudosquilla ciliata*; G.c., *Gonodactylus chiragra*; L.t., *Lysiosquilla tredecimdentata*; C.s., *Coronis scolopendra*; O.s., *Odontodactylus scyllarus*; DH, dorsal hemisphere; VH, ventral hemisphere; MB, mid-band.

two peripheral portions of retina where there are no notable modifications to the rhabdoms, it is by differential arranging the ommatidial units relative to the incoming light, that PS is achieved.

Other crustacean eyes also contain modified rhabdoms, at least some of which seem concerned with the analysis of polarized light. The crayfish *Procambarus* and *Astacus*, the water flea *Polyphemus* and the porcellanid crab *Petrolisthes* all possess rhabdoms, or portions of rhabdoms, which resemble stomatopod row five and six R8s (Waterman 1977; Krebs & Lietz 1982; Odselius & Nilsson 1983; Eguchi *et al.* 1982). The rhabdoms are spindle-shaped (or in the case of *Polyphemus*, round-shaped) in transverse section and, more significantly, all possess unidirectional microvilli. In all but *Petrolisthes*, where all the R1–7 cells form this rhabdomal region these modifications are apparently aimed at enhancing the analysis of polarized light (Waterman 1981; Odselius & Nilsson 1983). This is discussed further in §4*b*.

There is good neuroanatomical evidence that crayfish direct information from each orthogonal retinular cell population into two separate laminar layers, suggesting the existence of a dual-input system (Nässel 1976; Sabra & Glantz 1985). As with the squilloid *Oratosquilla oratoria* (Yamaguchi *et al.* 1976), retinular

cells and optic nerve fibres from many crustaceans have been shown by intracellular recording, to have PS (Leggett 1976; Waterman 1977). There have been a limited number of behavioural studies attempted on crustaceans (see, for example, Jander & Waterman (1960); Daumer *et al.* (1963); Waterman (1988)), but the results have rarely been clear-cut.

The PS capabilities that we speculate for each of the various regions of stomatopod retina, are considered in the next two sections. The first of these looks at retinal areas that are adapted to be blind to polarized light, and the second section discusses retinal areas that seem specifically adapted for PS.

(*a*) *Structural adaptations for destroying* PS

Two groups of receptors, the R8 cells throughout the retina and R1–7 in mid-band rows one to four, seem organized so as to be polarization-blind. With the exception of rows five and six, all R8 cell rhabdoms possess orthogonally arranged microvilli (figure 49). By having bi-directional microvilli provided by a single cell, the polarization sensitivities of the two sets of microvilli cancel out, making these cells equally sensitive to any direction of polarized light. Similar R8 microvillar patterns are found in other malacostracans (Waterman 1981) and in some insects (Meyer-Rochow 1971, 1974; Maida 1977; Gordon 1977; Kolb 1977) and here they are also presumed to allow insensitivity to polarized light. The same effect could be gained by having a random arrangement of microvilli, an adaptation found in the R8 cells of *Ocypode* for example (Kunze & Boschek 1968) and also, to some extent, in insects with layered orthogonal rhabdoms (Meyer-Rochow 1974).

The other polarization-insensitive retinal region occurs in R1–7 of mid-band rows one to four. The main rhabdoms of ommatidia from these four rows are divided into two tiers, DR1–7 and PR1–7, made from three or four retinular cells. Each tier is constructed from cells that, in typical crustacean retinae, would lay down microvilli in a single direction, for example, three cells (1, 4 and 5) horizontally and four cells (2, 3, 6 and 7) vertically (see Hallberg 1977). One might, therefore, expect microvilli in each of the tiers in these four rows to be aligned in a single direction. Both DR1–7 and PR1–7 tiers, however, possess orthogonally arranged microvilli (figures 28–33). On close examination (figures 30 and 31) it can be seen that each cell in these rows contain orthogonal microvilli, rather like the situation in R8 cells. This 'secondary' orthogonality thus seems to be concerned with making sure that these cells cannot analyse polarized light.

Layers of microvilli in row one-to-four rhabdomeres are often irregular in depth (figure 43 and table 2). Stowe (1983) has argued that keeping the orthogonal microvillar layers equal in thickness in a rhabdom is possibly important for maximizing PS. The lack of such order in these mid-band rows suggests that polarized light is not important here.

In both retinal sub-sets described, R8 and DR1–7 and PR1–7 bi-directional microvilli produced by one cell is the mechanism for attaining polarization insensitivity. This insensitivity may be desirable to avoid confusion between different visual parameters: rows one to four, for instance, are probably concerned with colour vision (paper II). Similar functional divisions in other compound eyes also involve polarization insensitivity in favour of, colour sensitivity for example. Mechanisms to achieve this include neural or optical coupling (Snyder 1973; Zufall *et al.* 1989) and rhabdomeric twist or jitter (Nilsson *et al.* 1987; Wehner *et al.* 1975).

(*b*) *Structural adaptations for enhancing* PS

Two regions of the stomatopod eye, the hemispheres and mid-band rows five and six, contain rhabdomal structures that suggest that they are capable of analysing polarized light. Both these retinal areas can be further divided into two subsets of ommatidia, between which a rotational relationship exists. The dividing lines are between row five and row six, and between dorsal and ventral hemisphere. In both the hemispheres and rows five and six, a comparison of the signal arising from retinular cells on either side of their respective lines of symmetry could allow a very comprehensive interpretation of incoming polarized light. This is now discussed with reference to these two retinal regions.

The ommatidia of the two hemispheric retinae are mirror images of each other. This symmetry has its line of reflection between rows two and three of the mid-band and, indeed, includes the mid-band rows. A dorso-ventral mirror symmetry in dipteran compound eyes was noted early in this century by Dietrich (1909). This bisects the eye approximately along its mid-line (Franchescini 1975) and can be seen in the overall retinular cell arrangement as it is set up during development (Tomlinson 1988). Other arthropod compound eyes also show such mirror symmetry and it is possible that all compound eyes realize their final form via similar developmental pathways (Hallberg 1977; Nässel 1976). In *Drosophila* the final arrangement of the ommatidia in top and bottom 'halves' of the eye involves 90° rotation in opposing directions for each hemisphere during development (Ready *et al.* 1975). There are also, however, some structural differences delineating top and bottom hemispheres before this transformation occurs (Tomlinson & Ready 1987).

For many crustaceans examined to date, whichever way this symmetry comes about, the resultant microvillar directions in dorsal and ventral halves of the eye are in two directions only, (↔) and (↕). As a result it is unlikely that anything more than a two input or 'two dimensional' PS system could operate here (Bernard & Wehner 1977). A good example of just such a microvillar arrangement is seen in *O. solicitans*, figures 26 and 47, the line of symmetry being between the two mid-band rows. For both hemispheres and the mid-band, cells 1, 4 and 5 produce (↔) microvilli and cells 2, 4, 6 and 7 (↕), the two inputs here, therefore, would come from the two populations of cells, 1, 4 and 5 and 2, 3, 6 and 7.

In most species examined here, one hemisphere is rotated 45° relative to the other, as summarized in

figure 49. This means that the R1–7 cell microvilli are arrayed in four different directions; (↔) and (↕) in one hemisphere and (↗) and (↖) in the other. If this is significant for PS some knowledge of the neural interconnections of these cells is required, in particular the projection of retinular cell axons onto the lamina ganglionaris, the first integrative neuropile in the eye stalk.

The neural structures subserving the retina, in stomatopods, are not well known. In *Squilla mantis* the lamina, like the retina, is divided into two discrete areas, and within each, unusually for malacostracans, three layers are observable (Bullock & Horridge 1965; Strausfeld & Nässel 1981; Schiff *et al.* 1986*b*). The lamina of species with a six-row mid-band is divided into three areas, one under each hemisphere and one for the mid-band rows (unpublished observation). For the crayfish *Procambarus clarkii* the lamina is arranged such that the axons for the three cells with horizontal microvilli (↔) and the four cells with vertical microvilli (↕), terminate in two discrete laminar layers. Thus separate information channels may exist for horizontally and vertically polarized light (Nässel & Waterman 1977; Sabra & Glanz 1985).

Stomatopod retinae sampling four directions of polarized light could construct four information channels for polarized light, oriented (↕) and (↔) in one lamina and (↗) and (↖) in the other. It is important to remember here, that many of the ommatidia of top and bottom hemispheres which provide input to these four hypothesized channels, view the same points in space (Marshall 1988). In such a system an object could be comprehensively examined for any patterns of polarized light reflected or scattered from it by a static eye. In life the eyes rotate freely over 70° or more. If receptors could also sample the environment in a temporal fashion, the PS capabilities of the eye becomes more complex still (Kirschfeld 1973).

Given the potentially elaborate PS system of the peripheral retina it is surprising that rows five and six of the mid-band also seem specifically adapted to be sensitive to polarized light. Here a novel rotational symmetry exists such that the retinular cells of row five are rotated 90° relative to those of row six. No mirror symmetry exists between these two rows as they both lie in the ventral side of the overall retinal mirror symmetry which divides rows two and three of the mid-band. The row five and six retinular cell arrangement is the same in all species examined.

These two rows could represent a pair of three-channel analyser systems (Marshall 1988). Like the R8 microvilli of the peripheral retina, those in rows five and six are at 45° to the underlying R1–7 microvilli. However unlike the periphery, R8 microvilli of row five and six are laid down in one orientation only (figures 24 and 49) and thus could provide the third input to a three channel system.

Two pieces of evidence suggest that such a three channel system may not be in operation here. Firstly, where their structure is known, crustacean R8 cell axons pass through the lamina ganglionaris and terminate in the medulla externa (Waterman 1981). For *Squilla mantis* Strausfeld & Nässel (1981) describe a single neural fibre arising from each ommatidium, which passes through the lamina and terminates in the medulla. This is possibly the axon of R8. For a three dimensional PS system, all three receptor axons might be expected to terminate or make connections in the same neural region.

Secondly the visual pigment in row five and six R8 cells is probably unlike that of R1–7. The R1–7 cells in rows five and six, in stomatopod species examined to date, possess visual pigments with peak absorbance values at around 500 nm but no visual pigment has yet been identified in R8 (Cronin & Marshall 1989*b*). The receptors of a three dimensional system should be sensitive to the same wavelength of light so as to prevent ambiguity between colour and polarization information.

The shape and orientation of the row five and six R8 rhabdomeres is indicative of some form of PS system. In transverse section they are elliptical (figures 24 and 27). The microvillar axes all run perpendicular to the ellipse long axis (figure 49), suggesting that high PS may be gained from a rhabdom designed to provide many microvilli arrayed in one direction. Row six ellipses have their long axes parallel to the line of the mid-band, while those of row five are perpendicular to it (figure 27). Thus the R8 microvilli are orthogonal to each other in these two rows (figure 49). It is therefore possible that these R8 cells represent components of a two-channel PS system which would operate at short wavelengths. At longer wavelengths PS would be analysed in the same ommatidia by the R1–7 cells.

Several other features exist in rows five and six which suggest they are concerned with analysis of polarized light.

1. The orthogonal microvillar layers of R1–7 are very thin and regular. In all species, rows five and six layers were found to be around four microvilli deep compared with seven deep in the peripheral regions or five to twenty deep in rows one through four (figures 42–44 and table 2). Thin orthogonal layers minimize self screening in the rhabdomere and therefore increase PS (Snyder 1973; Stowe 1983).

2. R8 rhabdoms are in optical series with R1–7 and may therefore, act as filters, changing the quality of light transmitted to more proximal layers. Presuming maximum PS is parallel to the microvilli of each layer the PS of the proximal retina, with horizontal microvilli (↔), can be enhanced by overlaying it with microvilli orthogonal to it (↕). This filtering effect will be greater the longer the R8s are. R8s in these two rows are unusually long, contributing around 25% of the rhabdom, and this may be to maximize the PS enhancement on more proximal regions (Snyder 1973).

Trujillo-Cenoz & Bernard (1972) suggest a similar function for the rhabdomal arrangement in *Sympyncus lineatus*; and Snyder (1973) has quantified this effect using the tiered R7–R8 rhabdomere in flies as a model. The unusually long nature of these R8 rhabdoms does mean that their own PS may be degraded due to self screening (Snyder 1973). However the unusual length of row five and six R8s may be explained by the fact that they are presumed sensitive to the region of the spectrum below 400 nm (Cronin & Marshall 1989*b*).

Light of these wavelengths is in relatively short supply (Jerlov 1976) and the R8 photoreceptors may need to be long to increase their sensitivity (see Schlecht (1979) for a discussion of matching photoreceptor length to the task required).

3. Because of the 90° rotation of these two rows relative to each other, for the left eye, the microvilli of cells 1, 4 and 5 in row five are oriented (↗) and those of cells 1, 4 and 5 are oriented (↖) in row six. Cells 2, 3, 6 and 7 possess microvilli oriented (↖) in row five and (↗) in row six. Interpretation of these observations with regards to the putative two-channel PS system requires knowledge of the retinal wiring before further speculation is profitable.

4. A fascinating possibility arising from the arrangement of the row five and six rhabdomeres (suggested to us by Professor H. B. Barlow) is that these two rows may be sensitive to elliptically polarized light, or, more exactly, circularly polarized light, a special case of elliptical polarization. This would involve the R8 cells of these two rows acting as quarter-wavelength retarders so as to convert a circularly polarized light beam into two orthogonally oriented linear ones. These are then analysed by the R1–7 cells underneath which are ideally arranged for this purpose. Neville & Luke (1971) have shown that certain areas of crustacean cuticle reflect elliptically polarized light although those mentioned are not in a position to be easily detected. Waterman (1975) also suggests looking for retarders in eyes potentially sensitive to *E*-vectors.

5. In all species, R1–7 microvilli in rows five and six are particularly regular in the way they are situated in the rhabdom. In transverse section these rows always appear as strikingly neat squares and this almost crystalline arrangement is indicative of an attempt to maximize PS (Snyder 1973). The same is also true of all *O. solicitans* rhabdoms and the rhabdoms of the hemispheres in Lysiosquilloid species. Correlated with this rhabdomeric neatness is a yellow palisade layer (in cryosection), apparently a yellow 'oil' or some substance in solution in the clear liquid which fills the palisade.

It is possible that in such a position, this yellow sheath around the rhabdom could act as a lateral filter, in this case removing the highly scattered, short wavelengths, which could corrupt the quality of the PS information gathered by the rhabdom. In other words this yellow filter is acting as a haze filter and as such may be more to do with sharpening visual acuity rather than specifically helping with PS (Lythgoe 1979). However, the association of this filter with potential PS retinal regions is striking. This is discussed further in §4*d* of paper II.

(*c*) *Conclusion*

It is worth stating again that, as many authors have pointed out, possessing an eye structurally capable of PS, does not necessarily imply that analysis of polarized light as a sensory quality is achieved (Bernard & Wehner 1977). Even showing polarotactic behaviour in an animal does not allow the term 'polarization vision' (PV) to be used. Such behaviour may be present due to the perception of light in different polarization states as different brightnesses. Thus PS is distinct from PV (Kirschfeld 1973) and true PV has not yet been shown for any crustacean (Wehner 1983).

Stomatopod eyes have the capacity for three or four dimensional, static PS. Combined with the eyes rotational ability, the potential exists for an exhaustive analysis of polarized light (Kirschfeld 1973; Land *et al.* 1990; Bernard & Wehner 1977). However we are still ignorant of retinular cell sensitivities and the behaviours they drive. It is possible that rather than seeking a broad polarization sense, the various subsections of this eye are designed for very specific tasks.

Some stomatopods are reported to be able to return directly to their burrows from several meters away (R. L. Caldwell, personal communication). It is unknown, however, whether this ability utilizes environmental polarization cues.

As many stomatopods live in sight of the surface, the air–water interface may also provide them with important information, part of which could involve polarized light. Any reflected light would obviously be from the under-surface of the water and would necessarily lie outside Snell's window (Ivanoff & Waterman 1958*a*). It may also be significant that, at around the angle of total internal reflection, underwater, elliptically polarized light is at a maximum (Ivanoff & Waterman 1958*b*).

Contrast enhancement is another possible function of PS. The visibility of objects may be enhanced either when objects are viewed against a background containing scattered or polarized light (Lythgoe 1979; Odselius & Nilsson 1983) or, to break down the reflected silvery camouflage of, for example, fish (Lythgoe 1979). Fish are an important constituent of the diet of some stomatopods.

We are especially grateful to Simon Laughlin, Roger Hardie and Tom Collett for help and advice at various stages in the preparation of this work. Research was supported in the U.K. by the S.E.R.C grant no. GR/E 42532 and in the U.S.A. by the N.S.F. grant nos. BNS – 8518769 and BNS – 8917183.

REFERENCES

Bernard, G. D. & Wehner, R. 1977 Functional similarities between polarisation vision and colour vision. *Vis. Res.* **17**, 1019–1028.

Bullock, T. H. & Horridge, G. A. 1965 *Structure and function in the nervous system of invertebrates*, vol. II. San Francisco: W. H. Freedman.

Caldwell, R. L. & Single, H. 1976 Stomatopods. *Scient. Am.* **234** (1), 80–89.

Consi, T. R., Passani, M. B. & Macagno, E. R. 1990 Eye movements in *Daphnia magna*. Regions of the eye are specialised for different behaviours. *J. comp. Physiol.* **166**, 411–420.

Cronin, T. W. & Marshall, N. J. 1989*a* A retina with at least ten spectral types of photoreceptors in a mantis shrimp. *Nature, Lond.* **339**, 137–140.

Cronin, T. W. & Marshall, N. J. 1989*b* Multiple spectral classes of photoreceptors in the retinas of gonodactyloid stomatopod crustaceans. *J. comp. Physiol.* **166**, 261–275.

Cronin, T. W., Nair, N. J., Doyle, R. D. & Caldwell, R. L. 1988 Ocular tracking of rapidly moving visual targets by stomatopod crustaceans. *J. exp. Biol.* **138**, 155–179.

Daumer, K., Jander, R. & Waterman, T. H. 1963 Orientation of the ghost-crab *Ocipode* in polarised light. *Z. vergl. Physiol.* **47**, 56–76.

Dietrich, W. 1909 Die facettenaugen der dipteren. *Z. wiss. Zool.* **92**, 465–593.

Eguchi, E. & Waterman, T. H. 1966 Fine structure patterns in crustacean rhabdoms. In *The functional organisation of the compound eye* (ed. C. G. Bernard), pp. 105–124. Oxford: Pergamon Press.

Eguchi, E. & Waterman, T. H. 1968 Cellular basis for polarised light perception in the spider crab *Libina*. *Z. Zellforsch. microsk. Anat.* **84**, 87–101.

Eguchi, E., Goto, T. & Waterman, T. 1982 Unorthodox pattern of microvilli and intercellular junctions in regular retinular cells of the porcellanid crab *Petrolisthes*. *Cell Tiss. Res.* **222**, 493–513.

Exner, S. 1891 *Die physiologie der facettirten augen von krebsen und insecten*. Liepsig, Wein: Deuticke.

Franceschini, N. 1975 Sampling of the visual environment by the compound eye of the fly: fundamentals and applications. In *Photoreceptor optics* (ed. A. W. Snyder & R. Menzel), pp. 98–125. New York, Heidelberg, Berlin: Springer-Verlag.

Gordon, W. C. 1977 Microvillar orientation in the retina of the Nymphalid butterly. *Z. Naturf.* **32c**, 662–664.

Hateren, J. H. van, Hardie, R. C., Rudolph, A., Laughlin, S. B. & Stavenga, D. G. 1989 The bright zone, a specialised dorsal eye region in the male blowfly. *Chrysomyia megacephala*. *J. comp. Physiol.* A **164**, 297–308.

Hallberg, E. 1977 The fine structure of the compound eyes of mysids (Crustacea: Mysidacea). *Cell Tiss. Res.* **184**, 45–65.

Hallberg, E. & Elofsson, R. 1989 Construction of the pigment shiel of the crustacean compound eye: a review. *J. Crust. Biol.* **9** (3), 359–372.

Hardie, R. C. 1986 The photoreceptor array of the dipteran retina. *T.I.N.S.* **9** (9), 419–423.

Hardie, R. C. 1988 The eye of the mantid shrimp. *Nature, Lond.* **333**, 499–500.

Horridge, G. A. 1978 The separation of visual axes in apposition compound eyes. *Phil. Trans. R. Soc. Lond.* B **285**, 1–59.

Horridge, G. A. 1977 Insects which turn and look. *Endeavour* (new series), **1** (1), 7–17.

Ivanoff, A. & Waterman, T. H. 1958*a* Factors, mainly depth and wavelength, affecting the degree of underwater light polarisation. *J. Mar. Res.* **16**, 283–307.

Ivanoff, A. & Waterman, T. H. 1958*b* Elliptical polarisation of submarine illumination. *J. Mar. Res.* **16**, 225–282.

Jander, R. & Waterman, T. H. 1960 Sensory discrimination between polarised light and light intensity patterns by arthropods. *J. cell. comp. Physiol.* **56**, 136–160.

Jerlov, N. G. 1976 *Marine optics*. Amsterdam, London, New York: Elsevier.

Kirschfeld, K. 1973 Vision of polarised light. In *Symposium proceedings of the 4th international biophysical congress, Moskow.* **4**, pp. 289–296. (Ed. by Int. Union for Pure and Applied Biophysics, Acad. Sci. USSR.)

Kolb, G. 1977 The structure of the eye of *Pieris brassicae* L. (Lepidoptera). *Zoomorphologie* **87**, 123–146.

Krebs, W. & Leitz, R. 1982 Apical region of the crayfish retinula. *Cell Tiss. Res.* **222**, 409–415.

Kunze, P. & Boschek, C. B. 1968 Elektronenmikroskopische underschung zur form der achten retinulazelle bei *Ocypode*. *Z. Naturf.* **23b**, 568–569.

Land, M. F. 1989*a* Variations in the structure and design of compound eyes. In *Facets of vision* (ed. D. G. Stavenga & R. C. Hardie), pp. 90–111. Heidelberg, Berlin: Springer-Verlag.

Land, M. F. 1989*b* The eyes of hyperiid amphipods: relations of optical structure to depth. *J. comp. Physiol.* A **164**, 751–762.

Land, M. F., Burton, F. A. & Meyer-Rochow, V. B. 1979 The optical geometry of euphausid eyes. *J. comp. Physiol.* A **130**, 49–62.

Land, M. F., Cronin, T. W. & Marshall, N. J. 1990 The eye-movements of the mantis shrimp *Odontodactylus scyllarus* (Crustacea: Stomatopoda). *J. comp. Physiol.* A **167**, 155–166.

Leggett, L. M. W. 1976 Polarised light-sensitive interneurons in a swimming crab. *Nature, Lond.* **262**, 709–711.

Lythgoe, J. N. 1979 *The ecology of vision*. Oxford: Clarendon Press.

Miada, T. M. 1977 Microvillar orientation in the retina of a Pierid butterly. *Z. Naturf.* **32c**, 660–661.

Manning, R. B., Schiff, H. & Abbott, B. C. 1984 Cornea shape and surface structure in some stomatopod crustacea. *J. Crust. Biol.* **4** (3), 502–513.

Marshall, N. J. 1988 A unique colour and polarization vision system in mantis shrimps. *Nature, Lond.* **333**, 557–560.

Marshall, N. J., Land, M. F., King. C. A. & Cronin, T. W. 1991 The compound eyes of mantis shrimps (Crustacea, Hoplocarida, Stomatopoda). II. Colour pigments in the eyes of stomatopod crustaceans: polychromatic vision by serial and lateral filtering. *Phil. Trans. R. Soc. Lond.* B **334**, 57–84. (Following paper.)

Meinertzhagen, I. A., Menzel, R. & Kahle, G. 1983 The identification of spectral receptor types in the retina and lamina of the dragonfly *Sympetrum rubicundulum*. *J. comp. Physiol.* A **151**, 295–310.

Menzel, R. 1981 Spectral sensitivity and colour vision in invertebrates. In *Handbook of sensory physiology*, vol. VII/6A (ed. H. Autrum), pp. 503–580. Berlin, Heidelberg, New York: Springer.

Meyer-Rochow, V. B. 1974 Fine structural changes in dark-light adaptation in relation to unit studies of an insect compound eye with a crustacean-like rhabdom. *J. Insect Physiol.* **20**, 537–589.

Meyer-Rochow, V. B. 1971 A crustacean-like organisation of insect-rhabdoms. *Cytobiologie* **4**, 241–249.

Nässel, D. R. 1976 The retina and retinal projection on the lamina gangloinaris of the crayfish *Pacifastacus leniusculus* (Dana). *J. comp. Physiol.* **167**, 341–360.

Nässel, D. R. & Waterman, T. H. 1977 Golgi EM evidence for visual information channelling in the crayfish lanina gangloinaris. *Brain Res.* **130**, 556–563.

Neville, A. C. & Luke, B. M. 1971 Form optical activity in crustacean cuticle. *J. Insect. Physiol.* **17**, 519–526.

Nilsson, D.-E., Labhart, T. & Meyer, E. 1987 Photoreceptor design and optical properties affecting polarization sensitivity in ants and crickets. *J. comp. Physiol.* A **161**, 645–658.

Odselius, R. & Nilsson, D.-E. 1983 Regionally different ommatidial structure in the compound eye of the waterflea *Polyphemus* (Cladocera, Crustacea). *Proc. R. Soc. Lond.* B **217**, 177–189.

Ready, D. F., Hanson, T. E. & Benzer, S. 1976 Development of the *Drosophila* retina, a neurocrystalline lattice. *Devl Biol.* **53**, 217–240.

Rossel, S. 1989 Polarisation sensitivity in compound eyes. In *Facets of vision* (ed. R. C. Hardie & D. G. Stavenga), pp. 298–316. Heidelberg, Berlin: Springer-Verlag.

Sabra, R. & Glanz, R. M. 1985 Polarization sensitivity of

crayfish photoreceptors is correlated with their termination sites in the lamina ganglionaris. *J. comp. Physiol.* A **156**, 315–318.

Schiff, H., Abbott, B. C. & Manning, R. B. 1986*a* Optics, rangefinding and neuroanatomy of the eye of a mantis shrimp *Squilla mantis* (Linnaeus) (Crustacea: Stomatopoda Squillidae). *Smithson. Contr. Zool.* **440**, pp. 1–32.

Schiff, H., Manning, R. B. & Abbott, B. C. 1986*b* Structure and optics of ommatidia from eyes of stomatopod crustaceans from different luminous habitats. *Biol. Bull.* **170**, 461–480.

Schiff, H. & Abbott, B. C. 1989 Stomatopod Vision. In *Biology of stomatopods*. Selected symposia and monographs U. Z. I. (ed. E. A. Ferrero), pp. 11–38. Moderna: Mucchi.

Schiff, H. 1963 Dim light vision in *Squilla mantis* (L.). *Am. J. Physiol.* **205** (5), 927–940.

Schlecht, P. 1979 Colour discrimination in dim light: an analysis of photoreceptor function in the moth *Dielephila* **129**, 257–267.

Schönenberger, N. 1977 The fine structure of the compound eye of *Squilla mantis* (Crustacea, Stomatopoda). *Cell Tiss. Res.* **176**, 205–233.

Sherk, T. E. 1978 Development of the compound eyes of dragonflies (Odonata). III. Adult compound eyes. *J. exp. Zool.* **203**, 61–80.

Snyder, A. W. 1973 Polarisation sensitivity of individual retinular cell. *J. comp. Physiol.* **83**, 331–360.

Stowe, S. 1977 The retina-lamina projection in the crab *Leptograpsus varigatus*. *Cell Tiss. Res.* **185**, 515–525.

Stowe, S. 1983 A theoretical explanation of intensity-independent variation of polarisation sensitivity in crustacean retinular cells. *J. comp. Physiol.* **153**, 435–441.

Strausfeld, N. J. & Nässel, D. R. 1981 Neuroarchitecture of brain regions that subserve the compound eyes of crustaceans and insects. In *Handbook of sensory physiology*, vol. VII/6A (ed. H. Autrum), pp. 1–132. Berlin, Heidelberg, New York: Springer-Verlag.

Tomlinson, A. 1988 Cellular interactions in the developing *Drosophila* eye. *Development* **104**, 183–193.

Tomlinson, A. & Ready, D. F. 1987 Neuronal differentiation in the *Drosophila* ommatidium. *Devl Biol.* **120**, 366–376.

Trujillo-Cenoz, O. & Bernard, G. D. 1972 Some aspects of the retinal organisation of *Sympyncus lineatus* (Diptera, Dolichopodidae). *J. Ultrastruct. Res.* **38**, 149–160.

Waterman, T. H. 1981 Polarization sensitivity. In *Handbook of sensory physiology*, vol. VII/6C (ed. H. Autrum), pp. 281–469. Berlin, Heidelberg, New York: Springer-Verlag.

Waterman, T. H. 1977 The bridge between visual input and central programming in crustaceans. In *Identified neurons and behaviour in arthropods* (ed. G. Hoyle), pp. 371–386.

Waterman, T. H. 1988 Polarization of marine light fields and animal orientation. *S.P.I.E.* **925**, 431–437.

Waterman, T. H. 1975 The optics of polarization sensitivity. In *Photoreceptor optics* (ed. A. W. Snyder & R. Menzel), pp. 339–371. Berlin, Heidelberg, New York: Springer.

Wehner, R., Bernard, G. D. & Geiger, E. 1975 Twisted and non-twisted rhabdoms and their significance for polarisation detection in the bee. *J. comp. Physiol.* **104**, 225–245.

Yamaguchi, T., Katagiri, Y. & Ochi, K. 1976 Polarized light responses from retinular cells and sustaining fibers of the mantis shrimp. *Biol. J. Okayama Univ.* **17**, 61–66.

Zeil, H. 1983 Sexual dimorphism in the visual system of flies: the compound eyes and neural superposition in Bibionidae (Diptera). *J. comp. Physiol.* A **150**, 379–393.

Zufall, F., Schmitt, M. & Menzel, R. 1989 Spectral and polarized light sensitivity of photoreceptors in the compound eye of the cricket (*Gryllus bimaculatus*). *J. comp. Physiol.* **164**, 597–608.

KEY TO ABBREVIATIONS

AZ	acute-zone
BM	basement-membrane
MB	mid-band
DP	distal pigment
RP	retinular pigment
PP	proximal pigment
LRP	light-coloured reflecting pigment
GRP	green reflecting pigment
F1	distal filter
F2	proximal filter
R1–7	retinular cells 1–7
DR1–7	distal retinular cells
PR1–7	proximal retinular cells
D	facet diameter of each ommatidium
f	focal length of each ommatidium
a	aperture of each ommatidium
l	length of rhabdom or tier
d	diameter of rhabdom; maximum for each tier
Mv	microvilli
$\Delta\rho$	acceptance angle $= a/f \times 57.3$
$1/2\ A$	the wavelength at which the filters absorbance drops to 1/2 the peak value

Gonodactyloidea

G.o.	*Gonodactylus oerstedii*
G.c.	*Gonodactylus chiragra*
G.b.	*Gonodactylus bredini*
G.v.	*Gonodactylus viridis*
G.g.	*Gonodactylus glabrous*
P.c.	*Pseudosquilla ciliata*
O.s.	*Odontodactylus scyllarus*
M.sp.	*Mesacturus* sp.
H.g.	*Haptosquilla glyptocercus*
H.s.	*Haptosquilla stoliurus*
H.t.	*Haptosquilla trispinosa*
C.t.	*Chorysquilla trigibbosa*

Lysiosquilloidea

C.s.	*Coronis scolopendra*
L.sc.	*Lysiosquilla scabricauda*
K.su.	*Lysiosquilla sulcata*
L.t.	*Lysiosquilla tredecimdentata*
L.m.	*Lysiosquilla maculata*

Squilloidea

Ch.sp.	*Chloridopsis* sp.
O.o.	*Oratosquilla solicitans*

Received 30 January 1991; revised 30 May 1991; accepted 28 June 1991

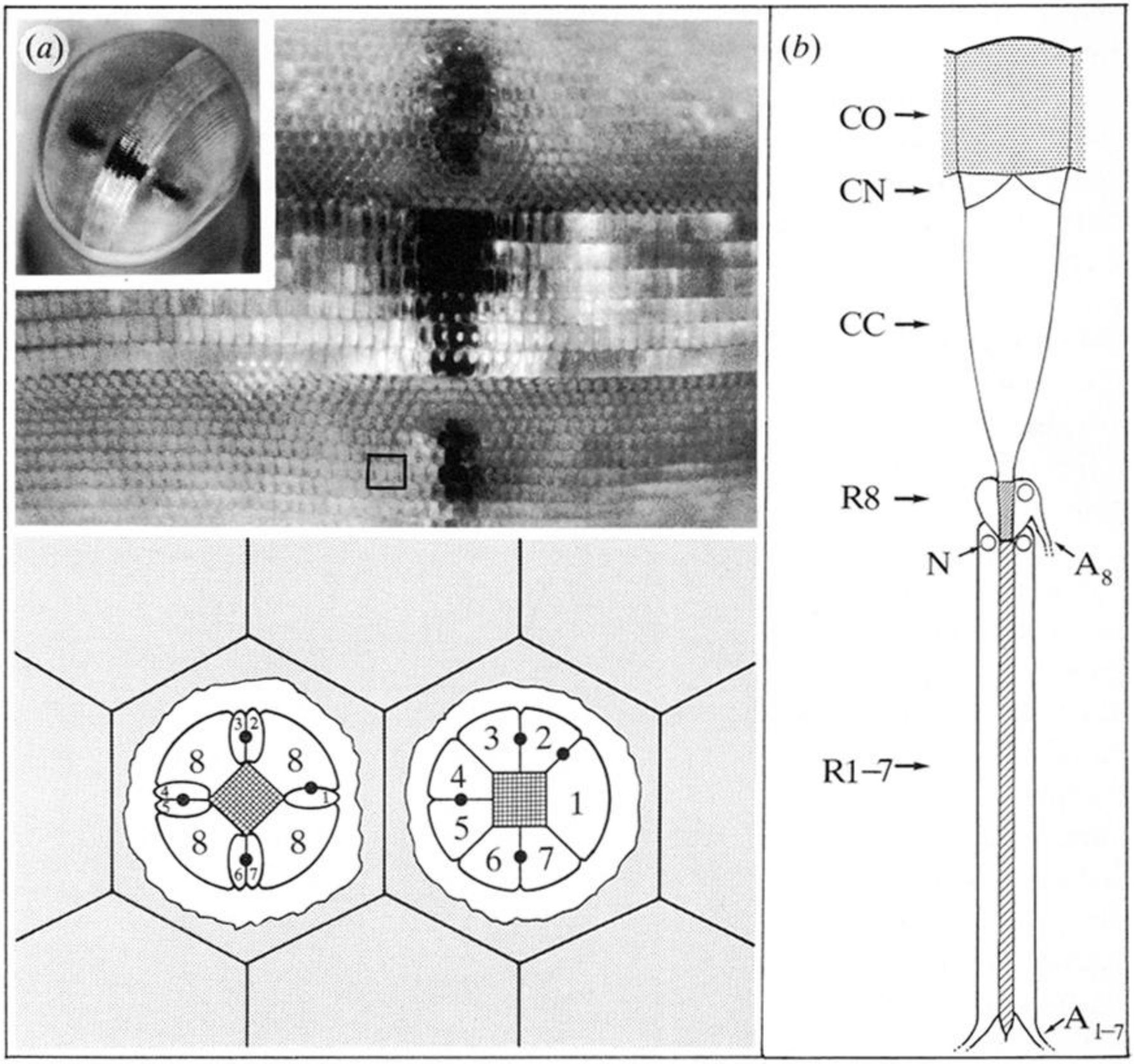

Figure 1. (*a*) Left eye of *Gonodactylus chiragra*. The photograph is of the mid-band with some peripheral ommatidia and the inset is a frontal view of the whole eye. Stomatopod eyes can rotate about the eye stalk axis by up to 70° and the mid-band is often not held horizontally. However, to simplify the description of the eye's anatomy (in particular the direction of microvilli relative to the outside world) the text and all subsequent figures presume the mid-band is horizontal, unless otherwise stated.

Beneath the photograph is an expanded, diagrammatic view of the portion of the ventral hemisphere within the box above. Two of the hexagonal facets found in the peripheral retinae are 'cut away' to reveal the arrangement of retinular cells in these ommatidia. The R8 cell level is shown on the left and the R1–7 level on the right (figure 16). As explained further in the text (§3*d*(iv)), the dorsal and ventral halves of the eye are mirror images of each other; as are the right- and left-hand eye. The cell arrangement shown here is for the bottom half of the left-hand eye, viewed looking into the eye from in front of the shrimp. The black dots mark the position of the four cone cell projections and cell numbering is based on the position of these relative to the R1–7 cells; it conforms with that of Hallberg (1977) and is not the same as that of Marshall (1988). Cell 1 is always the largest cell and cell 2 is flanked on both sides by cone cell projections. Note the two directions of microvilli in the rhabdoms represented by the cross-hatch.

(*b*) A generalized ommatidium in longitudinal (or sagittal) section: CO, cornea; CN, corneagenous cells; CC, crystalline cones; N, nucleus; A8, axon of retinular cell 8; A1–7, axons of R1–7 cells.

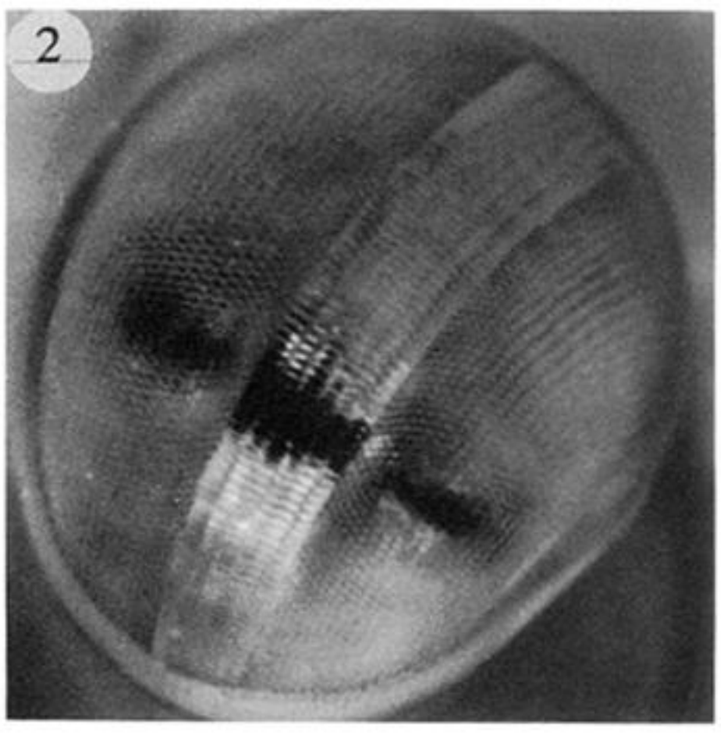

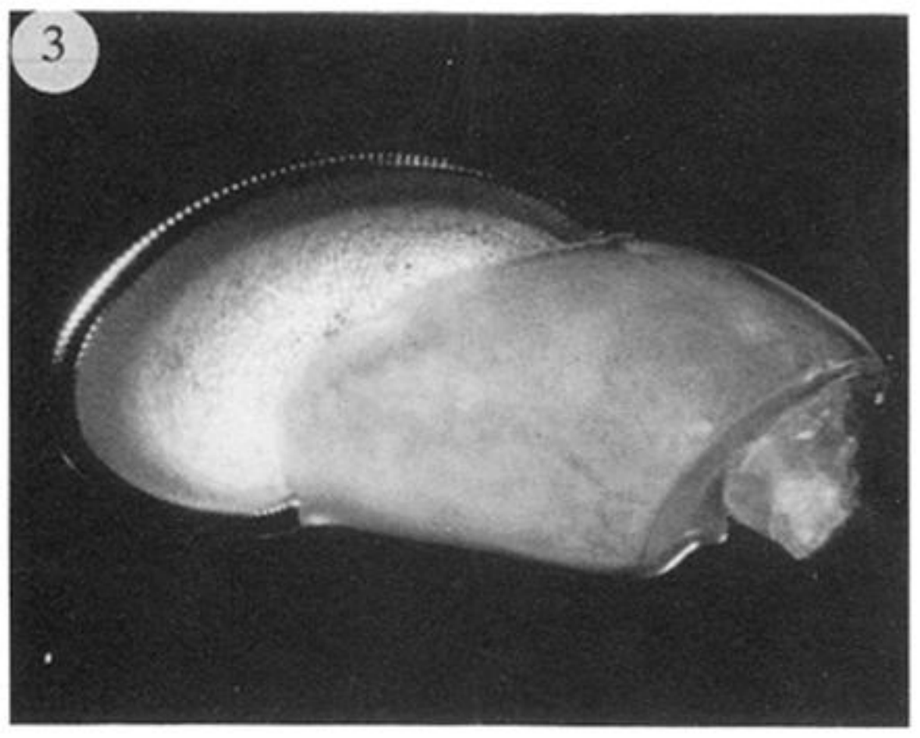

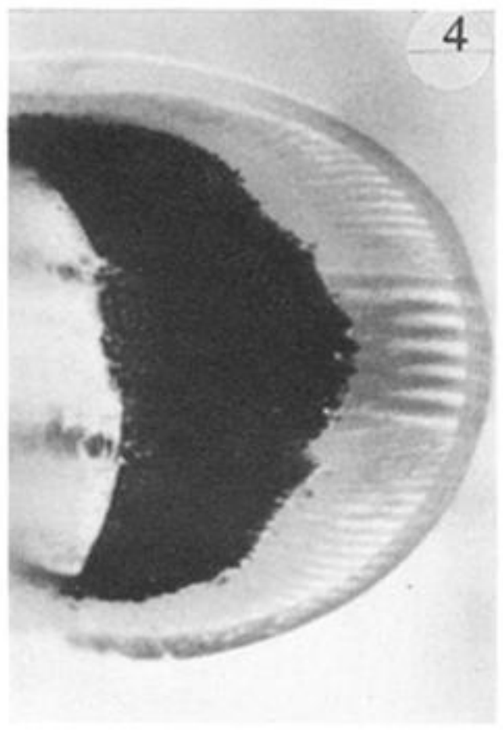

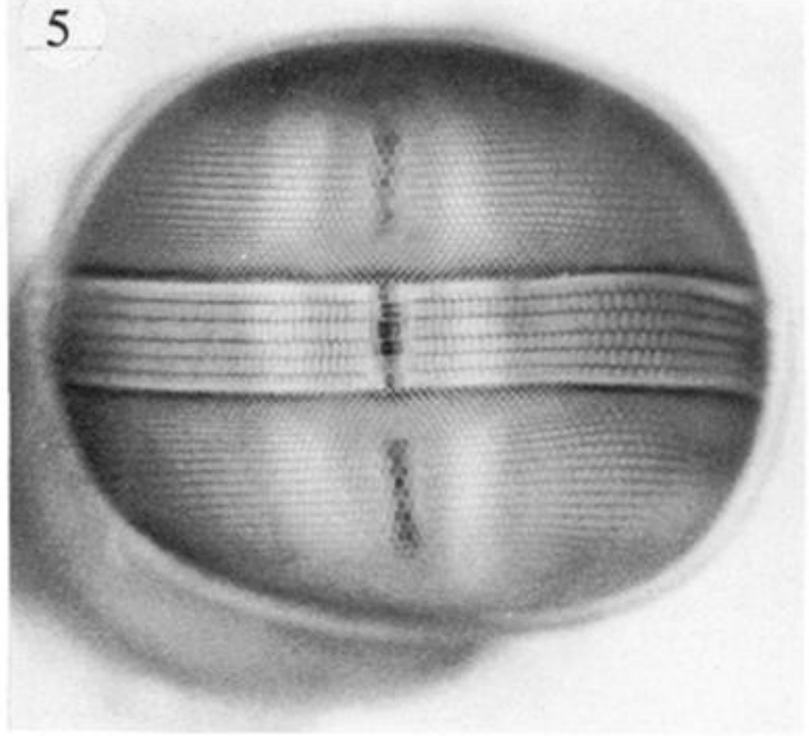

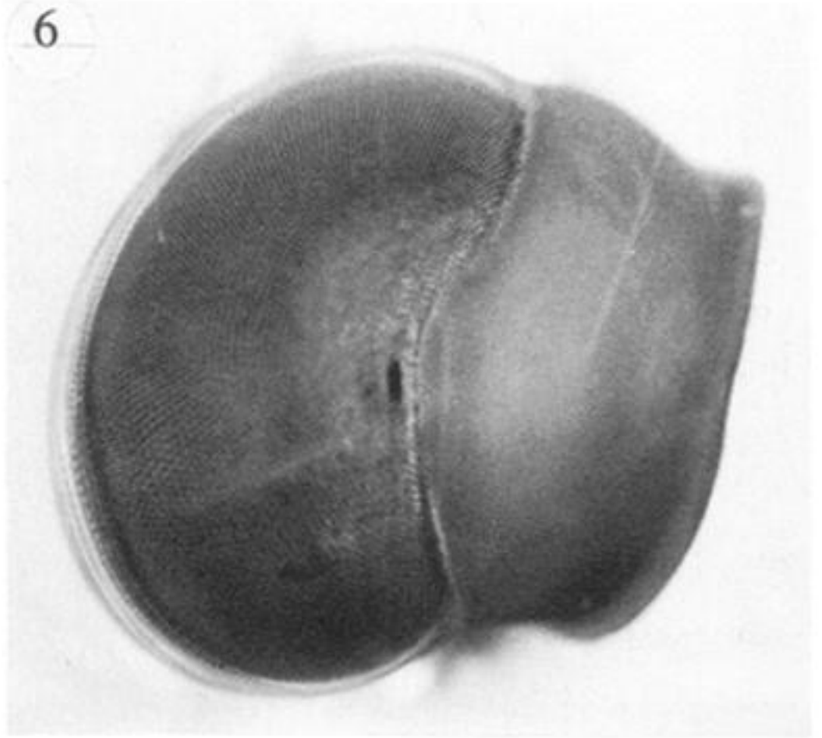

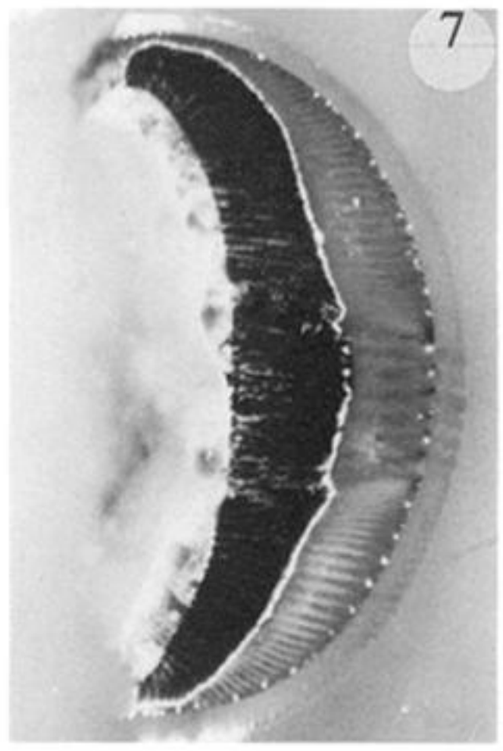

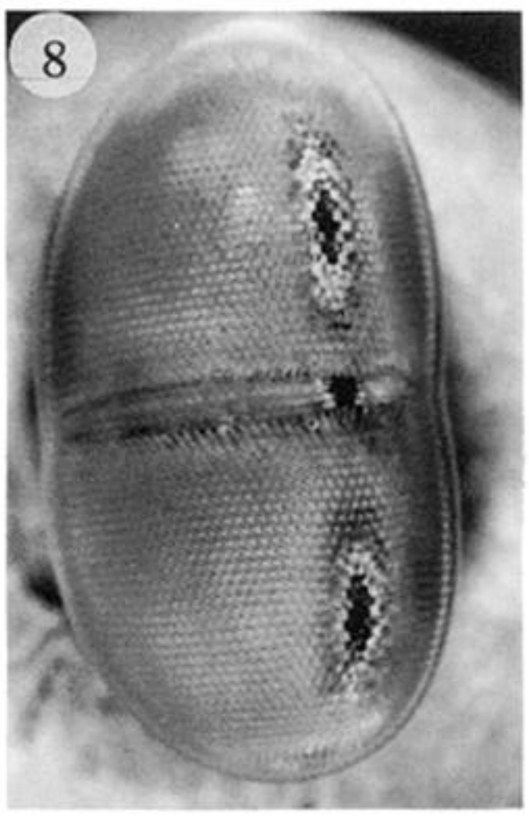

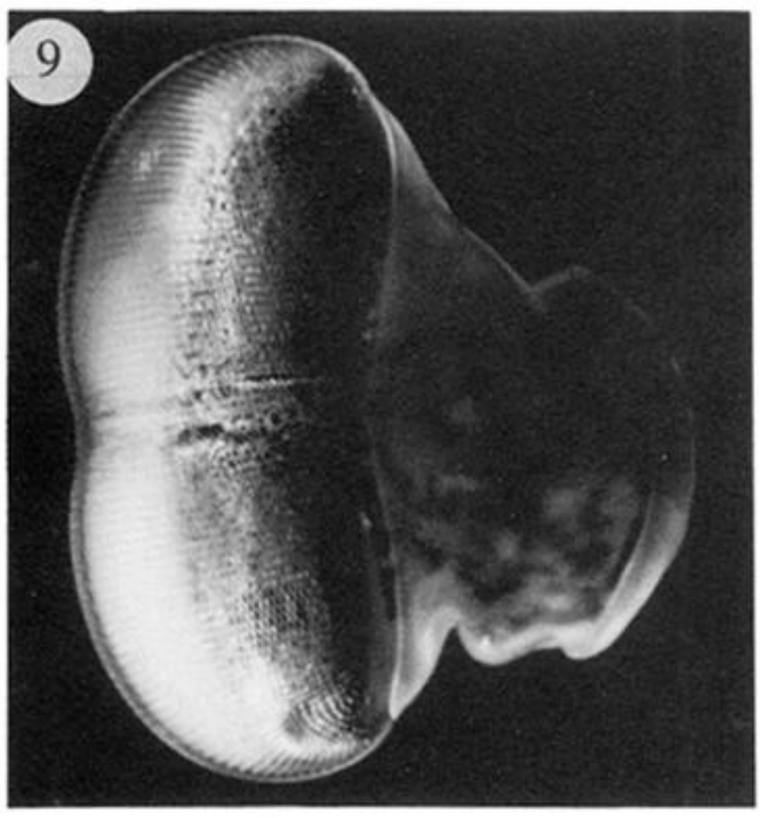

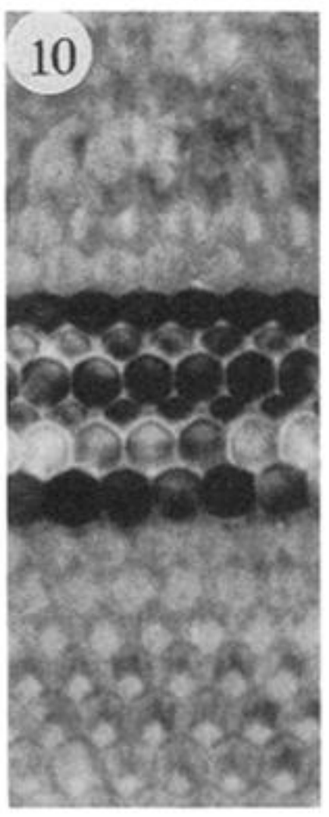

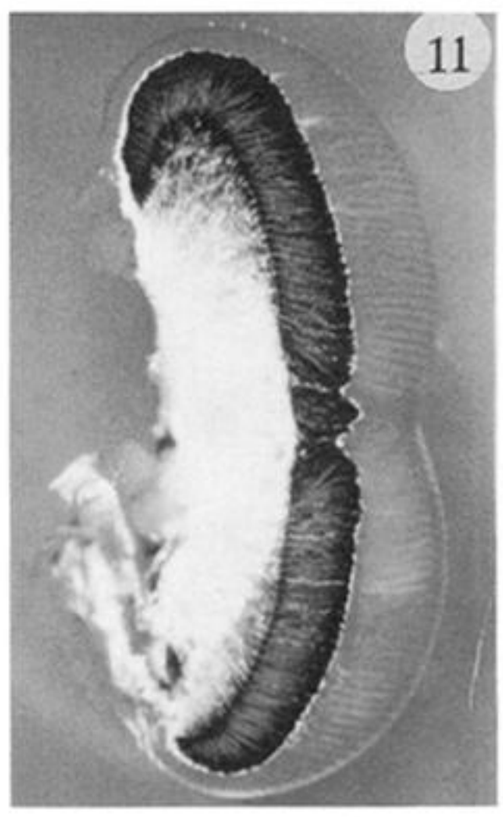

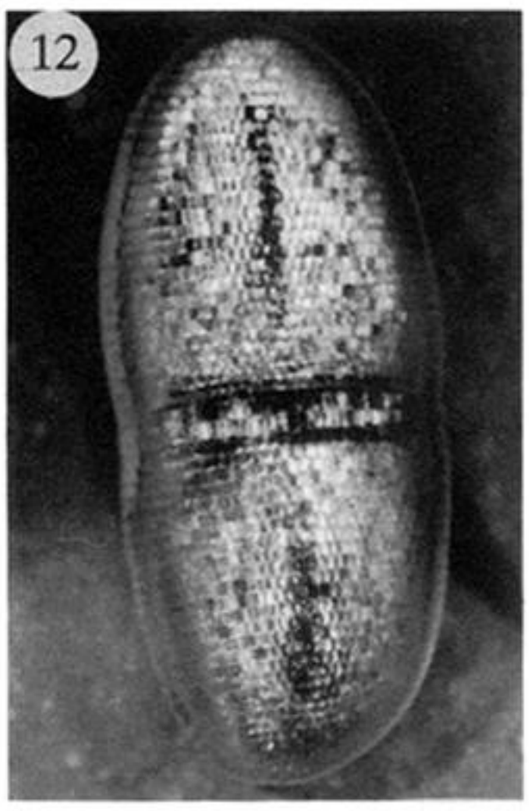

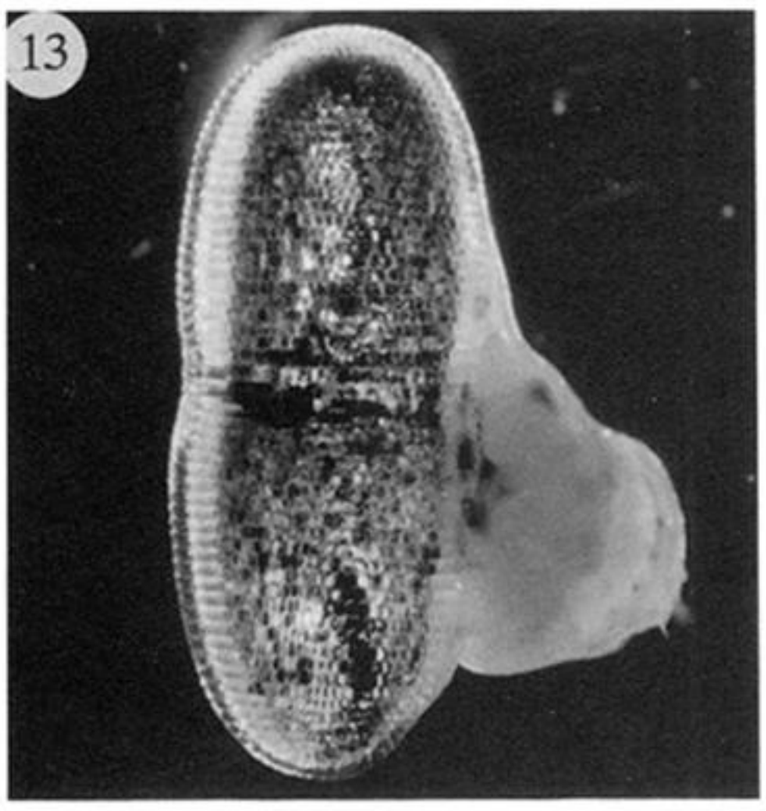

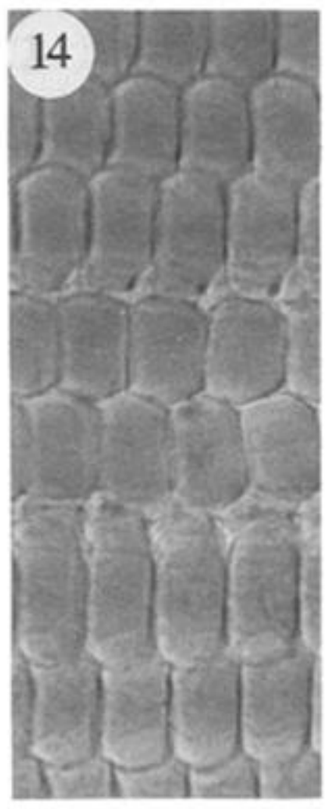

Figures 2–15. Stomatopod eyes.
Figure 2. Acute-zone in *Gonodactylus chiragra*, 15° off sagittal axis of eye.
Figure 3. Dorsal aspect of the eye of *Gonodactylus chiragra*.
Figure 4. Sagittal section through the eye of *Gonodactylus chiragra*.
Figure 5. Right eye of *Odontodactylus scyllarus* viewed from in front, directly on the sagittal axis.
Figure 6. Dorsal aspect of the eye of *Odontodactylus scyllarus*.
Figure 7. Sagittal section through the eye of *Odontodactylus scyllarus*.
Figure 8. Left eye of *Lysiosquilla tredecimdentata* viewed from in front, directly on the sagittal axis.
Figure 9. Lateral aspect of the left eye of *Lysiosquilla tredecimdentata*.
Figure 10. Close-up of the mid-band and surrounding ommatidia in *Lysiosquilla tredecimdentata*.
Figure 11. Sagittal section through the eye of *Lysiosquilla tredecimdentata*.
Figure 12. Left eye of *Oratosquilla solicitans* viewed from in front, directly on the sagittal axis. Note the position of the pseudopupil (dark facets) in this eye compared with figure 8. There is no acute-zone in this eye and only two rows of ommatidia in the mid-band.
Figure 13. Lateral aspect of the left eye of *Oratosquilla solicitans*.
Figure 14. Close-up of the mid-band and surrounding ommatidia in *Oratosquilla solicitans*; cornea dissected away and cleaned. The mid-band is flanked by two rows with small facets.
Figure 15. Sagittal section through the eye of *Oratosquilla solicitans*. Note the unusual upward skewing of the ommatidia in the ventral hemisphere.

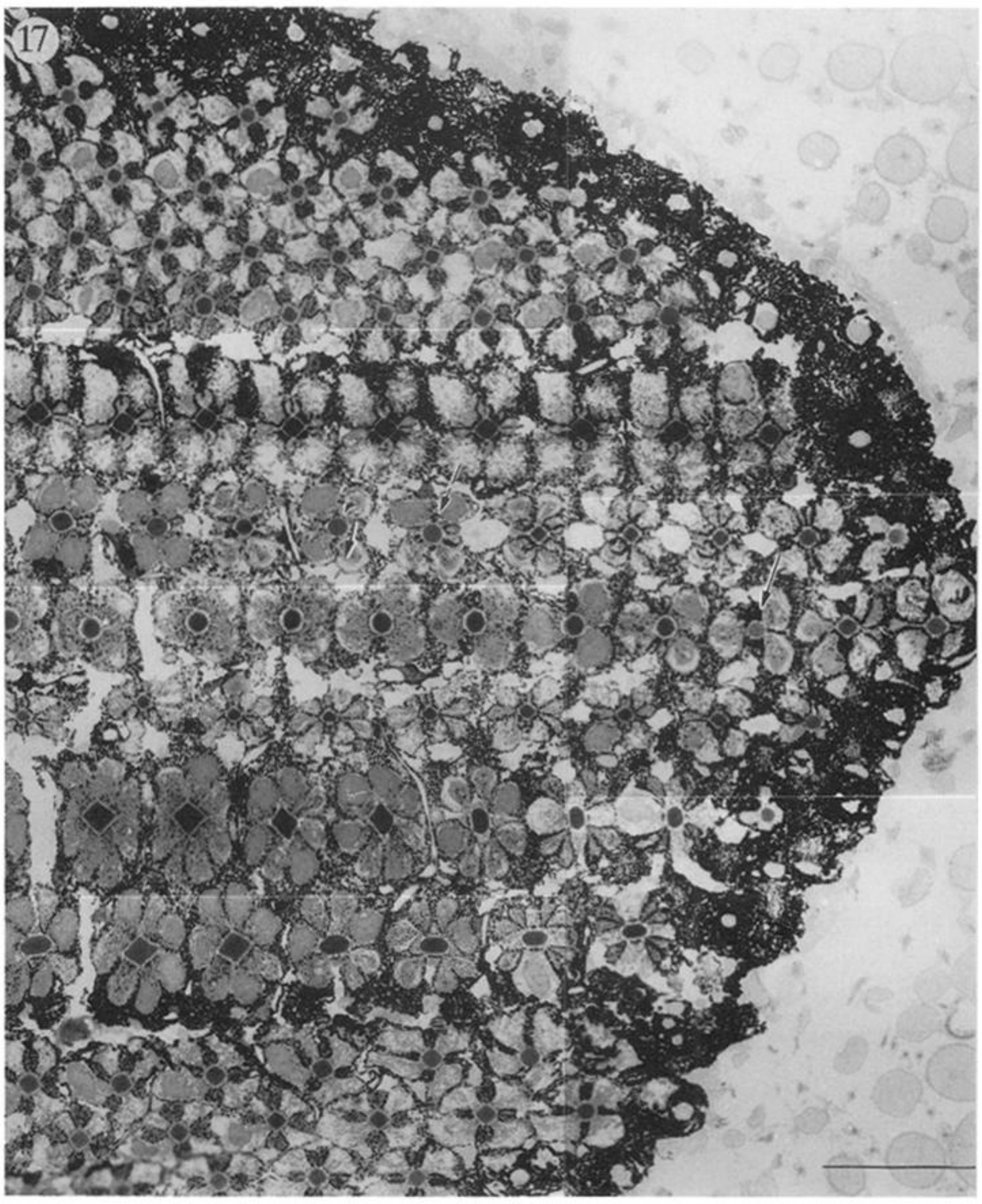

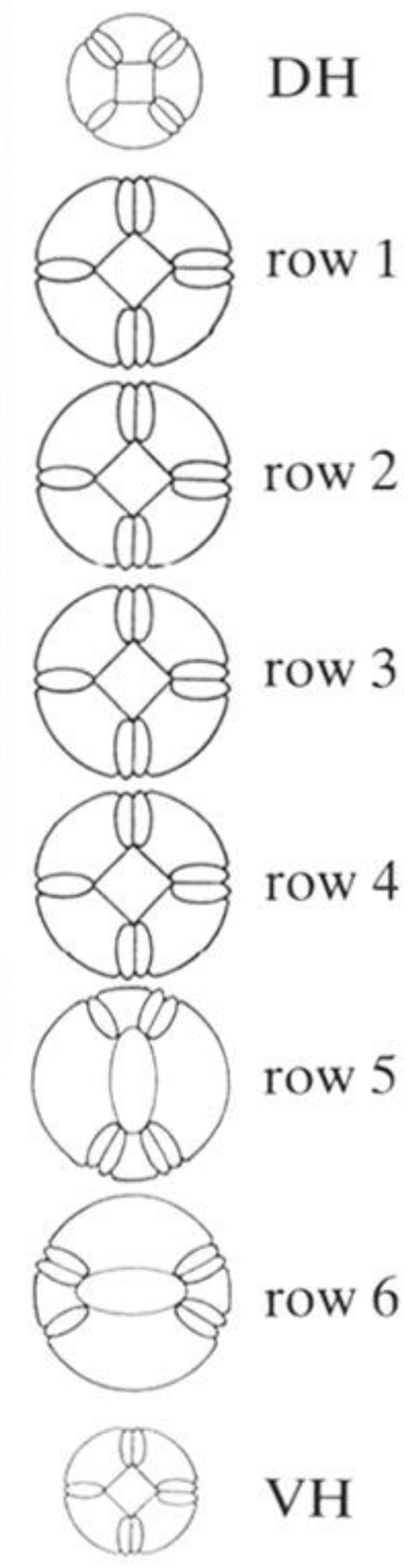

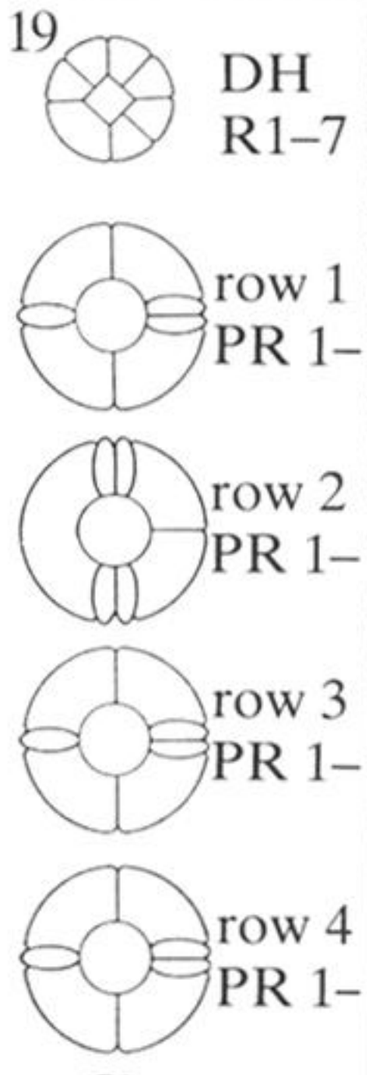

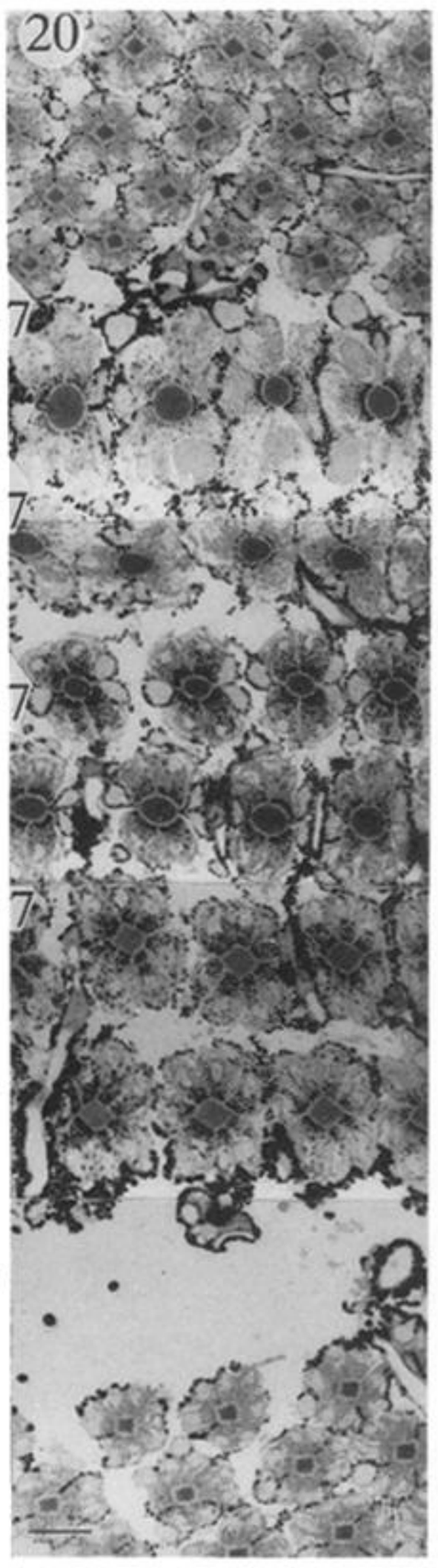

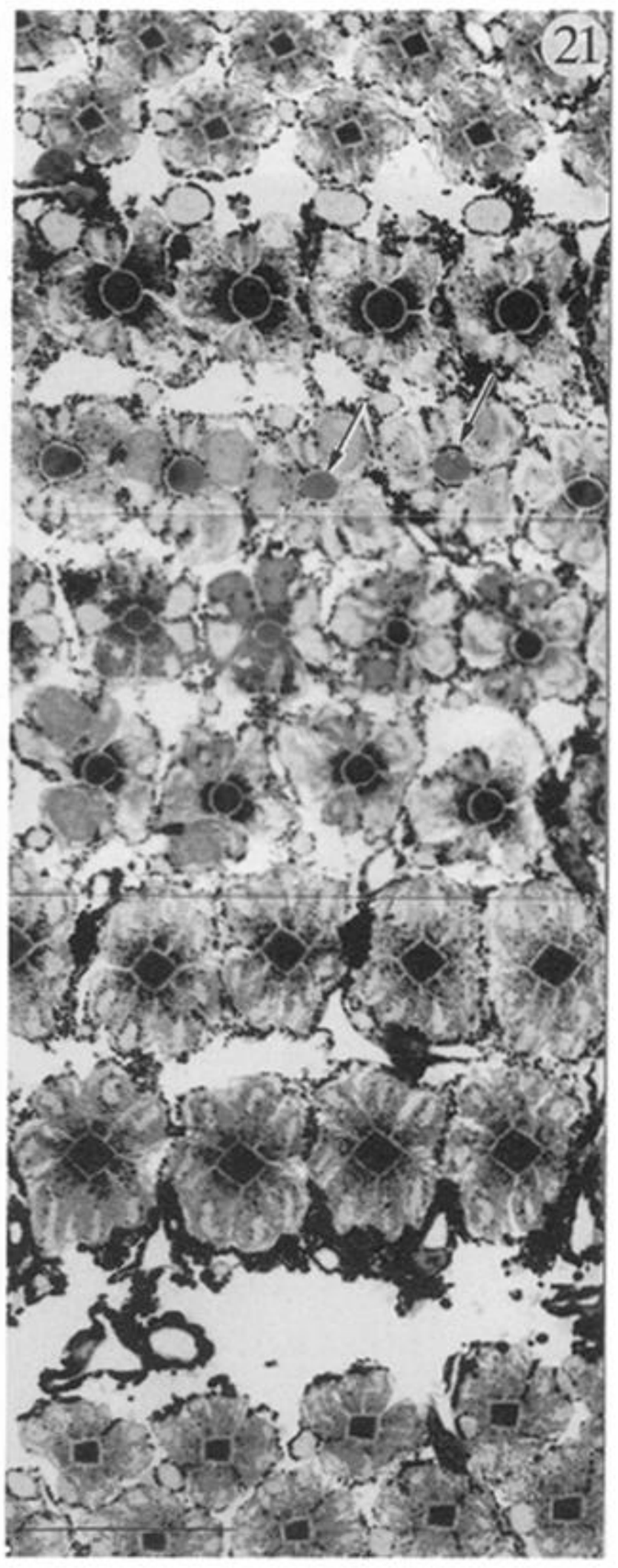

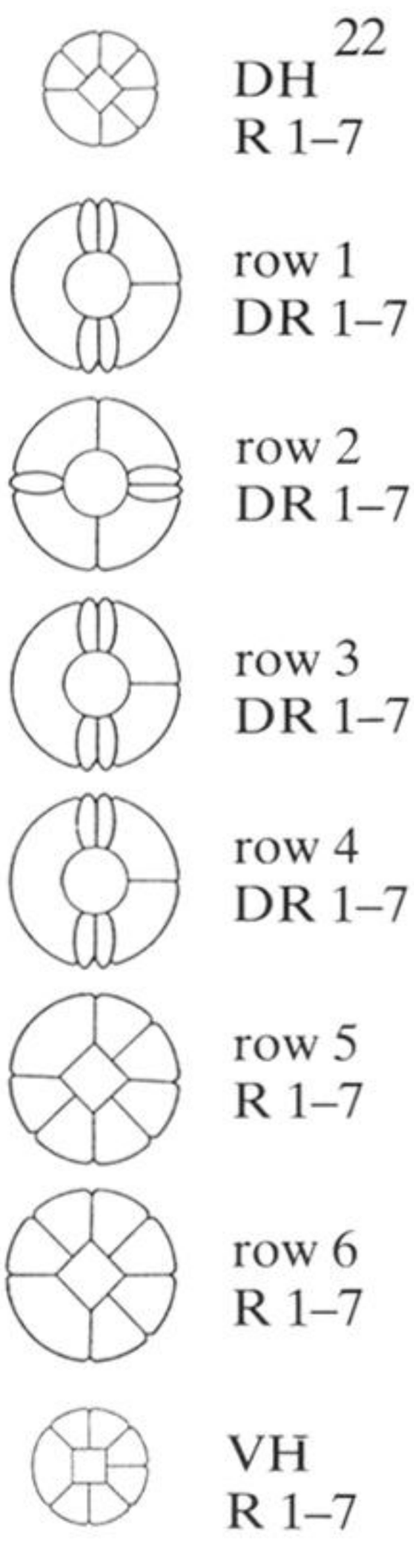

Figures 17–22. The retinular cells (levels A–R8, C–DR1–7 and E–PR1–7). Figures 17, 20 and 21 are arranged such that rhabdoms on the right of each figure are more distal than those on the left.

Figure 17. Transverse LM section of mid-band and periphery of the right eye of *Coronis scolopendra* at a distal level. Owing to the curvature of the retina, several different retinal levels, A, B and C (figure 16), can be seen in one section. In mid-band row one and four and in both hemispheres, only the R8 rhabdom (level A) is sectioned. In the remainder of the retina, R1–7, DR1–7 (level C), in rows two and three, and F1 filters (level B: arrowed in the figure) are sectioned (see figures 34–39). Scale 100 μm.

Figure 18. Diagrammatic representation of the R8 cells in figure 17 level A in the retina. R1–7 cells are also present at this level as thin upward projections between these four lobes of R8. Note the 'side-down' square shape of the R8 rhabdom in the dorsal hemisphere and the 'point-down' square shaped R8 rhabdom in the ventral hemisphere.

Figure 19. Diagrammatic representation of the retinular cells and rhabdoms in figure 20 (level E, figure 16). In mid-band rows one to four, the small cells are the axonal projections of the DR1–7 cells.

Figure 20. LM transverse section of the mid-band and hemispheres in *Coronis scolopendra* PR1–7. In row one the transition between DR1–7 and PR1–7 tiers is visible, all other rows are sectioned through the PR1–7 tier only. Scale 30 μm.

Figure 21. Transverse LM section of the mid-band and hemispheres in *Coronis scolopendra* DR1–7 (level C). F2 in row two (level B, arrowed) is also visible in this section, as are the PR1–7 cells (level E) in rows two and three. All other rhabdoms are sectioned through DR1–7 rhabdom. Scale 100 μm.

Figure 22. Diagrammatic representation of the DR1–7 cells in figure 21 or 24 (level C, figure 16).

Figures 23–27. The R8 cells.

Figure 23. TEM longitudinal section of the R8 cell rhabdom of row three in *Gonodactylus chiragra*. At the top the crystalline cones, surrounded by screening pigment, join the rhabdom and at the bottom the rhabdom joins the F1 filter of this row. Scale 10 μm.

Figure 24. TEM transverse section of row six R8 rhabdom in *Pseudosquilla ciliata*. The small distal protrusions of cells 1–7 are labelled. Scale 5 μm.

Figure 25. TEM transverse section of the R8 cell of row four in *Coronis scolopendra*. The four lobes of the R8 cell and the small upward projections of R1–7 are labelled. Note the orthogonal arrangement of microvilli. Scale 5 μm.

Figure 26. Transverse LM section of R8 (left) and R1–7 (right) cells and rhabdom in the dorsal hemisphere of the left eye of *Oratosquilla solicitans*. Note the R8 cell nucleus in the upper right limb of the 'X' and the four cone cell projections visible at the R8 cell level. Scale 20 μm.

Figure 27. LM transverse section of rows five and six R8 cells in *Coronis scolopendra*. Scale 50 μm.

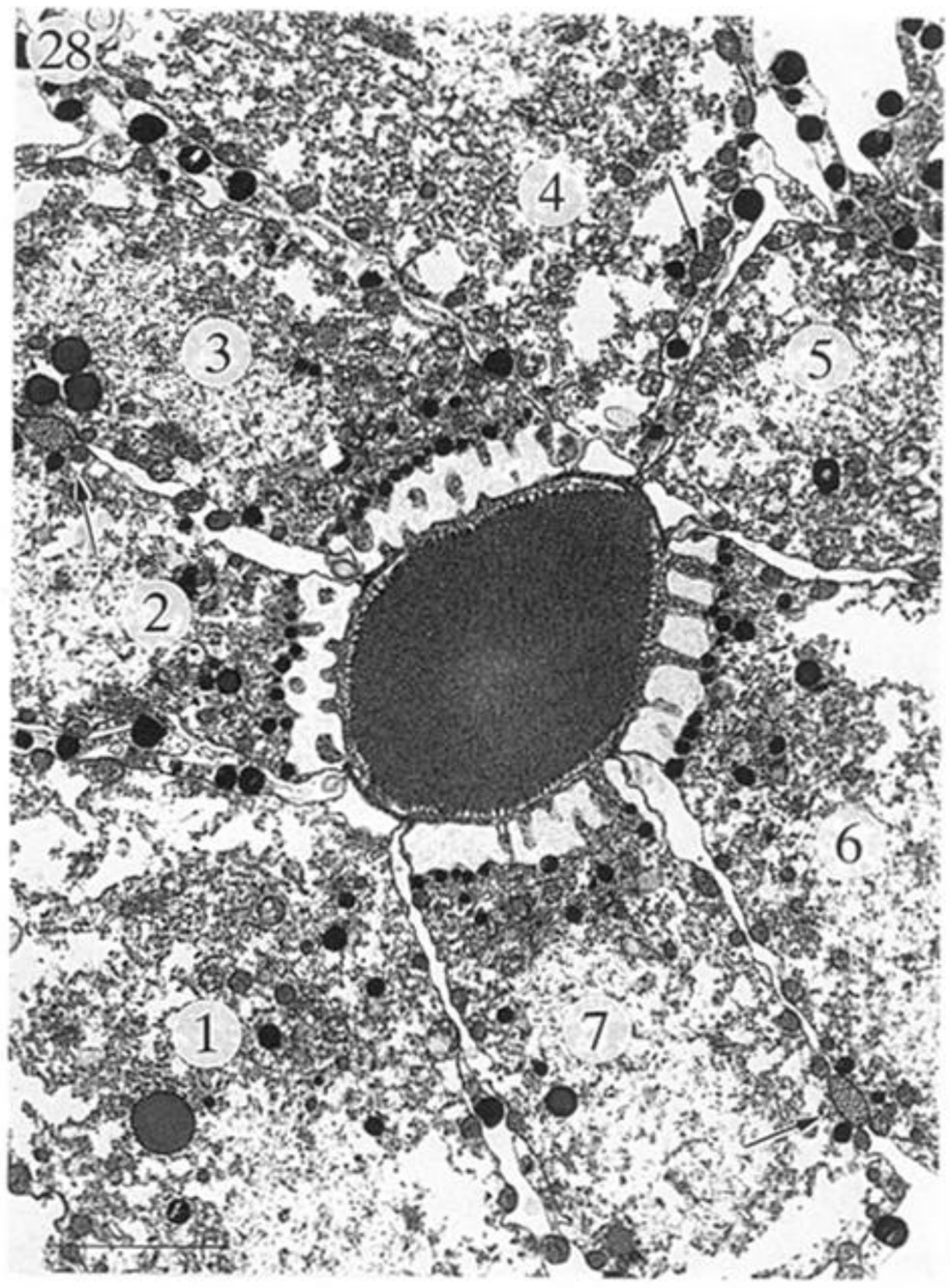

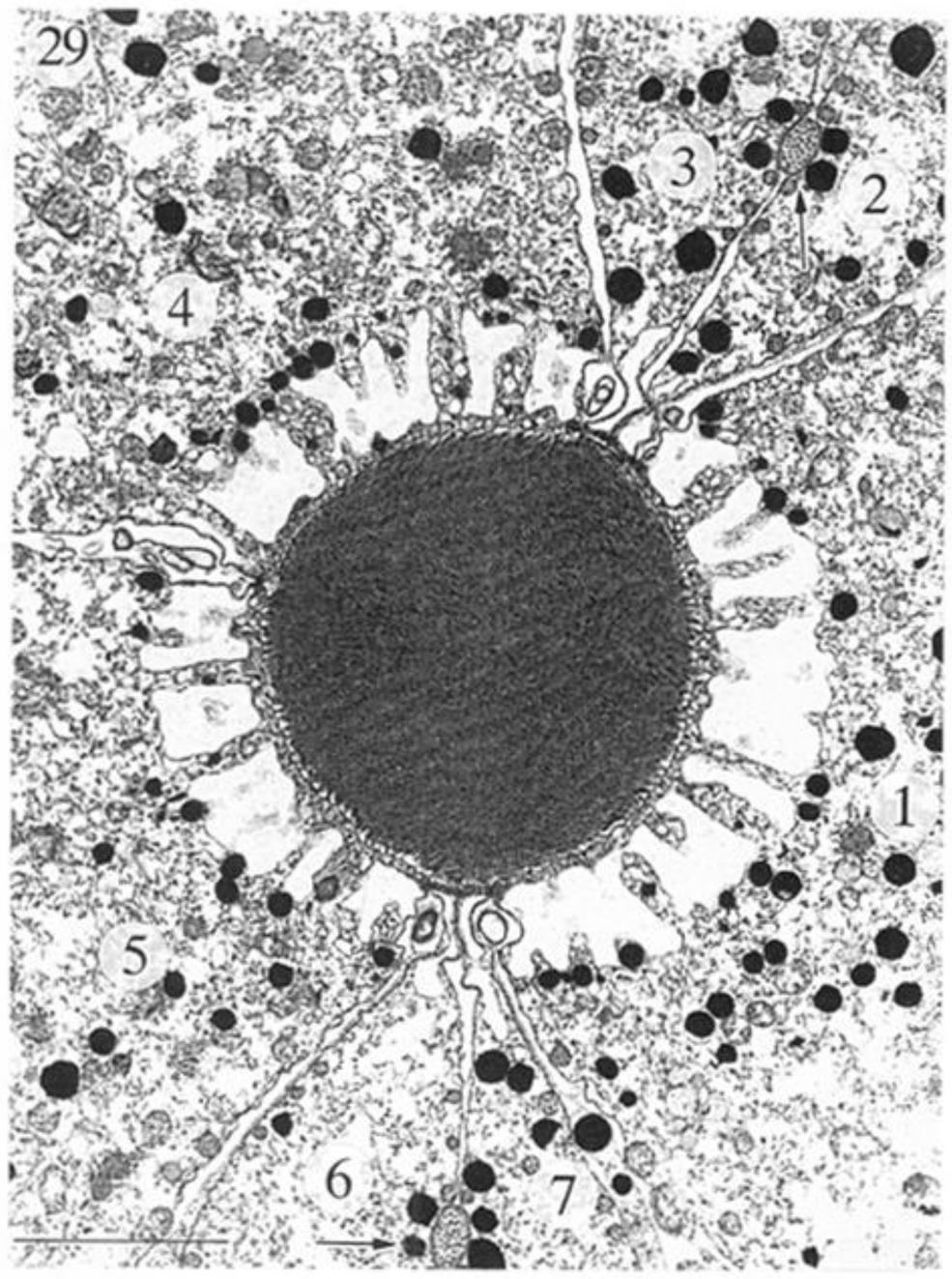

30

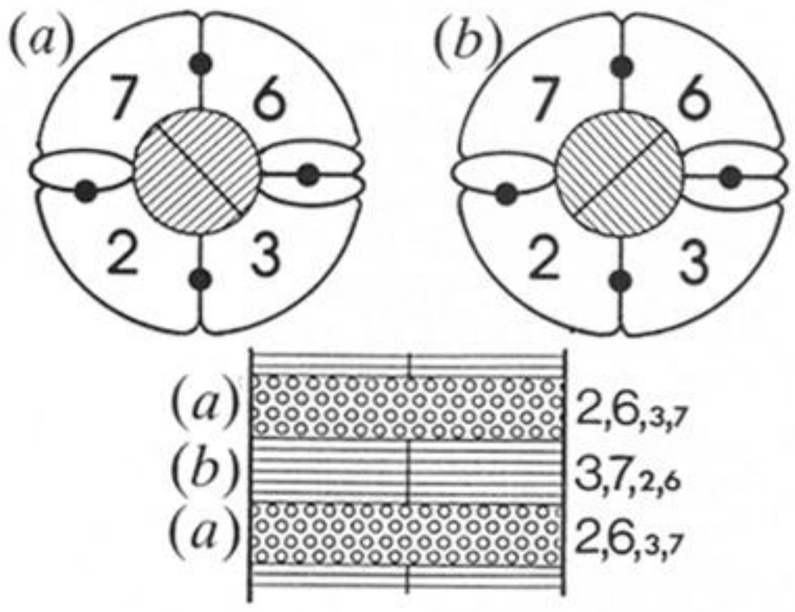

31

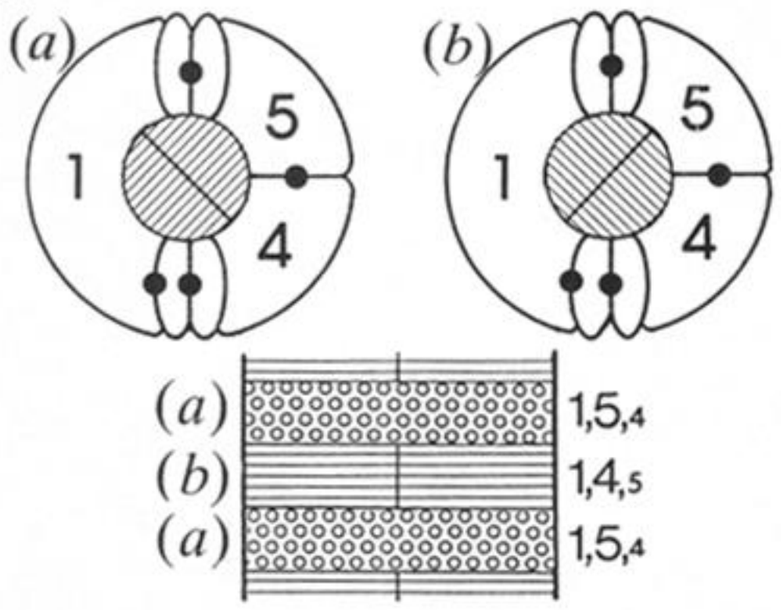

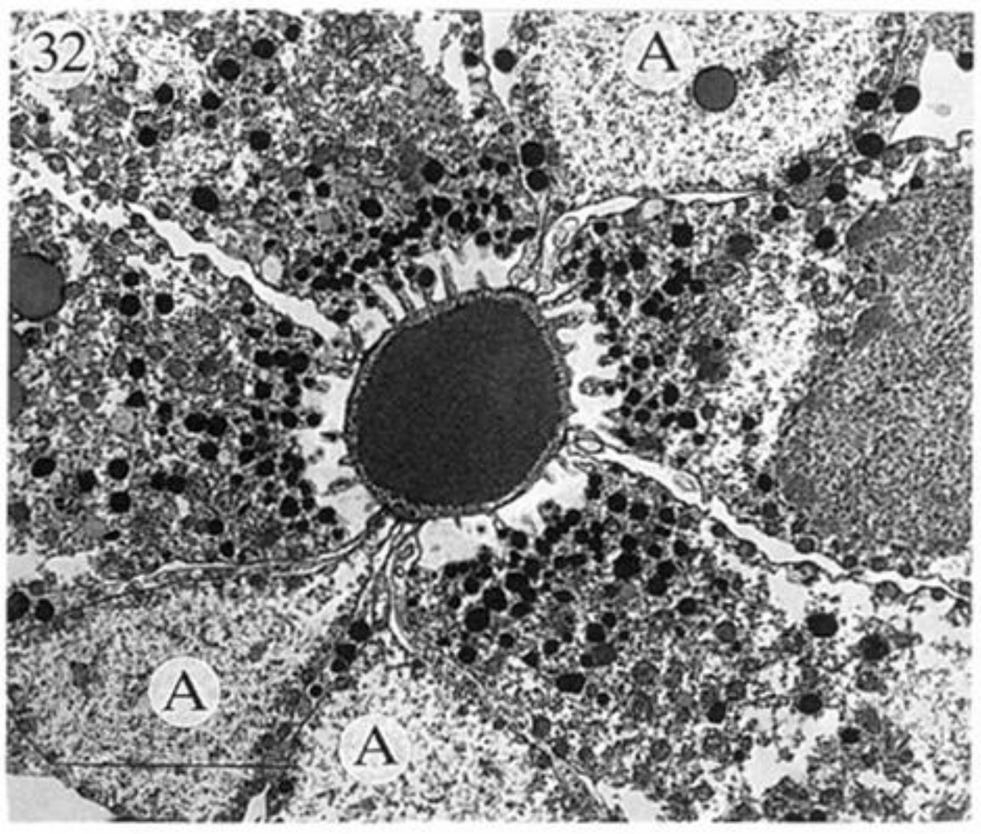

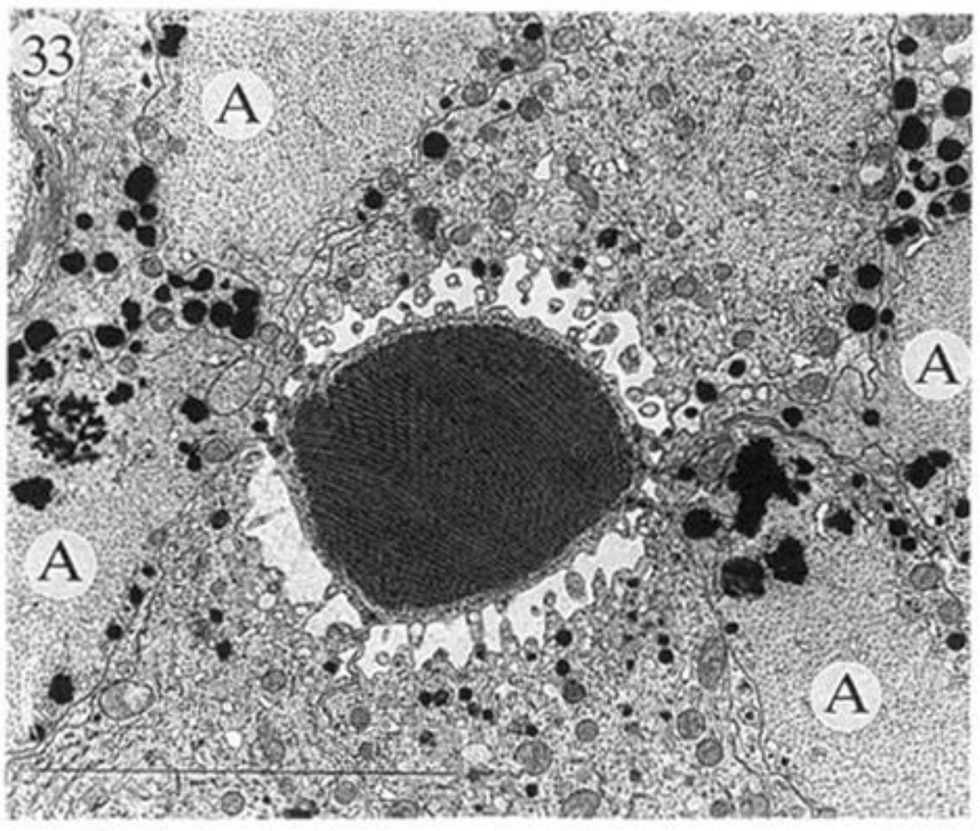

Figures 28–33. Cellular microvillar arrangement in rows one to four of the mid-band.

Figure 28. TEM transverse section of row two DR1–7 in *Coronis scolopendra*. Cells are numbered and three cone cell projections visible between cells 2 and 3, 4 and 5 and 6 and 7 are arrowed. Scale 5 μm.

Figure 29. TEM transverse section of row three DR1–7 in *Coronis scolopendra*. Cells are numbered and two of the cone cell projections visible between cells 2 and 3 and 6 and 7 are arrowed. Scale 5 μm.

Figure 30. Diagrammatic representation of a four-cell rhabdom found in the row two DR1–7 tier and rows one, three and four PR1–7 tiers (figure 16). The illustration is specifically of row one or two in a right eye (from the cone tail position, figure 1). The upper two diagrams (*a*) and (*b*) are transverse sections of layers (*a*) and (*b*) shown in the lower diagram which is a longitudinal section. The large and small numbers next to each layer are the cells responsible for the manufacture of microvilli; the large numbers are those cells which make most microvilli. Therefore in layer (*a*), for instance, cells 2 and 6 make most of the microvilli arrayed (↗) and cells 7 and 3 make a few microvilli arrayed (↗). In the next layer, (*b*), the roles are reversed to produce (↘) microvilli and cells 3 and 7 make most microvilli and cells 2 and 6 only a few.

Figure 31. Diagrammatic representation of a three-cell rhabdom found in the row two PR1–7 tier and rows one, three and four DR1–7 tiers (figure 31). Here cells 4 and 5 alternate in producing large or small amounts of microvilli for each of layers (*a*) and (*b*), and cell 1 contributes an equal amount to each layer.

Figure 32. TEM transverse section of a row three PR1–7 rhabdom in *Coronis scolopendra*. The three axons from the DR1–7 cells of this ommatidium, are labelled A. Scale 10 μm.

Figure 33. TEM transverse section of a row two PR1–7 rhabdom in *Lysiosquilla scabricauda*. The four axons of the DR1–7 cells are labelled A. Scale 10 μm.

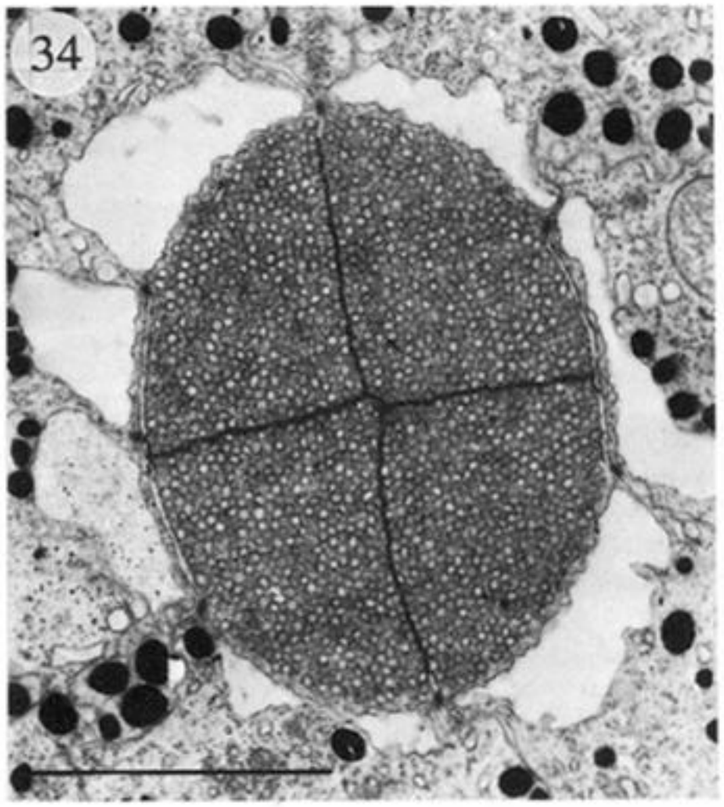

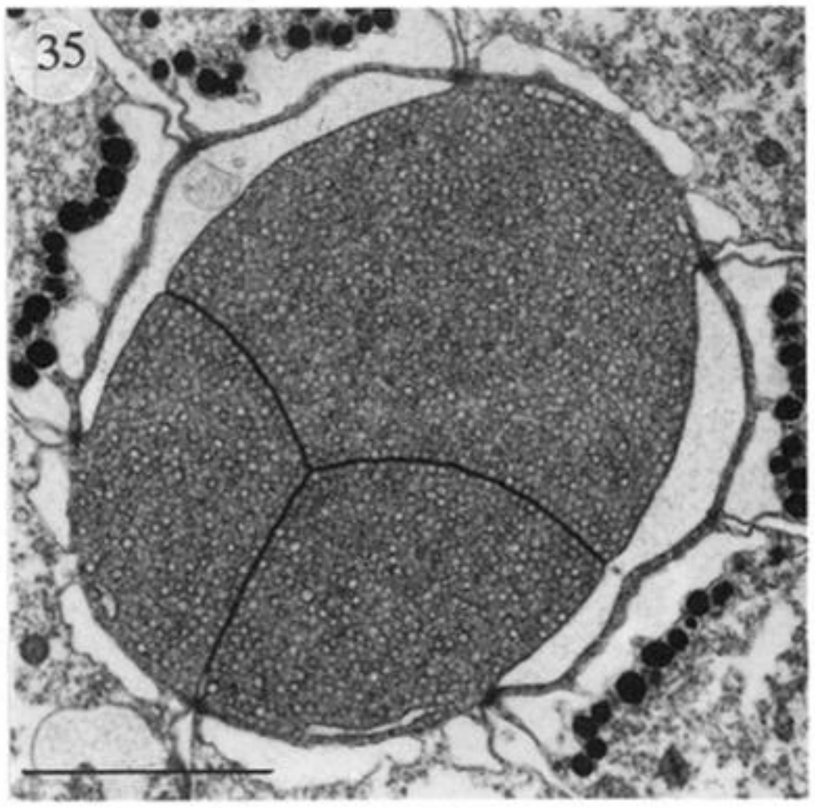

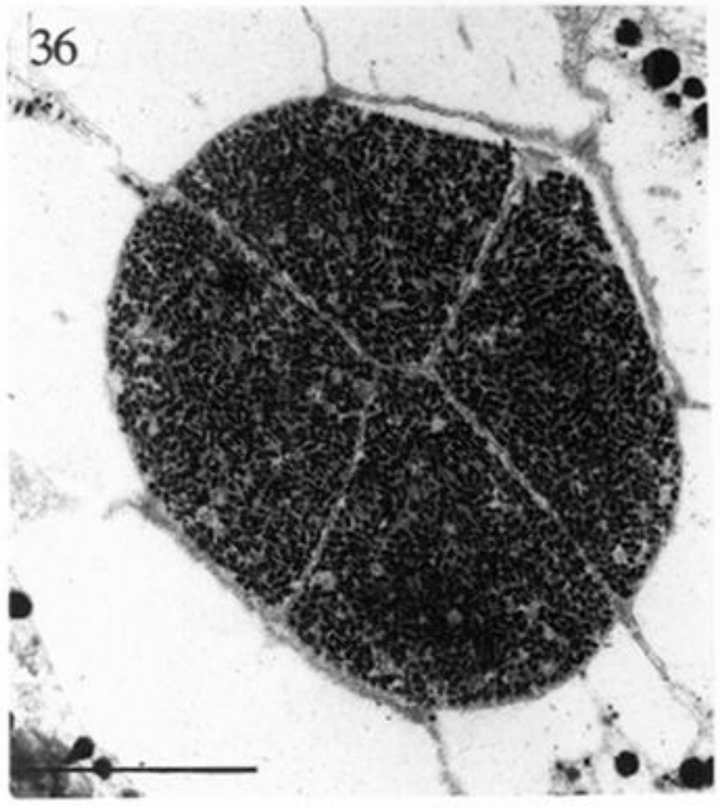

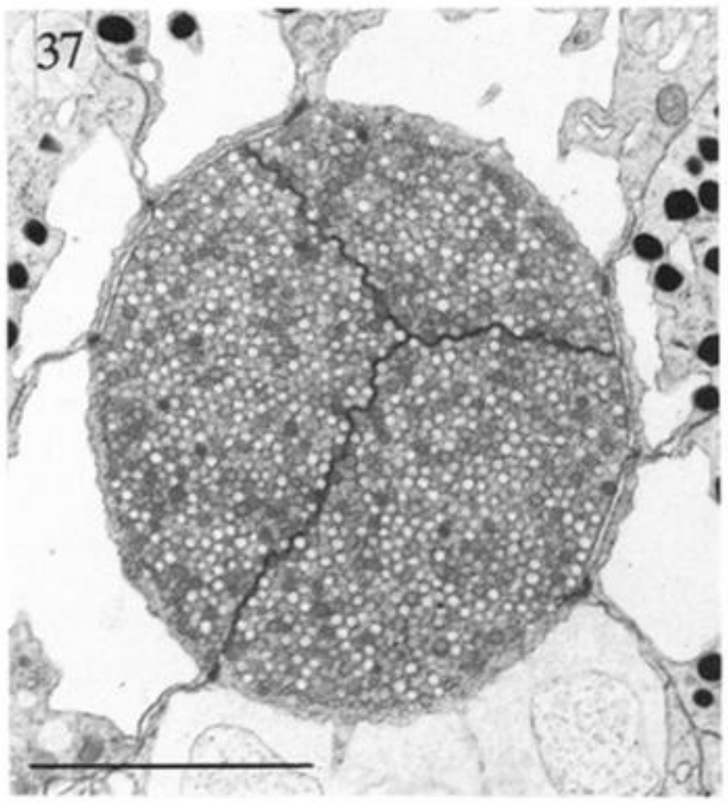

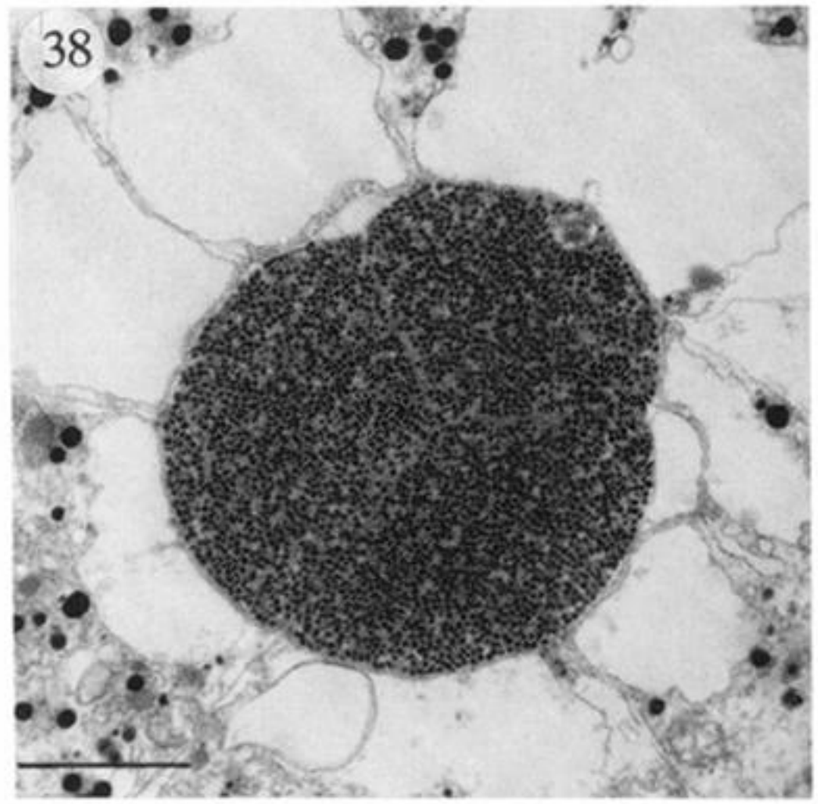

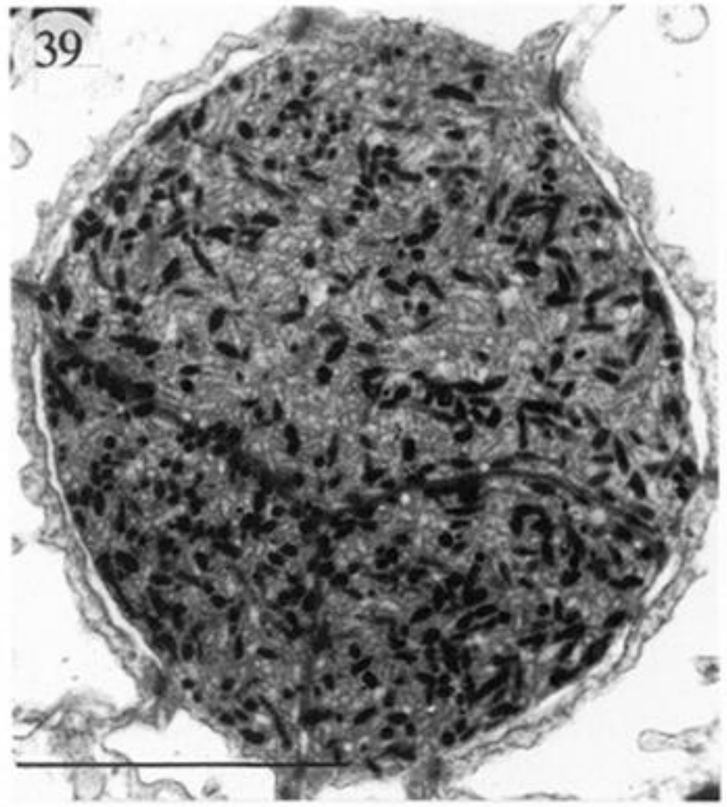

Figures 34–39. Distal and proximal filters (levels B–F1 and D–F2). Notable in these figures is the three or four part segmentation of filters depending on whether they are made by the four cell (DR1–7) tier in row two or the three cell (DR1–7) tier of row three. Differential staining of 'similar coloured' filters is also shown here. Filters in figures 36, 37 and 38 are all 'red'.

Figure 34. Row two F1 in *Gonodactylus oerstedii* (yellow, DR1–7). Scale 4 μm.

Figure 35. Row two F2 in *Coronis scolopendra* (yellow, DR1–7). Scale 4 μm.

Figure 36. Row two F2 in *Gonodactylus chiragra* (red, DR1–7). Scale 4 μm.

Figure 37. Row three F1 in *Coronis scolopendra* (red, DR1–7). Scale 4 μm.

Figure 38. Row three F2 in *Odontodactylus scyllarus* (red, DR1–7). Scale 4 μm.

Figure 39. Row three F2 in *Gonodactylus oerstedii* (purple, DR1–7). Scale 4 μm.

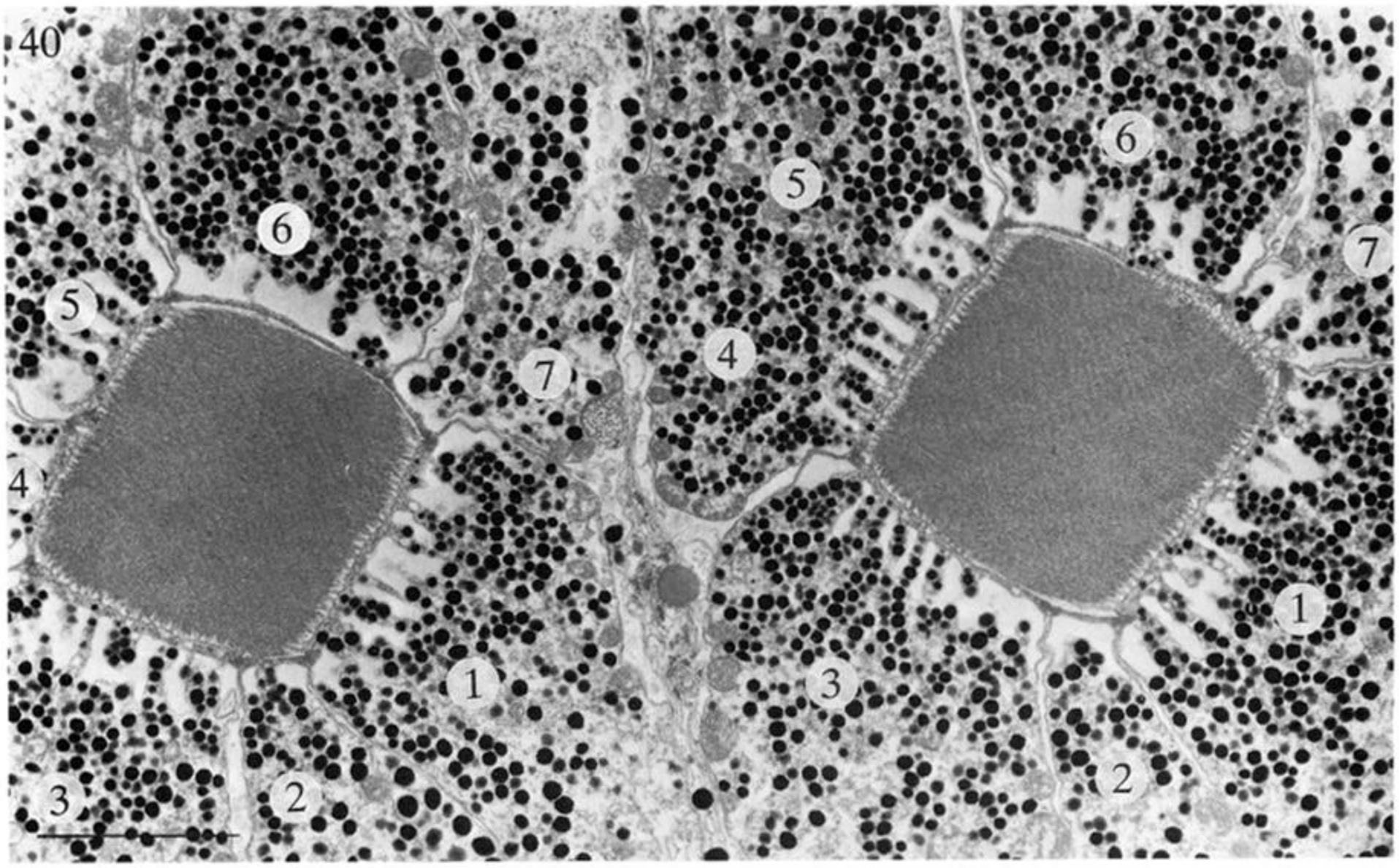

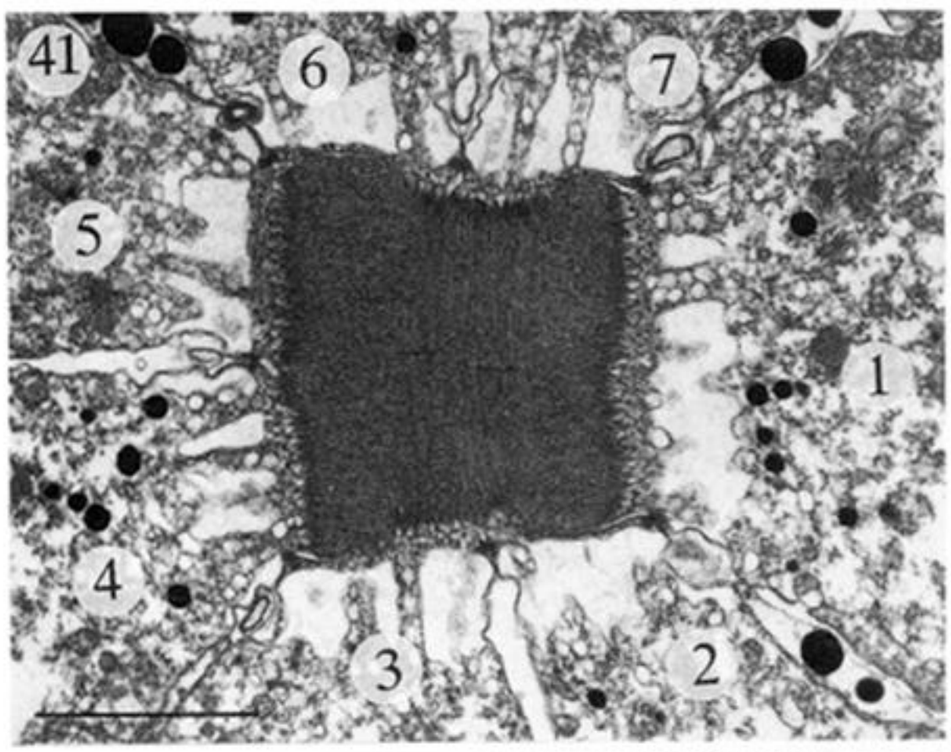

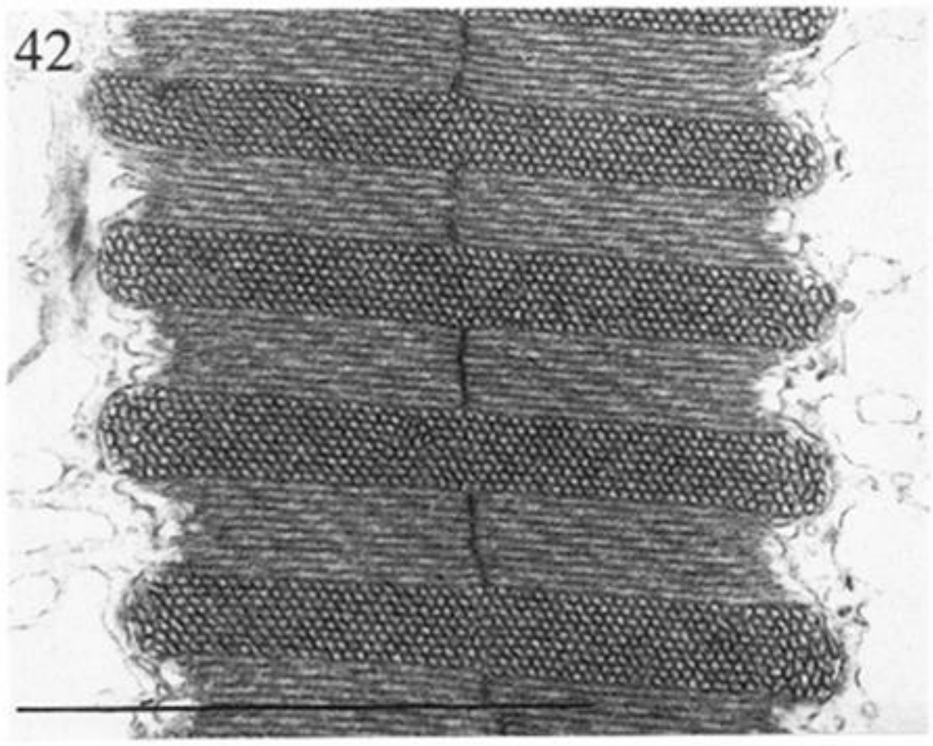

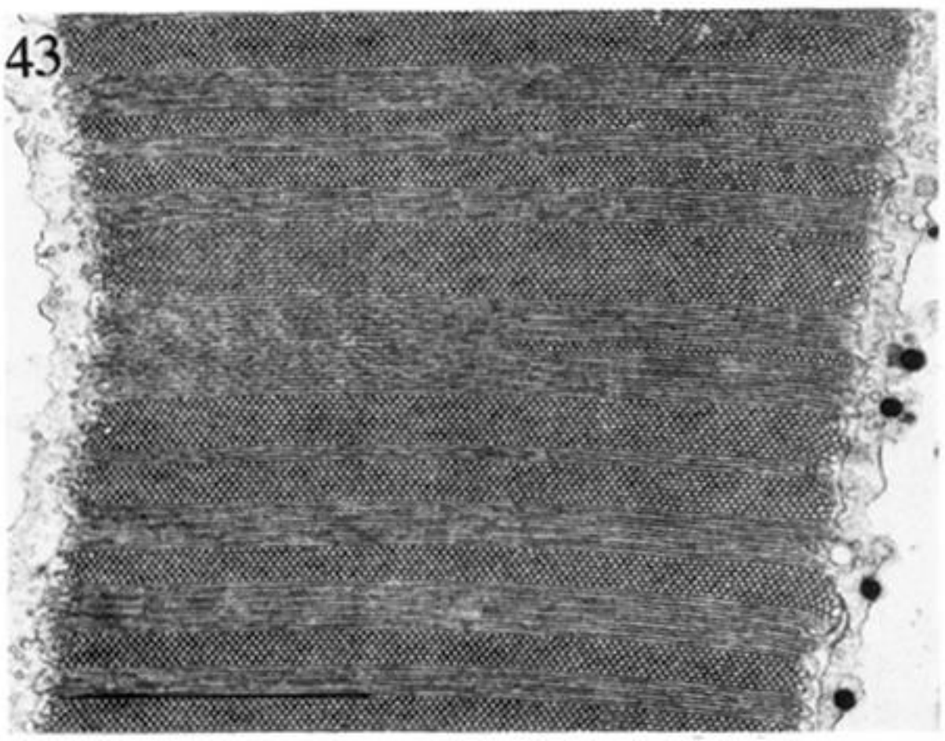

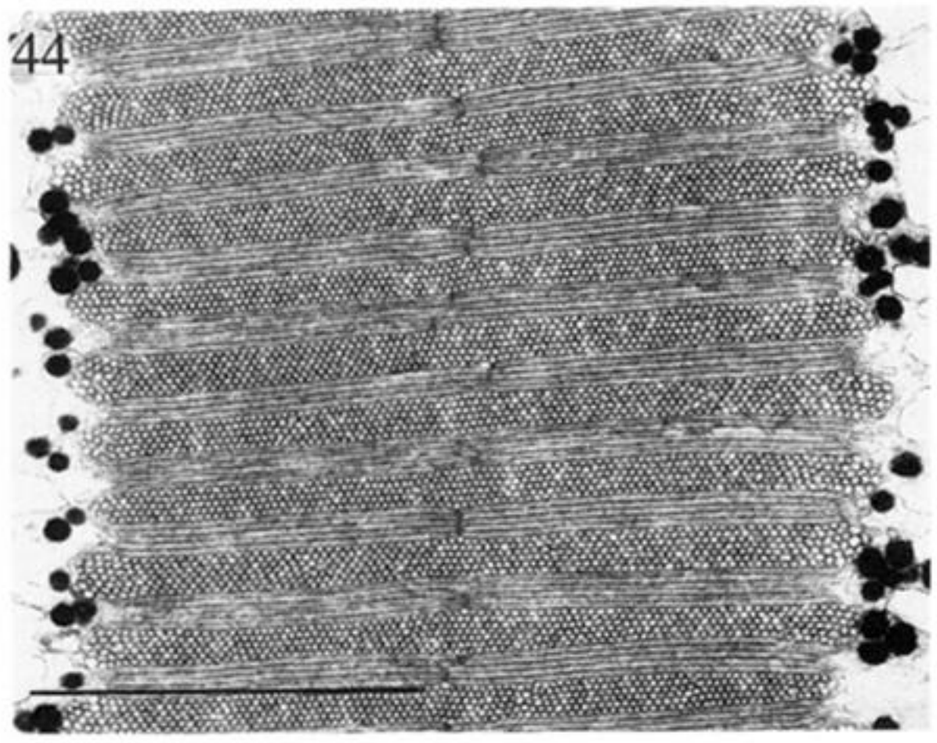

Figures 40–44. Cellular and microvillar arrangement in mid-band and periphery.
Figure 40. TEM transverse section of mid-band row six in *Pseudosquilla ciliata*, cells 1–7 are numbered. Scale 10 μm.
Figure 41. TEM transverse section of a rhabdom of the ventral hemisphere in *Coronis scolopendra*. Cells 1–7 are numbered. Scale 3 μm.
Figure 42. TEM of a dorsal hemisphere rhabdom in *Coronis scolopendra* cut in longitudinal section. Scale 3 μm.
Figure 43. TEM of row one PR1–7 *Gonodactylus chiragra* cut in longitudinal section. Scale 3 μm.
Figure 44. TEM of row six in *Gonodactylus chiragra* cut in longitudinal section. Scale 3 μm.